5-1-1993

A Unified Model for Multi-Phase Flow and Heat Transfer in Wellbores

Mohammad Mahbubul Ameen

A UNIFIED MODEL FOR MULTI-PHASE FLOW AND

HEAT TRANSFER IN WELLBORES

by

Mohammad Mahbubul Ameen

Bachelor of Science, Bangladesh University

of Engineering & Technology, 1988.

A Thesis

Submitted to the Graduate Faculty

of the

University of North Dakota

in partial fulfillment of the requirements

for the degree of

Master of Science

Grand Forks, North Dakota

May, 1993

This thesis, submitted by Mohammad Mahbubul Ameen in partial fulfillment of the requirements for the degree of Master of Science from the University of North Dakota, has been read by the Faculty Advisory Committee under whom the work has been done and is hereby approved.

(Chairperson)

This thesis meets the standards for appearance, conforms to the style and format requirements of the Graduate School of the University of North Dakota, and is hereby approved.

Dean of the Graduate School

4-28-93

ii

PERMISSION

Title   A Unified Model for Multi-Phase flow and Heat Transfer in Wellbores.

Department   Chemical Engineering

Degree   Master of Science

In presenting this thesis in partial fulfillment of the requirement for a graduate degree from the University of North Dakota, I agree that the library of this University shall make it freely available for inspection. I further agree that permission for extensive copying for scholarly purposes may be granted by the professor who supervised my thesis work, in his absence, by the chairperson of the department or the dean of Graduate School. It is understood that any copying or publication or other use of this thesis or part thereof for financial gain shall not be allowed without my written permission. It is also understood that due recognition shall be given to me and to the University of North Dakota in any scholarly use which may be made of any material in my thesis.

Signature _Mohammad Mahbubul Ameen._

Date _April 28, 93._

TABLE OF CONTENTS

LIST OF ILLUSTRATIONS

LIST OF TABLES

ACKNOWLEDGEMENT

ABSTRACT

Multiphase flow is a common occurrence in the chemical and petroleum industries. The objective of this study was to apply the principles of multiphase flow to the production of petroleum fluids. A unified model was developed to predict the pressure profiles in wellbores using models available in the literature, which was then used to develop a simulator. A rigorous approach was also taken to model heat transfer and predict the temperature profiles in wellbores under various circumstances.

Our model is capable of predicting the pressure profiles for various channel orientation and geometries. It can handle flow in vertical, and inclined system. Countercurrent flow and flow in downward direction can also be simulated. With appropriate value for the parameters, the model applies to liquid-liquid systems in addition to the gas-liquid systems.

The temperature profile in a wellbore is important to the petroleum industry. Fluid temperature determines various properties such as viscosity, density, the extent of dissolved gases etc. The pressure profile depends on these physical properties. In addition, the temperature profile is important in many production operations in arctic regions. A prior knowledge of the temperature and pressure profile enables the operators to take preventive measures against the clogging of pipelines due to hydrate or wax

x

formation. Accurate temperature estimation is also important during such operations as drilling, cementing etc.

Fluid temperature depends on the extent of heat loss from the wellbore, which in turn, depends on the formation temperature. The present approach of temperature estimation assumes a constant heat flux between the wellbore and formation throughout the entire operation time. However, quite often the heat transfer rate between the formation and wellbore changes with time. We used the superposition principle to account for the gradual change of heat flux with time. Analytical solutions with the assumption of invariant and linear variation of heat flux with depth, and numerical solution of the governing differential equation were obtained.

We developed expressions for fluid temperature during production, injection and mud circulation. The results showed variation in the temperature profiles when superposition is used during oil production and in mud circulation compared to solution without superposition. The solutions of linear variation of heat flux with depth assumption were close to the numercial solutions.

CHAPTER 1

INTRODUCTION

Multiphase flow is the simultaneous flow of more than one phase in a single conduit. The phases can be any combination of solids, liquids and gases. Multiphase flow is widely encountered in the petroleum industry and in the chemical process industry. It also occurs in steam generating boilers and nuclear power generators.

Each industry views multiphase flow from its own perspective. The petroleum industry has many unique features that create complications not encountered by other industries. The fluids involved are multicomponent mixtures whose phase behavior is extremely complex. The range of pressure and temperatures encountered in the petroleum industry is also very broad. It has been found that the pressure can range from 15,000 psia to near atmospheric conditions while the temperature can range from 400°F to below the freezing point of water. Pipes used in the production process from the reservoir can be either vertical or inclined. Transportation on the surface use the pipelines that are generally horizontal. Wells producing petroleum crudes can be from few hundred feet to more than 20,000 ft whereas the surface pipe can vary from a few feet to several hundred miles. Piping systems often involve significant variation in geometry, diameter, shape and inclination angle. Although most vertical and inclined systems involves cocurrent upflow,

it is not very uncommon to have downward multiphase flow in injection wells or downcomers connecting offshore platforms to subsea pipelines.

Engineers in petroleum industry are faced with the requirement to predict the relationships between flow rates and pressure drop throughout a reservoirs entire production life under different types of circumstances such as piping geometry, length, diameter, angle of inclination, etc. The pressure drops encountered during the production enter into a wide array of design calculations. The design considerations may include the tubing size and operating wellhead pressure in a flowing well; well completion or recompletion scheme; or artificial lift during gas lift or pump operation in a low energy reservoir. The pressure drop calculations are also needed in various equipment design calculation.

Simulation of multiphase flow in wells also requires the ability to predict fluid temperatures in a system that undergoes complex heat transfer between wellbore and the formation. It is essential to predict the fluid temperature with reasonable accuracy, because temperature determines various fluid properties, including the extent of dissolved hydrocarbon gases, which is a very important parameter in the process. Besides having influence on pressure profile, the temperature profile itself is also very important. For example, a very common problem in the arctic operation is due to the gas hydrate formation. The hydrates are formed at low temperature and high pressure. To design multiphase flow in a gas hydrate prone system, the phase behavior of gas hydrates, which is a function of temperature needs to be considered. Sometimes system pressure, temperature, and water contents are manipulated to avoid the gas hydrate phase envelope.

Heat transfer between the wellbore and formation plays an important role under such circumstances underscoring the importance of temperature prediction.

One of the objectives of this work is to develop a unified two-phase flow model that will be uniquely useful to the petroleum industry. The other important objective is to study some of the complex heat transfer problems encountered in wellbores. We take a rigorous approach to model heat transfer in wellbores with particular attention to appropriate boundary conditions. The models will predict temperature profiles during production, injection, and mud circulation. Superposition principle is used to account for gradual change in heat transfer with time.

CHAPTER 2

THEORY

Understanding the physical behavior of multiphase flow in wells is important because hydrocarbon production, as well as well testing/production logging, often involves the simultaneous flow of two or more phases in wells that have a variety of orientation and geometry. Designing such wells tubulars requires estimation of pressure drop. For existing wells, estimating productivity or designing artificial lift also demands pressure drop calculations.

The importance of multiphase flow in chemical and petroleum industries has led to proposals of many models and correlations for pressure gradient estimation. Most of these models recognize that the in-situ gas velocity is generally higher than the in-situ liquid velocity in up flow. The higher gas velocity is caused by the buoyancy effect and the tendency of the gas phase to flow through the central portion of the channel. The difference between the two phase velocity is called slip. The in-situ gas void fraction is different than the input gas void fraction because of this slip.

The extent of the slip between the phases depend on the various configurations the phases take up depending on the prevailing conditions. These distinctive patterns make the flow pattern approach superior to entirely empirical approaches. The pioneering effort of many workers in this area has made predicting flow pattern transitions quite reliable.

4

In this work the relationships for void fraction in terms of phase velocities and system properties are developed. In developing the models, extensive use is made of the published work in the area. As such, this work is an integration of the present knowledge on flow pattern approach in two-phase flow.

The mechanical energy balance for a flowing fluid over a differential pipe length dz without any energy input, may be written as,

$$\frac{dP}{dz} + \rho_m \frac{g}{g_c}\sin\theta + \frac{2f V_m^2 \rho_m}{g_c D} + \frac{\rho_m V_m}{g_c}\frac{dV_m}{dz} = 0 \qquad (2.1)$$

The last three terms in Equation 2.1 represent the potential energy loss, the friction loss, and the kinetic energy loss respectively. Hence, we may write the total pressure gradient, dP/dz, during single or multiphase flow as the sum of the gravitational (static head, dP/dz$_H$), frictional (dP/dz$_F$) and kinetic head (dP/dz$_A$) components:

$$\frac{dP}{dz} = \left[\frac{dP}{dz}\right]_H + \left[\frac{dP}{dz}\right]_F + \left[\frac{dP}{dz}\right]_A$$

$$= -\frac{1}{g_c}\left[g\,\rho_m \sin\theta + \frac{2f V_m^2}{D} + \rho_m V_m \frac{dV_m}{dz}\right] \qquad (2.2)$$

The problem for two-phase flow is to find an appropriate expression for the mixture density ρ_m and the mixture friction factor f_m. For vertical flow, the static head is the major contributor to the total head loss, and in some cases. (low gas fraction and low flow rates) it may account for more than 95% of the total gradient. Since the mixture density is related to the gas void fraction E_g (in-situ volume fraction of the gas) by.

$$\rho_m \ = \ \rho_g E_g \ + \rho_l (1 - E_g) \qquad\qquad (2.3)$$

Accurate estimation of the void fraction is of paramount importance in multiphase

flow analysis. The frictional head loss also requires an estimate of the mixture density

and, hence, the gas void fraction. The gas void fraction depends on the in-situ velocity

of the gas phase relative to the mixture. The gas phase velocity is influenced by the

buoyancy effect and the tendency of the gas phase to flow through the central portion of

the channel where the local mixture velocity is higher than the average velocity. Both

these effects depend on the particular flow pattern that exists under the given conditions

of flow, pressure and channel geometry. The various models available to estimate the

void fraction and the pressure gradient are discussed in chapter 3 and 4.

Heat transfer in wellbores affects the temperature of the hydrocarbon mixture and,

hence, the bubble point pressure. This in turn affect the gas volume fraction and pressure

drop. Models available at present do not adequately account for heat transfer between the

produced fluid and the formation. In this work, a rigorous approach has been taken to

model heat transfer with particular emphasis on appropriate boundary conditions.

When a liquid is produced from a reservoir, its temperature at the bottomhole may

be assumed to be same as that of the formation. While this is not true of gases, gas inlet

temperature may be estimated from the formation temperature if Joule-Thompson effect

is properly accounted for. Thus the bottomhole temperature of a produced fluid may be

reliably estimated. However, as the fluid rises up the well, its temperature soon becomes

significantly higher than the surrounding earth temperature because of general decline in

earth temperature with decreasing depth. The temperature difference between the

wellbore fluid and earth causes a transfer of heat from the fluid to the surrounding earth, and, therefore the fluid temperature decreases as it goes up. The transferred heat raises up the surrounding formation temperature near the wellbore. So, at any depth, the formation temperature would vary not only with the radial distance from the well, but also with production time. Hence, heat loss from the fluid decreases with time and depends on the various resistances to heat flow between the hot fluid in the tubing and the surrounding earth.

To derive an expression for fluid temperature as a function of depth and time, the formation temperature distribution needs to be established as a function of radial distance and time. An energy balance on the fluid in the wellbore can then be used to relate to the fluid temperature, the wellbore/earth interface temperature, and the heat flux between the formation and wellbore. The details of the energy balances are discussed in chapter 3 and 4.

CHAPTER 3

LITERATURE SURVEY

Design and operation of equipments involving multiphase flow often requires estimates of pressure drop within the equipment. Multiphase flow is much more complicated than single phase flow. The analysis of single phase flow is made easier if it can be established that the flow is either laminar or turbulent and whether any separation or secondary flow effect occurs. This information is equally useful in the multiphase flow, however, the geometry of the flow is of greater importance. The already intricate model developmental problem in multiphase flow is further complicated by complex heat transfer associated in the wellbores. In this chapter, we examine the various approaches presently available to estimate the void fraction and the pressure gradient in the vertical system. We also examine the heat transfer aspects associated in the wellbores.

3.1 Pressure Drop in Two-Phase Flow

Many models and correlations exist to predict pressure drop in vertical and inclined multiphase flow. Some of these were developed from large experimental data bases, relying almost entirely on empiricism. Other are mechanistically based models which are capable of accounting for the various flow patterns associated with the flow.

In this section, we first discuss models based on flow pattern. Then the other major approaches are presented.

3.1.1 Flow Pattern Approach

When multiphase flow occurs, the phases take up a variety of configurations, known as flow patterns. A particular flow pattern depends on the condition of pressure, flow rate, heat flux and channel geometry. Various techniques are available for the study of two-phase flow patterns in heated and unheated channels. In transparent channels at low velocities, it is possible to distinguish the flow patterns by direct visualization. At higher velocities where the pattern becomes indistinct, flash and cine photography can be used to slow the flow down and extend the range. Numerous other ingenious techniques are also in use to examine the flow patterns. In this work only those patterns that are clearly distinguishable and generally recognized will be considered. Four such flow patterns - **bubbly, slug, churn, and annular** are schematically shown in Figure 1.

At low gas flow rates, the gas phase rises through the continuous liquid medium as small discrete bubbles, thus the name bubbly flow. As the gas flow rate increases, the smaller bubbles begin to coalesce forming larger bubbles. At sufficiently high gas flow rates, the agglomerated bubbles become large enough to occupy almost the entire pipe cross section, separated from the pipe wall by a thin liquid film. These large bubbles, known as Taylor bubbles, separate the liquid **slugs** between them. The liquid slugs, which usually contain smaller entrained gas bubbles, give the name of the flow regime. At still higher flow rates the shear stress between the Taylor bubble and the liquid film increases, which finally causes a breakdown of the liquid film and the bubbles. The

| Bubbly | Slug | Churn | Annular |
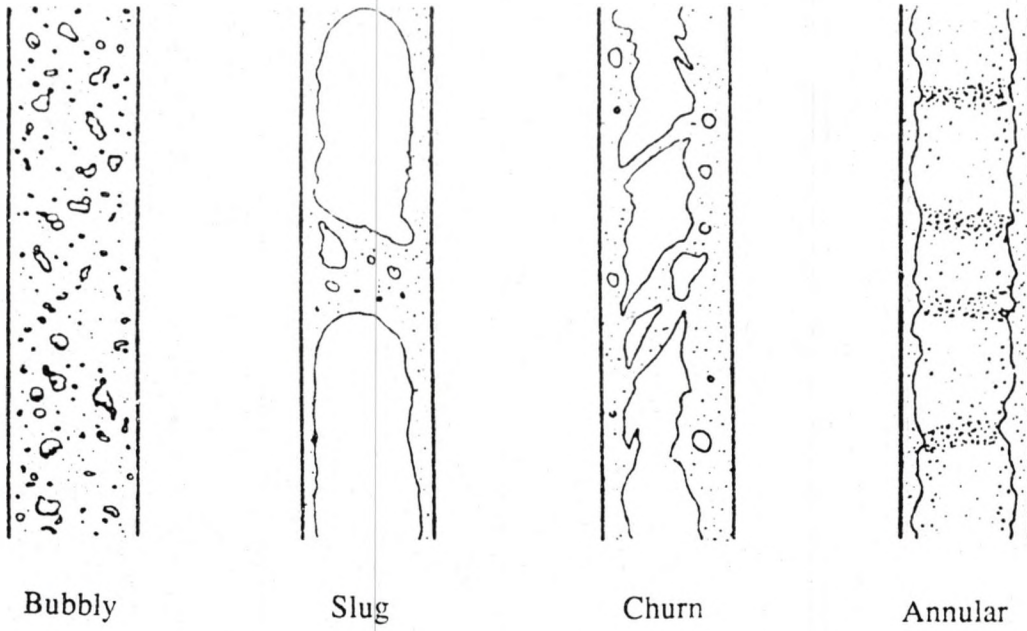
Figure 1. Flow Patterns in vertical co-current flow

resulting **churn**ing motion of the fluids gives rise to the name of this flow pattern. The final flow pattern, **annular** flow, occurs at extremely high gas flow rates which causes the entire gas phase to flow through the central portion of the pipe. Some liquid is entrained in the gas core as droplets while the rest of the liquid flows up the wall through the annulus formed by the tube wall and the gas core. Models presently available for vertical system for the various flow regimes are described below.

3.1.1.A Bubbly Flow

In bubbly flow the gas phase is distributed as discrete bubbles in a continuous liquid phase. At one extreme the bubbles may be small and spherical, and at the other extreme the bubbles may be large with a spherical cap and a flat tail. In this later state, although the sizes of the bubbles do not approach the diameter of the pipe, there may be some confusion with the slug flow.

If it is assumed that during bubbly flow most of the bubbles flow through the central portion of the channel, then the in-situ velocity of the gas phase, V_g, is the sum of the terminal rise velocity, V_t, and the mixture velocity at the channel center. If the central mixture velocity is designated to be C_o times the average mixture velocity, V_m, then it can be written that,

$$V_g = C_o V_m + V_t \qquad (3.1)$$

If the flow is "ideal" bubbly, which is possible at very low gas flow rates and with pure liquids, the bubbles do not affect each other's motion and Equation 3.1 is not strictly valid. In such cases, the Drift Flux model, developed by Ishii (1975), Zuber and Findlay

(1965), Wallis (1969) and others, should be used. Indeed, Equation 3.1, a special form of the Drift Flux model, is valid when the bubbles are affected by the tube wall and the wakes of other bubbles. For most practical systems, fluids are rarely pure and Equation 3.1 is quite appropriate.

Noting that the in-situ velocity, V_g, of the gas phase is equal to the superficial gas velocity divided by the gas void fraction, ($V_{sg} = V_g / E_g$). Equation 3.1 may be rewritten to arrive at the following expression for the gas void fraction,

$$E_g = \frac{V_{sg}}{C_o V_m + V_t} \tag{3.2}$$

For most cases, the terminal rise velocity, V_t, appears to be well represented by the Harmathy (1960) correlation. Hasan and Kabir (1988) also suggests the use of Harmathy correlation.

$$V_t = 1.53 \left[\frac{g \, \sigma \, (\rho_l - \rho_g)}{\rho_l^2} \right]^{0.25} \tag{3.3}$$

Value of the Flow Parameter C_o: Researchers analyzed various mixture velocity profiles and bubble distributions across the channel and arrived at expressions for C_o in terms of the parameters of these profiles. For most practical cases, Reynolds number based on bubble velocity is much greater than 2100. In turbulent flow the mixture velocity at the axis of the pipe is 1.2 times the average mixture velocity. If the gas bubbles are assumed to flow mostly through the central portion of the pipe, as has been shown to be the case for vertical flow, then the value of C_o is 1.2 as established in the classical work of Zuber and Findlay (1965) for an air-water system in a five cm pipe.

Hasan and Kabir recommended 1.2 for the flow parameter C_o to estimate the in-situ gas void fraction during vertical bubbly flow.

Dispersed Bubbly flow : Sometimes at higher flow rates, the turbulence breaks up the larger agglomerated bubbles and the resulting flow pattern is somewhat different than the bubbly flow. This type of bubbly flow which results from the breakdown and dispersion of larger bubbles in the liquid phase is known as dispersed bubbly flow. Under certain circumstances, this is the only type of bubbly flow that can be observed in inclined system. Although slightly different, the equations developed for bubbly flow are also applicable for dispersed bubbly flow.

3.1.1.B Slug Flow

In slug flow, the gas bubbles are approximately the diameter of the pipe and are known as Taylor bubbles. The nose of the bubble has a characteristic spherical cap and the gas in the bubble is separated from the pipe wall by a slowly descending film of liquid. The liquid flow is contained in liquid slugs which separate successive gas bubbles. These slugs may or may not contain smaller entrained gas bubbles carried in the wake of the large bubble. The length of the main gas bubble can vary considerably. The pattern has also been designated by some as plug or piston flow at low flow rates where the gas liquid boundaries are well defined, and as slug flow at higher rates where the boundaries are less clear.

The analysis for slug flow is very similar to that for bubbly flow. Indeed, Equation 3.2 applies for void fraction in slug flow as well, but with different constants.

Assuming there is no bubble in the liquid slug, the void fraction for ideal slug flow becomes,

$$E_{gT} = \frac{V_{sg}}{C_1 V_m + V_{tT}}$$

(3.4)

But slug flow is rarely ideal. The liquid slug contains gas bubbles in it. The cellular approach pioneered by Fernandes et al. (1983) accounts for the bubbles in the liquid slug. Hasan and Kabir simplified the Fernandes et al. (1983) approach to model slug flow. They denoted the in-situ gas fraction in the section with Taylor bubble as E_{gT}, and that in the liquid slug as E_{gs}, and obtained the following expression for average void fraction,

$$E_g = \left[\frac{L_T}{L_C}\right] E_{gT} + \left[\frac{L_S}{L_C}\right] E_{gs}$$

(3.5)

The terms L_s/L_C and L_T/L_C can be calculated from the following expressions,

$$E_g = \left[\frac{L_T}{L_C}\right] E_{gT} + 0.1 \qquad for \quad V_{sg} > 0.4 \quad m/s$$

$$E_g = \left[\frac{L_T}{L_C}\right] E_{gT} + 0.25 \, V_{sg} \qquad for \quad V_{sg} \leq 0.4 \quad m/s$$

(3.6)

Because the flow is almost surely turbulent, and the bubbles ride through the flat portion of the velocity profile, C_1 (as C_o in bubbly flow) is expected to be 1.2. This is
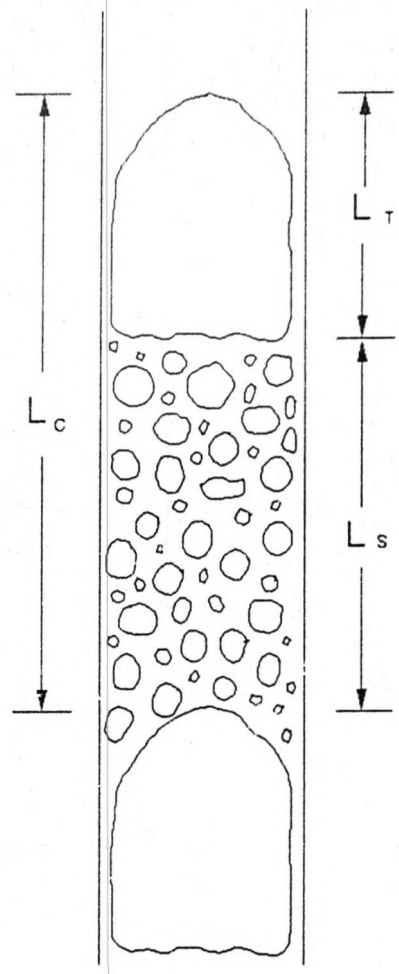
Figure 2.   A Model Cell in Slug Flow

indeed found to be the case by Nicklin et al. (1962), Hasan and Kabir (1988) and others

and 1.2 is the accepted value for the parameter.

The Taylor bubble rise velocity, V_{tT}, in slug flow is given by Nicklin (1962),

$$V_{tT} = C_2 \sqrt{gD \left[\frac{\rho_l - \rho_g}{\rho_l} \right]} \quad \propto \quad C_2 \sqrt{gD} \tag{3.7}$$

Extensive data and theoretical analyses by a number of researchers indicate that

C_2 is influenced by the forces of inertia, viscosity, and surface tension. The data of

White and Beardmore (1962), along with those of Dumitrescu (1943) have been

represented by the following single equation by Wallis (1969),

$$C_2 = 0.345 \left[1 - e^{-\frac{0.01 Nf}{0.345}} \right] \left[1 - e^{\frac{3.37 - Eo}{m}} \right] \tag{3.8}$$

where Nf is the dimensionless inverse viscosity number, $\sqrt{\{D^3 g(\rho_l - \rho_g)\rho_l / \mu_l\}}$, Eo is the

Eotvos number, $gD^2(\rho_l - \rho_g)/\rho$, and m is a parameter dependent on Nf. The value of m

is 10 when Nf is greater than 250, is 25 when Nf is less than 18 and is given by m =

69 $(Nf)^{-0.35}$ for 18 < Nf < 250. For large values of Nf (say >300) and Eo (>100),

Equation 3.8 reduces to $C_2 = 0.345$. For air-water flow through a 5 cm pipe at standard

conditions, Nf = 35000 and Eo = 322. Thus, for many practical systems (if diameter is

not too small) $C_2 = 0.345$

3.1.1.C   Churn Flow

Churn flow is formed by the breakdown of the large gas bubbles in slug flow.

The gas or vapor flows in more or less chaotic manner through the liquid, which is

mainly displaced to the channel wall. The flow has an oscillatory or time varying character; hence the descriptive name **churn** flow. This region is also sometimes referred to as semi-annular, annular-slug transition or froth flow (Govier-Aziz (1972), Aziz-Govier-Fogarasi (1972))

The churn or froth flow pattern has not been investigated extensively because of its chaotic nature. However, the analyses presented for bubbly and slug flow should also be applicable for the churn flow pattern. Thus the equation developed for predicting void fraction in slug flow (Equation 3.7) may be used for the churn flow regime as well. Although the bubble shape is quite different from the classical Taylor bubble, the bubble rise velocity during churn flow is probably not much different from that for slug flow. In addition, because the mixture velocity is much higher than the bubble rise velocity during churn flow, a slight error in estimating V_{tT} does not significantly affect void fraction estimation. On the other hand, an accurate estimate of the flow parameter C_1 is very important for predicting void fraction. The bubble concentration profile in churn flow is unlikely to be similar to that for slug flow because of the churning motion characteristic of this flow regime. Hasan and Kabir suggested a value of 1.15 for the parameter C_1. In this work we use Equation 3.5 and $C_1 = 1.15$ for the estimation of void fraction in churn flow.

3.1.1.D Annular Flow

In annular flow, the gas phase along with the entrained liquid droplets, flows through the core of the channel forming a continuous phase. The liquid phase is dragged along the pipe wall and appears to flow through the annulus formed by the channel wall

and the vapor core; hence the name annular flow. Large amplitude coherent waves are usually present on the surface of the liquid film and the continuous break-up of these waves forms a source for droplet entrainment, which occurs in varying amounts in the central gas core. The droplets are separate rather than agglomerated.

In ideal annular flow, when no liquid is being carried as droplets in the gas phase and the gas-liquid interphase is smooth, the estimation of pressure drop in annular flow reduces to that of estimating pressure drop in single phase gas flow. The liquid film thickness is typically less than 5 % of the tube diameter, thus introducing little error even if it is neglected in calculating the channel diameter for gas flow.

Unfortunately, however, annular flow is rarely ideal. Usually, a substantial fraction of the liquid is carried as droplets in the gas stream requiring estimation of the mixture density. In addition, the gas-liquid interface is usually wavy and determining the appropriate friction factor becomes very difficult.

The following equation may be used for the total pressure gradient during annular flow noting that V_g replaces V_{sg}.

$$-\frac{dP}{dz} = \frac{1}{g_c}\left[\frac{2f_f V_g^2 \rho_c}{D} + g\rho_c + \rho_c V_g \frac{dV_g}{dz}\right] \qquad (3.9)$$

The acceleration term in this equation contains the differential dV_g/dz. This term can be rewritten in terms of dP/dz and V_g using the gas law and thereby Equation 3.9 becomes

The problem then reduces to that of estimating the density of the fluid in the core, ρ_c, and estimating the friction factor f_f. To determine the density of the fluid flowing

$$-\frac{dP}{dz} = \frac{1}{g_c} \left[\frac{\frac{2 f_f V_g^2 \rho_c}{D} + g \rho_c}{1 - \frac{\rho_c V_g^2}{P g_c}} \right] \tag{3.10}$$

through the core it is necessary to estimate the entrainment. Hasan and Kabir (1988) recommended the following correlations proposed by Wallis and Steen (1964) for the estimation of entrainment.

$$E = 0.0055 \left[10^4 (V_{sg})_c \right]^{2.86} \qquad if \quad 10^4 (V_{sg}) < 4$$

$$E = 0.857 \log_{10} \left[10^4 (V_{sg})_c \right] - 0.20 \qquad if \quad 10^4 (V_{sg})_c > 4 \tag{3.11}$$

A number of correlations are available for predicting the film friction factor f_f. Hasan and Kabir (1988) recommended the one proposed by Wallis (1969), which probably is the best among these.

$$f_f = f_g \left[1 + 75 (1 - E_g) \right] \tag{3.12}$$

Some rigorous models, which incorporate velocity profile in the liquid and gas core have been developed in recent years. Considering the rarity of this flow regime in oilwell and the complexity of those models, we use the simple approach presented here.

3.1.1.E Transition criteria

The individual models discussed so far enables us to estimate void fraction and the pressure gradient once the flow pattern is established. But it is very difficult to

correctly determine exactly when transition from one flow pattern to another takes place. One reason behind this problem is the lack of agreement in the description of the flow pattern. Besides, the transition does not occur abruptly. In most cases gradual transition from one pattern to another is observed.

Bubbly-Slug Transition. Transition from the condition of small bubbles dispersed throughout the flow cross-section to the condition when the bubbles become large enough to fill almost the entire pipe cross-section, requires a process of agglomeration or coalescence. In general, bubbles, other than very small ones, follow a zig-zag path when rising through the liquid. This results in collision between the bubbles, with consequent bubble agglomeration and formation of larger bubbles. Obviously, collision frequency and bubble agglomeration increases with increasing gas flow rates. Radovich and Moissis (1962) theoretically examined the behavior of bubbles by considering a cubic lattice in which the individual bubbles fluctuate. It was found that at a void fraction of 0.3, the collision frequency becomes so high that a transition to slug flow is to be expected. Griffith and Snyder (1964) experimentally verified that the transition occurs at a void fraction of 0.25 to 0.3. Hasan and Kabir also found the transition to take place at a void fraction of about 0.25.

Thus $E_g = 0.25$ may be taken as the criteria for transition between bubbly and slug flow. This criteria when expressed in terms of the superficial velocities by equating the slip between the phases with the terminal rise of a single bubble then the relationship between V_{sg} and V_{sl} at the transition becomes.

$$V_{sg} = 0.429 \ V_{sl} + 0.357 \ V_t \qquad\qquad (3.13)$$

Since the transition from bubbly to slug flow is likely to be gradual, it is unlikely, although assumed in deriving the above equation that the void fraction relationship for bubbly flow would be applicable up to the point of transition. The appropriate expression in slug flow is similar to that of the bubbly flow with only exception in bubble rise velocity. However, the difference between V_{tT} and V_t is not large and the above equation is adequate in representing the transition between bubbly and slug flows.

Dispersed Bubbly Flow : The transition criteria discussed above applies only at low or moderate flow rates. At higher flow rates, the turbulence breaks up the larger agglomerated bubbles and inhibits transition to slug flow. The bubbly flow may persist even when the void fraction exceeds 0.25 in this case. Taitel et al. (1980) analyzed the onset of dispersed bubbly flow based on the maximum bubble diameter possible under highly turbulent conditions. They concluded that if the turbulence is high enough so that the bubbles are smaller than the critical diameter, agglomeration is suppressed and bubbly flow continues. They derived the following minimum mixture velocity for dispersed bubbly flow.

$$V_m = 4 \ (D)^{0.43} \left[\frac{(\rho_l - \rho_g) g}{\sigma} \right]^{0.446} \left[\frac{\rho_l}{\mu_l} \right]^{0.072} \left[\frac{\sigma}{\rho_l} \right]^{0.446} \qquad\qquad (3.14)$$

If the mixture velocity is higher than that given by the above equation, bubbly flow will persist even if the void fraction is higher than 0.25. However, it was found that

bubbly flow can not persist above a void fraction of 0.52. At higher void fractions, transition to either slug or churn flow will occur.

Slug-Churn Transition. A characteristic of slug flow is the liquid confined between the Taylor bubble and the tube wall. This liquid flows around the bubble as a falling film. The interaction between this falling film and the Taylor bubble increases with increasing flow rate. The upper limit of slug flow occurs when the interaction becomes high enough to break up the bubbles, causing transition to churn flow.

The most promising model for this transition appears to be the one proposed by Brauner and Barnea (1986). They analyzed the condition of the liquid slug following the Taylor bubble just before the transition to churn flow takes place. The normal upper limit of local gas void fraction in the liquid slug is about 25%, because at higher gas fraction, the smaller bubbles coalesce to give rise to more Taylor bubbles. If the mixture velocity is high enough for dispersed bubbly flow, the local in-situ gas volume fraction in the liquid slug could attain a maximum value of 52%. Thus Brauner and Barnea argue that the transition to churn flow occurs when the void fraction in the liquid slug, which would be approximately the same as the average void fraction in the pipe, is over 52% and the mixture velocity is high enough to sustain dispersed bubbly flow. They assumed that at high flow rates void fraction may be approximated by input volume fraction so that $E_g = V_{sg}/V_M$. Hence at transition from slug to churn flow,

$$\frac{V_{sg}}{V_{sg} + V_{sl}} > 0.52 : \quad Hence, \quad V_{sg} > 1.08 \, V_{sl} \tag{3.15}$$

Transition to Annular Flow. At high gas flow rates, transition from churn and slug flow to annular flow takes place. The liquid flows upward along the tube wall, while the gas flows through the center of the tube. The liquid film has a wavy interface and the waves could break away and be carried away as entrained droplets.

One approach to study the transition from churn (or slug) to annular flow is by analyzing the minimum gas flow rate required to reverse the direction of flow of a falling liquid film (Wallis (1969), Jones and Zuber (1978)). Another approach, adapted by Taitel et al. (1980), is to examine the drag force necessary to keep the entrained liquid droplets in suspension during annular flow. When the gas velocity is not sufficient to keep the liquid droplets in suspension, the droplets will fall back, accumulate, form a bridge, and finally establish churn or slug flow. The minimum velocity required to keep the droplets in suspension may be determined from a balance of the drag forces on these droplets and the gravitational forces acting on them

$$V_g = \frac{2}{\sqrt{3}} \sqrt{\frac{g(\rho_l - \rho_g)d}{\rho_g C_d}} \tag{3.16}$$

Substituting the droplet diameter d in the above equation by the maximum stable drop size, Taitel et al. (1980) arrived at the following minimum gas velocity for transition to annular flow:

$$V_{sg} = 3.1 \left[\frac{g \, \sigma (\rho_l - \rho_g)}{\rho_g^2} \right]^{0.25} \tag{3.17}$$

3.1.2   Other Approaches

A number of procedures have been reported in the petroleum engineering literature that attempts to predict pressure drop in vertical wells over a broad range of multiphase flow conditions. Four overall predictive schemes are described below because these are well known to the petroleum engineers. They are due to (1) Orkiszewski (1967), (2) Aziz, Govier and Fogarasi (1972), (3) Duns and Ros (1963), and (4) Beggs and Brill (1973).

3.1.2.A   Orkiszewski Method

In 1967, Orkiszewski examined the available correlations for predicting multiphase pressure drop in vertical wells in light of data from 148 wells. He proposed a composite method based on the flow pattern approach. He recognized four different flow patterns - bubbly, slug, transition (churn) and mist (annular). To estimate void fraction and pressure drop in bubbly flow, he accepted the suggestion of Griffith and Wallis (1961). The bubbly to slug flow transition is also given by Griffith and Wallis (1961), while the transition from slug to churn and churn to annular is given by the criteria suggested by Duns and Ros (1963).

The Orkiszewski method was an improvement over the methods generally used in the petroleum industries. At present, however, simpler models with better theoretical basis and greater accuracy are available.

3.1.2.B Aziz, Govier and Fogarasi Method

In 1972, Aziz et al. presented a procedure for predicting pressure drop in vertical oil wells by combining the available literature in the area. The method used the flow pattern map of Govier et al (1957). It restricts itself in developing a prediction procedure for bubbly and slug flow only, perhaps because of the rarity of the other two patterns in oil wells.

The Aziz et al. model is somewhat similar to the Hasan Kabir model. The difference between the prediction and actual data in the bubbly flow regime is slight, but the difference is large in slug flow, when the taylor bubble rise velocity is different from the terminal rise velocity of small bubbies. Moreover, this method neglects the acceleration term in the estimation of total pressure gradient.

3.1.2.C Duns and Ros Method

In the early sixties, Ros (1961) and Duns and Ros (1963) developed a general empirical correlation from a large set of laboratory data. The method is flow regime based, but the regime definitions are somewhat different from present standard definitions. They define region I as the flow regime where the liquid is the continuous phase, and hence, include bubble, froth (presumably dispersed bubbly), plug, and some slug flow. Region II covers situations when neither phase is continuous, and hence, include the rest of the slug flow and froth flow as well as 'heading' (or pulsating flow). When gas becomes the continuous phase, as in annular-mist flow, it is termed region III. Duns and

Ros also include a transition region (probably corresponding to churn flow) between Region II and Region III. The prediction by this method is quite accurate. However, its drawback is its non-standard flow pattern descriptions and transition criteria. It also contains a large number of empirically determined constants and its entirely empirical nature makes interpolation and extrapolation risky.

3.1.2.D Beggs and Brill Method

The classical study of Beggs and Brill probably gives the most comprehensive method available for predicting void fraction and pressure drop in inclined systems. Their correlation is based on a predictive method for the horizontal system and modifications to account for the inclination of the system. For estimating liquid holdup for a horizontal system, $E_{l,90}$ (= in situ liquid fraction = $1 - E_{g,90}$), they propose the following equation in terms of mixture Froude number, Fr_m (= V_m^2/gD) and the input liquid volume fraction E_{li}.

$$E_{l,90} = a \frac{E_{li}^b}{(Fr_m)^c} \qquad (3.18)$$

The values of the parameters a, b and c depend on the flow regime. For inclined systems, Beggs and Brill use the holdup calculated by Equation 3.18 and multiplies it by an inclination factor, $F(\theta)$. The value of the multiplier depends upon the pipe inclination, input liquid fraction, dimensionless liquid velocity number, the Froude number and the flow pattern that would exist in a equivalent horizontal system.

The predictions of the Beggs and Brill correlation are usually good for inclined systems. However, the complications involved in the calculation procedure and the methods exclusive reliance on empiricism, makes it less than completely satisfactory. One problem with the correlation is that liquid input fraction, E_{li}, is used to determine the horizontal flow pattern and the correction factor, $F(\theta)$. For stagnant liquid columns, when E_{li} is zero, the method cannot be used, and for small values of E_{li}, the predictions of the method would be unreliable.

3.2 Heat Transfer in Wellbores

The importance of various aspects of heat transfer between a wellbore fluid and the earth has generated a rich literature on the subject. The usefulness of fluid temperature measurement was pointed out as early as 1937 by Schlumberger et al. (1937). Fluid temperature depends on heat loss from the wellbore to the surrounding formation. The formation temperature distribution around a well was first modeled by Ramey (1962). He neglected the effect of kinetic energy and friction, and the model was applicable only to the flow of single phase fluids. Moreover, his assumption of a vanishingly small well radius in solving the formation temperature distribution proved untenable in some cases. Many other researchers have suggested various procedures for estimating wellbore fluid temperature. The following section discusses one such model, with appropriate initial and boundary conditions.

3.2.1 Formation Temperature Distribution

Heat diffusion in a three-dimensional solid may be mathematically treated as a two-dimensional problem if symmetry around the heat source (or sink) is assumed, as in the case of a producing or an injection well. In addition, if small increment of the vertical direction of the well is considered, the problem simplifies to one-dimensional heat diffusion, because vertical heat diffusion can be ignored due to small vertical temperature gradient. This approach proposed by Hasan and Kabir (1991) has been adapted in this work. It introduces very little error and allows analytical solution of the problem which is often preferable to the alternative of tedious and time consuming numerical solution. A number of interesting heat conduction problems of similar nature was earlier presented by Carslaw and Jaeger (1950).

In a short time-step, the heat flux from the wellbore may be assumed to remain constant at a given depth. An energy balance on the formation then leads to the following partial differential equation derived in cylindrical coordinates for the variation of formation temperature with radial distance from the well and time of production:

$$\frac{\partial^2 T_e}{\partial r^2} + \frac{1}{r}\frac{\partial T_e}{\partial r} = \frac{c_e \rho_e}{k_e}\frac{\partial T_e}{\partial t} \qquad (3.19)$$

where T_e is the temperature of earth at time t and radial distance r measured from the center of the wellbore. c_e, ρ_e and k_e are the heat capacity, density and thermal conductivity of formation. This equation is analogous to the pressure diffusion equation as used in the pressure transient literature.

Initially, formation temperature at any given depth is constant, leading to the following condition,

$$\underset{t \to 0}{Lim}\; T_e = T_{ei} \qquad\qquad (3.20)$$

At the infinite or outer boundary, formation temperature does not change with radial distance, i.e.,

$$\underset{r \to \infty}{Lim}\; \frac{\partial T_e}{\partial r} = 0 \qquad\qquad (3.21)$$

The other boundary condition is derived from the heat flow rate at the interface of wellbore and the formation, which is governed by Fourier's law of heat conduction. Rate of flow of heat per unit mass of wellbore fluid per unit length of the well, ϕ, is then given by,

$$\phi = - \frac{2 \pi k_e}{W} \frac{r\, \partial T_e}{\partial r} \bigg|_{r\ at\ wellbore} \qquad\qquad (3.22)$$

where W is the wellbore fluid mass flow rate, and r_{wb} is the outer radius of the wellbore.

To facilitate solution and to have more general applicability of the solution, the above equations were first recast in dimensionless variables and the solution was carried out using Laplace transformation (Lok (1991), Hasan and Kabir (1991)). The analysis resulted in the following expression for formation temperature as a function of radial distance and time.

The above equation shows that the computation of formation temperature requires evaluation of an integral involving modified Bessel function of zero and first order over

$$T\ (r_D, t_D)\ =\ T_{ei}\ +\ \frac{\phi}{\pi^2\ k_e}\ I$$

$$where,\quad I = \int_0^\infty \frac{1 - e^{-u^2 t_D}}{u^2}\ \frac{Y_1(u) J_0(ur_D) - J_1(u) Y_0(ur_D)}{J_1^2(u) + Y_1^2(u)}\ du \qquad (3.23)$$

the limits of zero to infinity for the dummy variable, u. Such computations are time consuming. Hasan and Kabir found that the following expressions approximate the actual solution quite reasonably.

$$T_D = 1.1281\sqrt{t_D}\left[1 - 0.3\sqrt{t_D}\right] \qquad\qquad if\ t_D \le 1.5$$

$$T_D = \left[0.4063 + 0.5\ln(t_D)\right]\left[1 + \frac{0.6}{t_D}\right] \qquad if\ t_D > 1.5 \qquad (3.24)$$

where ,

$$t_D \equiv \frac{\alpha t}{r_{wb}^2}\ ;\qquad\qquad T_D \equiv -\frac{2\pi k_e}{W \phi}(T_{wb} - T_{ei}) \qquad (3.25)$$

3.2.2 Wellbore Fluid Energy Balance

Heat loss experienced by the fluid as it flows up the well results in lowering of its temperature. An energy balance on the fluid may be done following any standard text on thermodynamics. Ramey (1962) made an energy balance on the fluid by assuming single-phase flow. Hasan and Kabir developed a more rigorous balance for a differential length dz, for a two-phase system.

$$\frac{dH}{dz} + \frac{g \sin\theta}{g_c J} + \frac{V}{g_c J}\frac{dV}{dz} = \frac{dq}{dz} = \phi \tag{3.26}$$

where g_c and J represent appropriate conversion factors.

Fluid enthalpy, H, depends on its pressure and its temperature, which allows to write the following expression for dH/dz,

$$\frac{dH}{dz} = \left(\frac{\partial H}{\partial P}\right)_{T_f}\frac{dP}{dz} + \left(\frac{\partial H}{\partial T_f}\right)_P\frac{dT_f}{dz}$$

$$= -C_J c_p\frac{dP}{dz} + c_p\frac{dT_f}{dz} \tag{3.27}$$

where C_J is the Joule-Thompson coefficient and c_p is the heat capacity of the fluid at constant pressure. Combining Equations 3.26 and 3.27,

$$\frac{dT_f}{dz} = \frac{1}{c_p}\frac{dH}{dz} + C_J\frac{dP}{dz}$$

$$= C_J\frac{dP}{dz} + \frac{1}{c_p}\left[\phi - \frac{g \sin\theta}{g_c J} - \frac{V}{g_c J}\frac{dV}{dz}\right] \tag{3.28}$$

The radial heat transfer between the fluid and the surrounding earth may be expressed in terms of an overall heat transfer coefficient following any standard text on heat transfer (McAdams, 1942) or on transport phenomena (Bird, Stewart, and Lightfoot, 1960). Ramey (1962) and Willhite (1967) presented detailed discussions which lead to the following equation for heat transfer rate, ϕ. and the wellbore temperature, T_{wb} ,

$$\phi = -\frac{2\pi r_{to} U_{to}}{W}(T_f - T_{wb}) \qquad (3.29)$$

The overall heat transfer coefficient based on tubing outside surface area, U_{to}, depends on resistance to heat flow from the tubing fluid to the surrounding earth and is discussed in detail in the appendix. In general, resistances to heat flow through the tubing or casing metal may be neglected. Usually natural convection is considered as the dominant heat transfer mechanism for the fluid in annulus. Resistance through the cement layer can be important depending on its thickness.

Using the definition of dimensionless temperature, T_D, in Equation 3.21, an expression for heat transfer from the wellbore/earth interface to the earth can be obtained,

$$\phi = -\frac{2\pi k_e}{W T_D}(T_{wb} - T_{ei}) \qquad (3.30)$$

Combining Equations 3.29 and 3.30 to eliminate the wellbore temperature, T_{wb},

$$\phi = -\frac{2\pi}{W}\left[\frac{r_{to} U_{to} k_e}{k_e + T_D r_{to} U_{to}}\right](T_f - T_{ei}) \qquad (3.31)$$

3.2.3 Wellbore Fluid Temperature Distribution

Hasan and Kabir (1991) obtained an expression for variation of fluid temperature with well depth by substituting the expression for ϕ from Equation 3.31 into Equation 3.28.

$$\frac{dT_f}{dz} = \frac{T_{ei}-T_f}{A} - \frac{g}{g_c}\frac{\sin\theta}{Jc_p} + C_J\frac{dP}{dz} - \frac{V\,dV}{g_cJc_p} \tag{3.32}$$

$$where, \quad A = \frac{c_pW}{2\pi}\left[\frac{k_e+(r_{to}U_{to}T_D)}{r_{to}U_{to}k_e}\right] \tag{3.33}$$

The undisturbed earth temperature, T_{ei}, is generally assumed to vary linearly with depth. Thus,

$$T_{ei} = T_{eibh} - g_T z \tag{3.34}$$

where g_T represents the geothermal gradient and T_{eibh} is the undisturbed (static) earth temperature at the bottomhole. Even when different geologic formations are encountered at various depths, the computation may be divided into a number of zones with constant geothermal gradient being applied to each zone. If we assume that the sum of the last two terms in Equation 3.32 does not vary with well depth then Equation 3.32 becomes a linear differential equation,

$$\frac{dT_f}{dz} = \frac{T_{ei}-T_f}{A} - \frac{g}{g_c}\frac{\sin\theta}{Jc_p} + \sigma$$

$$where \quad \sigma = C_J\frac{dP}{dz} - \frac{V\,dV}{g_cJc_p} \tag{3.35}$$

Equation 3.35 may be integrated for a constant A and appropriate boundary conditions. Thus, for a producing well at the bottomhole condition ($z = z_{bh}$), fluid and earth

temperatures are generally known ($T_f = T_{fbh}$, and $T_{ei} = T_{eibh}$), giving the following expression for fluid temperature as a function of well depth and production time,

$$
T_f = T_{ei} + A \left(-\frac{g}{g_c} \frac{\sin\theta}{J c_p} + \sigma + g_T \right)
$$

$$
+ e^{(z_M - z)/A} \left[T_{fwh} - T_{ewh} + A \left(\frac{g}{g_c} \frac{\sin\theta}{J c_p} - \sigma - g_T \right) \right] \qquad (3.36)
$$

The value of the parameter, σ, used in Equation 3.36 would depend on a number of variables such as flow rates, gas/liquid ratio, wellhead pressure, etc. In their work, Hasan and Kabir used the empirical expression for σ developed by Sagar et al. (1989). It should be pointed out that Equation 3.35 may be integrated for other conditions also. For example, for an injection well the wellhead fluid and earth temperatures are used as boundary conditions. In addition, for gas-lift with gas injection at known depths, or formations with numerous zones with different properties, such as geothermal gradients or conductivities. Equation 3.35 may also be integrated separately for each section, using the fluid temperature calculated at the previous section as the input for the next one.

CHAPTER 4

PROPOSED APPROACH

One of the objective of this work is to develop a multiphase flow simulator which can predict pressure profile under different type of circumstances. This thesis uses the basic model of Hasan and Kabir which has been described in chapter 3. In the first section of this chapter, we describe modifications that are needed to use the basic model for other systems. The second and third sections deal with the heat transfer aspects in the wellbores. The concept of varying heat flux is introduced first and then its application to different systems are discussed.

4.1 Unification of Two-Phase Flow Model

We have already discussed the Hasan-Kabir model to estimate the void fraction and pressure drop when the flow is in the vertical upward direction. In the following three sections, we show how the same model with some modifications can be used for the inclined systems, liquid-liquid systems, countercurrent systems, systems where flow is in downward direction and also to the conduits other than conventional circular ones.

4.1.1 Inclined Flow

The proposed unified model utilizes the flow pattern approach of Hasan and Kabir with modification for the system deviation from vertical orientation. It should be noted that for annular and dispersed bubbly flow the flow rates are very high. Consequently, the influence of buoyancy is small, and hence the effect of pipe inclination is negligible. Therefore, for the annular and the dispersed bubbly flow regimes, the relationships developed for vertical system can be used without any modification. However, this two flow patterns are not very common in petroleum production. This leaves the bubbly and intermittent flow patterns, for which the predictive scheme is described below.

Bubbly Flow. The procedure for estimating void fraction, and pressure drop in inclined system, is similar to the vertical flow. However, we would need values of flow parameter C_o and bubble rise velocity V_t for an inclined system. For vertical systems, we are able to reason that the value of flow parameter C_o should be 1.2 because the flow is turbulent and the bubbles ride the central portion of the channel where the mixture velocity is 1.2 times the cross-sectional average velocity. One would expect the value of the parameter C_o to be influenced by the deviation of the pipe, since the bubble concentration profile would be affected by the pipes inclination. But, this effect has been experimentally observed to be very small, and the value of C_o has been generally found to be 1.2 . In addition, the bubble rise velocity has been found to remain unchanged with pipe inclination.

In a vertical system, the transition from bubbly to slug flow occurs at a void fraction of about 0.25. This criteria for the transition from bubbly to slug flow should also be applicable to inclined systems. However, in an inclined pipe the gas phase tends to flow along the upper wall of the pipe, thereby increasing the actual local void fraction. Conceivably, this local void fraction in the upper section of the channel may exceed 0.25, even when the cross-sectional average void fraction is much smaller than 0.25. As a result, in an inclined pipe transition to slug flow occurs at a cross- sectional average void fraction of less than 0.25.

For vertical systems, void fraction in bubbly flow is given by,

$$E_g = \frac{V_{sg}}{C_o(V_{sl} + V_{sg}) + V_t} \tag{4.1}$$

This relationship may be applied locally in the case of an inclined pipe if the actual superficial velocity of the gas phase at the upper section of the pipe is used rather than the cross-sectional average value. In an inclined pipe, it is reasonable to assume that the actual cross-sectional area available for the gas to flow is the projection of the cross-sectional area on a horizontal plane. The local superficial velocity of the gas phase therefore, is $(V_{sg})_{loc} = q_g/A \sin \theta = V_{sg}/\sin \theta$. Using $(V_{sg})_{loc}$ in place of V_{sg} in the void fraction relationship, we obtain the local void fraction at the upper portion of the pipe wall, $E_{g, loc}$,

$$E_{g,loc} = \frac{[V_{sg}/\sin \theta]}{C_o[V_{sl} + (V_{sg}/\sin \theta)] + V_t} \tag{4.2}$$

Rearranging and using $E_g = 0.25$ and $C_o = 1.2$ at transition,

$$V_{sg} = \left[0.43\, V_{sl} + 0.357\, V_t \right] \sin \theta \tag{4.3}$$

Slug Flow. Hasan and Kabir (198?) found that their model for vertical upward flow can be used for inclined systems with some modifications. The models remain almost the same, but value of some of the parameter changes. The value of C_1 in vertical flow, was taken as 1.2. Experimental verification of this value for C_1 for inclined systems has been provided by Patel (1986). However, the terminal rise velocity of a Taylor bubble is significantly influenced by the pipe inclination. This fact is evident from the classical work of Runge and Wallis (1965) and Zukoski (1966). Their data generally indicate that the Taylor bubble rise velocity increases with increasing deviation of the pipe from vertical, until a maximum is reached for a deviation angle of about 50°. The terminal rise velocity then gradually decreases with increasing deviations and finally becomes zero for horizontal systems.

An expression for the rise velocity of a bubble may be derived by balancing the buoyancy force against the drag force experienced by a rising bubble. Such an expression for the rise velocity of a Taylor bubble in an inclined pipe, $V_{tT\theta}$, can be derived in the in terms of the rise velocity in a vertical pipe, V_{tT}, and the angle of inclination θ.

$$V_{tT\theta} = V_{tT} \sqrt{ (\sin \theta)(1 + \cos \theta)^{1.2} } \tag{4.4}$$

4.1.2 Downward Flow

Downward simultaneous flow of gas and liquid, although less common than two-phase up-flow, is important in chemical process industries and petroleum crude production. Wet steam injection into high viscosity oil bearing formations is an example of the two phase down-flow. As in the up-flow, the static head is quite often the major contributor to the total head loss, especially for vertical and near vertical systems. Consequently, an accurate estimation of gas void fraction, E_g, is required because the mixture density is related to the void fraction.

For up-flow, the effect of buoyancy and the tendency of the gas phase to flow through the channel center causes in-situ gas velocity to be higher than the mixture velocity. For down-flow, buoyancy will oppose the downward flow of the gas phase. The cross-sectional distribution of the gas phase in the channel may also be different from that in the up-flow. The effect of buoyancy and bubble distribution across the flow channel also depend on the existing flow pattern. The relationship for void fraction in terms of phase velocities and system properties and the upper limit for the flow regime is described in this section.

Bubbly Flow. Equation 4.1 would also apply to downward bubbly flow in vertical and inclined systems. But, because in downward flow the terminal rise velocity acts opposite to the direction of flow, the expression for void fraction can be written as,

$$E_g = \frac{V_{sg}}{C_o(V_{sl} + V_{sg}) - V_t} \tag{4.5}$$

Hasan (1989) found that the Harmathy correlation applicable to the bubble rise velocity in both vertical and inclined pipes. He also found that a value of 1.2 for the flow parameter C_o to agree with the data of Mukherjee (1978) and Beggs (1972). The same value has been used in this work.

The transition from bubbly to slug flow has been found to occur at a void fraction of about 0.25 in upward flow. This criteria would apply to downward flow as well. Using a void fraction of 0.25 Hasan and Kabir arrived at the following expression,

$$V_{sg} = \left[0.43 V_{sl} - 0.36 V_t \right] \sin \theta \qquad (4.6)$$

Slug Flow. Slug flow is characterized by a Taylor bubble that fills up almost the entire pipe cross-section followed by a liquid slug that contains small gas bubbles. Hasan (1989) simplified the cellular approach of Hasan and Kabir (1988) for vertical up-flow for adaptation to down-flow. The analysis is similar to that of up-flow, except that the terminal rise velocity acts opposite to the mixture flow direction.

Taylor Bubble Rise Velocity : In upward flow the variation in Taylor bubble rise velocity with pipe inclination has been given by Hasan and Kabir. The same expression can be successfully used in downward flow.

Flow Parameter C_o: Hasan (1989) tried different values for the parameter C_o to fit the experimental data of Mukherjee (1978). It was been found that $C_o=1.12$ serves the purpose quite reasonably. Therefore, a constant value of 1.12 for C_o has been used for the downward slug flow in this model.

4.1.3 Flow in Different Geometries

The majority of two-phase flow occurs in circular conduit. But flow through other geometries, especially through annuli is very common. This section deals with the flow pattern transition and void fraction estimation in non-circular channels.

Flow Through Annuli. The presence of an inner tube does not appear to influence the bubble concentration profile in bubbly flow. The value of the flow parameter C_o, for annuli has been found to remain essentially the same as that for the circular channel. Bubbly-slug transition was found to take place at the same void fraction of 0.25 in the annular geometry. Thus, the transition criteria remains the same as that of circular channels. The dispersed bubbly model described for the circular channels applies to the annuli also.

Although the presence of a inner tube does not affect the bubbly or dispersed bubbly flow, but a significant effect is found in slug flow. The nose of the Taylor bubble becomes sharper which causes an increase in the rise velocity V_{tT}. We use the following expression suggested by Hasan and Kabir for estimation of Taylor bubble rise velocity.

$$V_{tTa} = \left[0.345 + 0.10 \, (D_i/D_o) \right] \left[\sqrt{g \, D_o \, (\rho_l - \rho_g)/\rho_l} \right] \qquad (4.7)$$

where D_i and D_o represents the tube and annular diameter.

Sadatomi et al. (1982) defined 'Equi-peripheral' diameter as the wetted perimeter of the channel divided by π, which is $D_i + D_o$ for the annulus and used that in estimation of Taylor bubble rise velocity. The equi-peripheral diameter is different than the equivalent diameter which is $D_o - D_i$. But the agreement of Sadatomi et al. correlation with

their data from annuli is less satisfactory than data with other channels. We use Equation 4.7 in our model.

The slug-churn and churn-annular transition remains similar to that of circular channels. Void fraction and pressure gradient can be estimated in a fashion similar to that for circular channels.

Flow Through Other Geometries. Sadatomi et al. (1982) found that the geometry of the pipe does not influence the bubble concentration profile considerably. The models for circular conduits can be used with other geometries also. The diameter of the circular pipe should be replaced by the equi-periphery diameter which is expressed in terms of periphery, $D_e =$ Periphery $/ \pi$.

4.1.4 Countercurrent Flow

Countercurrent two-phase flow is encountered occasionally in oil and gas production, in well testing, and in production logging. Little research have been done to understand countercurrent system, where the liquid flows downward while the gas moves upward.

The models for two-phase flow described in chapter 3 can be used for countercurrent system with some modifications. The mixture velocity is the difference between the gas and liquid superficial velocity instead of their sum used in earlier situations. Recognizing this modification, the void fraction in **bubbly flow** becomes,

$$E_g = \frac{V_{sg}}{C_o(V_{sg} - V_{sl}) + V_t} \qquad (4.8)$$

A value of 2.0 for C_o and Harmathy equation for V_t has been found to well represent the experimental data (Srinevasan (1993)).

Transition from bubbly to slug is also expected at a void fraction of 0.25 during the countercurrent flow. Using this value for void fraction the following transition criteria in terms of superficial velocity is obtained,

$$V_{sg} = \frac{V_t - C_o V_{sl}}{4 - C_o} \sin\theta \qquad (4.9)$$

The void fraction in slug flow can be calculated using the general approach described in chapter 3 with the modifications noted for the bubbly flow region. The terminal rise velocity V_t should be replaced by the Taylor bubble rise velocity, V_{tT} , and C_o value changes from 2.0 to 1.2 . The churn and annular flow regions are rarely observed in countercurrent situations and little has been understood about their behavior.

4.1.5 Liquid - Liquid Flow

Liquid-liquid two-phase flow is commonly encountered in chemical process industries and is quite prevalent in the production of petroleum crudes. Although a lot of work has been done to understand the gas-liquid two-phase flow, few investigators have attempted to explain the mechanics of simultaneous flow of two immiscible liquids. The physics of liquid-liquid flow is different from that of the gas-liquid flow. However,

there are some similarities between them as well. The model for two phase flow described earlier can be used for liquid-liquid system with some modifications.

The in-situ volume fraction of the lighter phase (i.e. oil in a mixture of oil-water) depends on its in-situ velocity relative to the mixture. The in-situ oil velocity, V_o, is influenced by the tendency of the oil droplets to flow through the central portion of the channel where the local mixture velocity is greater than the cross-sectional average velocity. We use the approach suggested by Hasan and Kabir (1987) and Wallis (1969). According to them, the density difference between phases give rise to drift flux, j_{ow}, which adds velocity to the lighter phase. Hence, lighter phase velocity becomes,

$$V_o = C_o V_m + \frac{j_{ow}}{E_o} \qquad (4.10)$$

where $j_{ow} = V_t E_o (1-E_o)^2$, as suggested by Wallis (1969).

For ideal bubbly flow, when the bubbles do not interact, taking Wallis suggestion into account, the following expression for lighter fluid volume-fraction is obtained,

$$E_o = \frac{V_{so}}{1.2 V_m + V_t (1-E_o)^2} \qquad (4.11)$$

Hasan and Kabir (1987) found Harmathy equation suitable in estimating the terminal rise velocity in liquid-liquid systems. The following expression represents the transition from bubbly to slug flow,

$$V_{so} = 0.43 V_{sw} + 0.20 V_t \qquad (4.12)$$

The expressions derived for bubbly flow are also applicable for slug and churn flow. However, Hasan and Kabir suggested to change the value of the flow parameter C_o from 1.2 to 1.15 for churn flow. Mist flow, analogous to annular flow in gas-liquid system is less frequent and should be treated as homogeneous flow.

4.2 Heat Transfer During Production and Injection

The steps involved in formulating an expression for fluid temperature has been described in detail in chapter 3. One of the underlying assumptions in the process was that the heat flux from the formation to the fluid remained constant throughout the entire production time. In order to estimate the fluid temperature more accurately it is essential to incorporate changes that will account for the variation of heat flux with production time. We will develop the concept of varying heat flux in the following section and use it in subsequent sections.

4.2.1 Effect of Varying Heat Flux

The rate of heat transfer, ϕ, from the wellbore to the formation (or vice versa) at the formation/wellbore interface per unit depth of the well is given by

$$W\,\phi \;=\; -\frac{2\,\pi\,k_e}{T_D(t_D)}\left(T_{wb}-T_{ei}\right) \tag{4.13}$$

The dimensionless temperature, $T_D(t_D)$, is a function of dimensionless time, $t_D = \alpha t/r^2$, and can be easily estimated from (Hasan and Kabir, 1991),

$$T_D = 1.1281\sqrt{t_D}\left[1 - 0.3\sqrt{t_D}\right] \qquad\qquad if \ \ t_D \leq 1.5$$

$$T_D = \left[0.4063 + 0.5\ln(t_D)\right]\left[1 + \frac{0.6}{t_D}\right] \qquad\qquad if \ \ t_D > 1.5 \qquad (4.14)$$

However, Equation 4.13 is only valid for constant heat flux at the wellbore/formation interface. In general, fluid temperature within the wellbore tends to approach the temperature of the formation surrounding it, thereby decreasing heat transfer rate with time. It is possible to account for this changing heat flux by using the superposition principle. Lets consider a new well that has produced fluids at a constant rate for a time t. To estimate fluid temperature at time t, we divide the total into n periods (not necessarily equal) - $(t_1 - 0)$, $(t_2 - t_1)$, $(t_3 - t_2)$, ..., $(t_{n-1} - t_n)$. We assume that the heat flux at each of these time periods is constant. Thus, at the first time step,

$$\phi_1 = -\frac{2\pi k_e}{W \, T_D(t_D)}\left(T_{wb} - T_{ei}\right)_1 \qquad\qquad (4.15)$$

Or,

$$T_{ei} - T_{wb,1} = \frac{W}{2\pi k_e}\phi_1 \, T_D(t_D) \qquad\qquad (4.16)$$

The heat flow rate, ϕ_2, during the second time step, $t_2 - t_1$, will be different from ϕ_1. This situation will be represented by adding another constant heat source, which supply heat to the well at time $> t_1$ and whose magnitude is equal to $\phi_2 - \phi_1$. The

wellbore/formation interface temperature at this step, $T_{wb,2}$, is then the sum of the effects of these two heat sources and is given by,

$$T_{ei} - T_{wb,2} = \frac{W}{2\pi k_e}\left[\phi_1 T_D(t_D) + (\phi_2 - \phi_1) T_D(t_D - t_{D,1}) \right] \qquad (4.17)$$

Similarly, the third time period can be represented by three sources of heat supplying ϕ_1 from zero time, $\phi_2 - \phi_1$ since t_1, and $\phi_3 - \phi_2$, since t_2. Hence,

$$T_{ei} - T_{wb,3} = \frac{W}{2\pi k_e}\left[\phi_1 T_D(t_D) + (\phi_2 - \phi_1) T_D(t_D - t_{D,1}) + (\phi_3 - \phi_2) T_D(t_D - t_{D,2}) \right] \qquad (4.18)$$

Hence for the nth time period,

$$T_{ei} - T_{wb,n} = \frac{W}{2\pi k_e} \Sigma_n \qquad (4.19)$$

Where

$$\Sigma_n = \sum_{i=1}^{n} (\phi_i - \phi_{i-1}) T_D(t_D - t_{D,i-1}) \qquad (4.20)$$

and both ϕ_o and T_{D0} are zero.

The flowing wellbore fluid temperature is obtained from an energy balance between the wellbore fluid and the surrounding formation at the time of interest, t. The rate of heat transfer from the wellbore fluid to the wellbore/formation interface, in terms of the overall heat transfer coefficient for the wellbore, is given by,

$$\phi_n = -\left(2\pi r_{to} U_{to}\right)\left(T_f - T_{wb}\right)_n / W \qquad (4.21)$$

48

Hence,

$$T_{wb,n} = T_{f.} + \frac{W \, \phi_n}{2 \, \pi \, r_{to} \, U_{to}} \tag{4.22}$$

Substituting this expression for $T_{wb,n}$ into Equation 4.19,

$$T_{ei} - T_{f,n} = \frac{W \, \phi_n}{2 \, \pi \, r_{to} \, U_{to}} + \frac{W}{2 \, \pi \, k_e} \sum_{n-1}$$

$$+ \frac{W}{2 \, \pi \, k_e} (\phi_n - \phi_{n-1}) \, T_D(t_D - t_{D,n-1}) \tag{4.23}$$

Where,

$$\sum_{n-1} = \sum_{i=1}^{n-1} (\phi_i - \phi_{i-1}) \, T_D(t_D - t_{D,i-1}) \tag{4.24}$$

Or,

$$T_{ei} - T_{f,n} = \frac{\phi_n \, W}{2 \, \pi} \left[\frac{1}{r_{to} \, U_{to}} + \frac{T_D(t_D - t_{D,n-1})}{k_e} \right]$$

$$+ \frac{W}{2 \, \pi \, k_e} \sum_{n-1} - \frac{W}{2 \, \pi \, k_e} (\phi_{n-1}) \, T_D(t_D - t_{D,n-1}) \tag{4.25}$$

Or,

$$T_{ei} - T_{f,n} = \frac{\phi_n \, W}{2 \, \pi} \left[\frac{k_e + r_{to} \, U_{to} \, T_D(t_D - t_{D,n-1})}{k_e \, r_{to} \, U_{to}} \right]$$

$$+ \frac{W}{2 \, \pi \, k_e} \sum_{n-1} - \frac{W}{2 \, \pi \, k_e} (\phi_{n-1}) \, T_D(t_D - t_{D,n-1}) \tag{4.26}$$

Rewriting Equation 4.26 for ϕ_n,

$$\phi_n = \frac{c_p}{A_n}\left(T_{ei} - T_{f,n}\right) + T_D(t_D - t_{D,n-1})\frac{\phi_{n-1}}{B_n} - \frac{1}{B_n}\sum_{n-1} \qquad (4.27)$$

Where,

$$A_n = \frac{W c_p}{2\pi}\left[\frac{k_e + r_{to}U_{to}T_D(t_D - t_{D,n-1})}{k_e r_{to}U_{to}}\right] \qquad (4.28)$$

And,

$$B_n = \frac{k_e + r_{to}U_{to}T_D(t_D - t_{D,n-1})}{r_{to}U_{to}} \qquad (4.29)$$

Energy balance on the flowing fluid for a differential depth, dz, gives,

$$\frac{dT_f}{dz} = \frac{1}{c_p}\left[\phi_n - \frac{g\sin\theta}{g_c J} - \frac{V}{g_c J}\frac{dV}{dz}\right] + C_J\frac{dP}{dz} \qquad (4.30)$$

Substituting the expression for ϕ_n from Equation 4.27 into Equation 4.30, we obtain,

$$\frac{dT_{f,n}}{dz} = \frac{T_{ei} - T_{f,n}}{A_n} - \frac{g\sin\theta}{g_c J c_p} - \frac{V}{g_c J c_p}\frac{dV}{dz} + C_J\frac{dP}{dz}$$

$$+ T_D(t_D - t_{D,n-1})\frac{\phi_{n-1}}{c_p B_n} - \frac{1}{c_p B_n}\sum_{n-1} \qquad (4.31)$$

Or,

$$\frac{dT_{f,n}}{dz} = T_{ei} - \frac{T_{f,n}}{A_n} - \frac{g\sin\theta}{g_c J c_p} + \psi \qquad (4.32)$$

Where,

$$\psi = \sigma + T_D(t_D - t_{D,n-1})\frac{\phi_{n-1}}{c_p B_n} - \frac{1}{c_p B_n}\sum_{n-1} \qquad (4.33)$$

And,

$$\sigma = C_j \frac{dP}{dz} - \frac{V(dV/dz)}{g_c J c_p} \tag{4.34}$$

The effect of various parameters on the term, σ (Equation 4.34), was investigated by Sagar et al. (1990) who proposed an empirical expression for its evaluation. This correlation is valid for flow rates less than 5 lb/sec and is shown below.

$$\phi = -0.00298 + 1.006 \times 10^{-6} P_{wh} + 1.91 \times 10^{-4} W - 1.05 \times 10^{-6} GOR$$
$$+ 3.229 \times 10^{-5} API + 0.004 \gamma_g - 0.3551 g_T \tag{4.35}$$

Heat flow from the wellbore to the formation will vary with well depth. At the bottomhole, where the fluid temperature is the same as formation temperature, ϕ is zero. As the fluid moves upward in the well, the temperature difference between the wellbore fluid and the formation increases with consequent increase in the transfer of heat between the formation and the wellbore. Analytical expressions for wellbore fluid temperature as a function of well depth may be obtained from Equation 4.32 for two different assumptions about the variation of wellbore/formation interface heat fluxes, ϕ_n, as functions of well depth. It should be noted that we assume the geothermal gradient to be linear with depth, i.e,

$$T_{ei} = T_{eibh} - g_T z \tag{4.36}$$

4.2.1.A Analytical Solution (Constant ψ)

Equation 4.32 can be rearranged as shown below as Equation 4.37,

$$\frac{dT_{f,n}}{dz} + \frac{T_{f,n}}{A_n} = \left[-\frac{g \sin \theta}{g_c J c_p} + \psi + \frac{T_{ei}}{A_n} \right] - \frac{g_T z}{A_n} \tag{4.37}$$

When heat fluxes are assumed not to vary significantly with depth, the terms in bracket on the right hand side of Equation 4.37 are constants while the last term is linear in the independent variable, z. Equation 4.37 is, therefore, a first order linear differential equation, which can be solved using integrating factor, I.F, given by,

$$I.F = e^{\int \frac{1}{A} dz}$$
$$= e^{z/A} \tag{4.38}$$

Multiplying each term by the I.F., we obtain,

$$\frac{d\left(T_{f,n} e^{z/A}\right)}{dz} = \left[-\frac{g \sin \theta}{g_c J c_p} + \psi + \frac{T_{ei}}{A_n} \right] e^{z/A} - \frac{g_T z}{A_n} e^{z/A} \tag{4.39}$$

To Integrate Equation 4.39 with respect to z, we note that the integral of $e^{z/A}$ is $Ae^{z/A}$ and that,

$$\frac{1}{A} \int e^{z/A} g_T z \, dz = g_T z e^{z/A} - \int g_T e^{z/A} \, dz \tag{4.40}$$
$$= g_T z e^{z/A} - A g_T e^{z/A}$$

Hence the solution to Equation 4.37 is,

$$T_{f,n} \, e^{Z/A} = A \, e^{Z/A} \left[-\frac{g \sin\theta}{g_c J c_p} + \psi + \frac{T_{eibh}}{A} \right] \qquad (4.41)$$
$$- g_T z \, e^{Z/A} + A \, g_T \, e^{Z/A} + IC$$

And,

$$T_{f,n} = A \left[-\frac{g \sin\theta}{g_c J c_p} + \psi + \frac{T_{eibh}}{A} \right] - g_T z + A g_T + IC \, e^{-Z/A} \qquad (4.42)$$

where IC represents the integration constant. Noting that $T_{eibh} - zg_T$ equals formation temperature at the given depth, T_{ei}, we obtain,

$$T_{f,n} = T_{ei} + A \left[-\frac{g \sin\theta}{g_c J c_p} + \psi + g_T \right] + IC \, e^{-Z/A} \qquad (4.43)$$

To evaluate the integration constant, IC, we use the condition that at the bottomhole (z=0) the fluid temperature is equal to the formation temperature ($T_{fn} = T_{eibh}$). Thus,

$$T_{fbh,n} = T_{eibh} + A \left[-\frac{g \sin\theta}{g_c J c_p} + \psi + g_T \right] + IC \qquad (4.44)$$

Or,

$$IC = T_{fbh,n} - T_{eibh} - A \left[-\frac{g \sin\theta}{g_c J c_p} + \psi + g_T \right] + IC \qquad (4.45)$$

Hence,

$$
\begin{aligned}
T_{f,n} &= T_{ei} + A_n \left(-\frac{g}{g_c} \frac{\sin\theta}{J c_{pm}} + \psi + g_T \right) \\
&\quad + e^{-Z/A} \left(T_{fbh} - T_{ebh} \right) \\
&\quad - e^{-Z/A} A_n \left(-\frac{g}{g_c} \frac{\sin\theta}{J c_{pm}} + \psi + g_T \right)
\end{aligned}
\tag{4.46}
$$

4.2.1.B Analytical Solution (Linear Variation of Heat Flux with depth)

Although the variation in heat flux with depth is small, it is possible to allow for this variation by using a linear variation of all ϕ's with depth. Heat flux is zero at the bottomhole and attains a maximum negative value (heat flow is from the wellbore to the formation) at the wellhead. Thus, at any depth, z, heat fluxes, ϕ_i, are written (analogous to geothermal gradient) as,

$$
\phi_i = F_i z
\tag{4.47}
$$

where F_i are positive numbers.

The parameter, ψ, given by Equation 4.33, is rewritten as,

$$
\psi = \sigma + T_D(t_D - t_{D,n-1}) \frac{z F_{n-1}}{c_p B_n} - \frac{z}{c_p B_n} \sum_{n-1}'
\tag{4.48}
$$

where,

$$
\sum_{n-1}' = \sum_{i=1}^{n-1} (F_i - F_{i-1}) T_D(t_D - t_{D,i-1})
\tag{4.49}
$$

Equation 4.37 then becomes,

$$\frac{dT_{f,n}}{dz} = -\frac{T_{f,n}}{A_n} + \frac{T_{eibh}}{A} - \frac{g \sin\theta}{g_c J c_p} + \sigma$$

$$+ \left[T_D(t_D - t_{D,n-1}) \frac{F_{n-1}}{c_p B_n} - \frac{1}{c_p B_n} \sum_{n-1}' - \frac{g_T}{A_n} \right] z \qquad (4.50)$$

Equation 4.50, is very similar to Equation 4.37. The last term in Equation 4.50, which is linear in z, contains constants in addition to g_t. The IF remains the same and the solution is also very similar.

$$T_{f,n} = T_{eibh} - z F_T + A_n \left(-\frac{g}{g_c} \frac{\sin\theta}{J c_{pm}} + \sigma + F_T \right)$$

$$+ e^{-Z/A} \left(T_{fbl} - T_{ebh} \right)$$

$$- e^{-Z/A} A_n \left(-\frac{g}{g_c} \frac{\sin\theta}{J c_{pm}} + \sigma + F_T \right) \qquad (4.51)$$

Where,

$$F_T = g_T - T_D(t_D - t_{D,n-1}) \frac{A_n F_{n-1}}{B_n c_p} + \frac{A_n}{c_p B_n} \sum_{n-1}' \qquad (4.52)$$

Here F_T is a function of n, but is independent of well depth.

4.3 Temperature Profile During Mud Circulation

Mud recirculation through tubings and tubing/casing annuli occurs during numerous operations, such as drilling, well kill operations, etc. The mud can enter either through the annulus or through the tube. If the mud enters through the annulus, then it returns through the tube and vice versa. The entering mud temperature at the wellhead is generally much lower than the bottomhole formation temperature. Thus, in flowing down through one channel and backing up through the other, the mud gains heat from the formation. The heat transfer rate for the mud in the annulus depends both on the formation temperature from which it gains heat, as well as on the tubing mud temperature to which it loses heat.

In the first two sections of this chapter we present two analytical solutions for the flowing mud temperature in the annulus and in the tubing for the two different system as a function of well depth. The solution is based on equating the heat loss from the formation to the heat gained by the mud in the tubing and in the annulus. The modeling approach utilizes the expression for the formation temperature distribution developed by Hasan and Kabir (1991). The resulting second order linear differential equation is solved in usual manner by adding the solution of the homogeneous equation to the particular solution for the inhomogeneous equation to obtain the final analytical expression.

One of the underlying assumptions of the above systems was the heat flux from the formation to the annular fluid remained constant throughout the entire operation. The effect of varying heat flux with operation time has been studied at the end of this chapter.

56
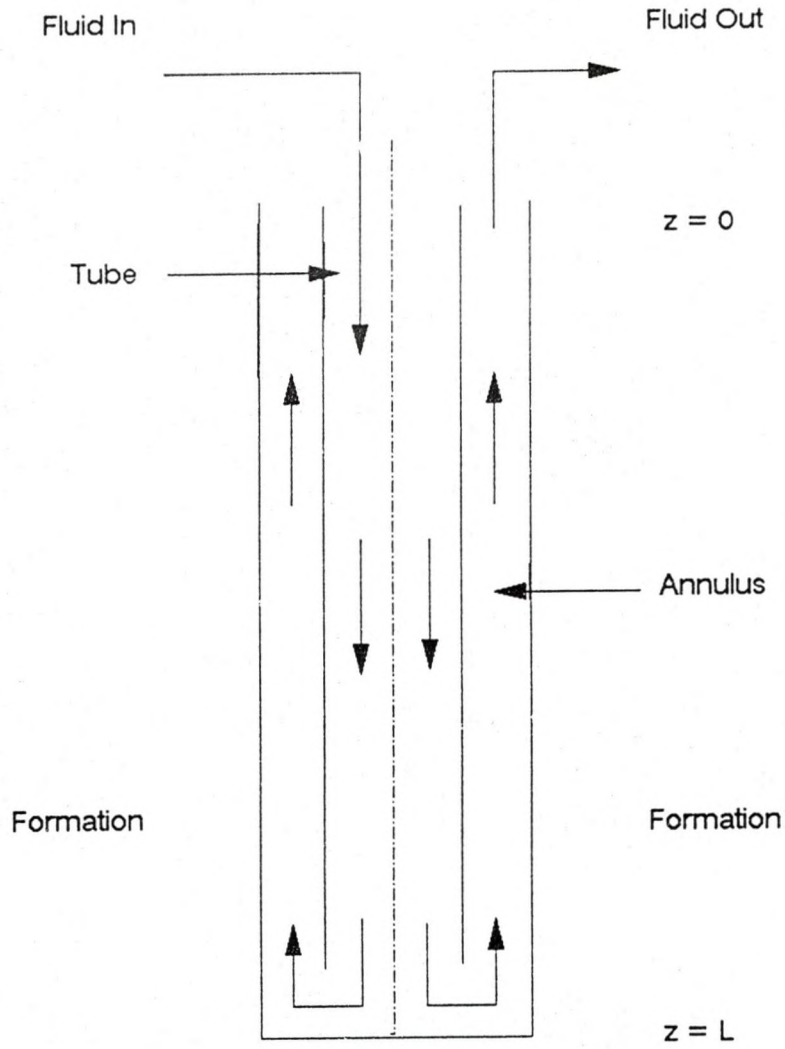
Figure 3.   Circulating Fluid System

4.3.1 Mud Flow Down the Annuli and Up the Tubing

During a kill operation, mud is recirculated through tubing/casing annuli. In these and other cases, such as during drilling, it is necessary to estimate the flowing mud temperature in both the tubing and the annulus as a function of depth.

The entering mud temperature at the annulus wellhead, T_{ai}, could be either slightly higher or slightly lower than the surface formation temperature. However, the formation temperature at the bottomhole is generally much higher than the annulus mud temperature. Thus, in flowing down the annulus and back up the tubing, the mud gains heat from the formation. The heat transfer rate for the mud in the annulus depends both on the formation temperature from which it generally gains heat, as well as on the tubing mud temperature to which it loses heat.

To obtain expressions for flowing mud temperature in the annulus and the drill tube, we set up an energy balance over a differential element of length, dz, of the annulus fluid as shown in Figure 4. Note that z is positive in the downward direction. Heat enters the element by convection at z, $q_a(z)$, and by conduction from the formation, q_F. Heat leaves the element by convection at z+dz, $q_a(z+dz)$ and by conduction and convection to the drill tube fluid, q_{ta}. Thus,

$$q_a(z) - q_a(z+dz) = q_{ta} - q_F \qquad (4.53)$$

Or,

$$c_P \left[T_a(z) - T_a(z+dz) \right] = q_{ta} - q_F \qquad (4.54)$$
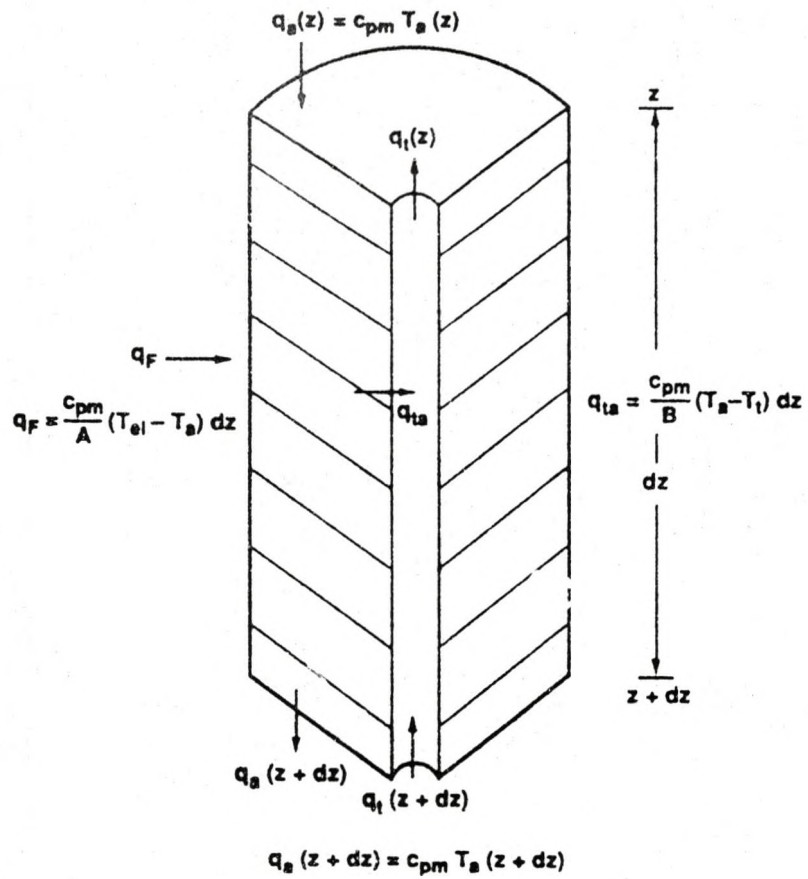
Figure 4.   Schematic of Heat balance for Tubulars and Formation

Heat flow, q_F, from the formation to the wellbore is given by,

$$q_F = \frac{2\pi k_e}{W T_D}(T_{ei} - T_{wb}) \, dz \tag{4.55}$$

where q_F is heat transfer rate per unit length of the well per unit mass of mud. The dimensionless temperature, T_D, can be easily estimated from Equation 4.14 (Hasan and Kabir, 1991),

The wellbore/formation interface temperature, T_{wb} is related to the annulus mud temperature, T_a, by the overall heat transfer coefficient of the annulus system as follows,

$$q = \frac{2\pi r_c U_a}{W}(T_{wb} - T_a) \tag{4.56}$$

The overall heat transfer coefficient, U_a, depends on the resistances to heat flow through the annulus mud, casing metal, and the cement, and is discussed in detail by Hasan and Kabir (1991).

Noting that the heat flowing from the formation to the annulus, q_F, equals q given by Equation 4.56, we eliminate T_{wb} from Equations 4.55 and 4.56 to we obtain the rate of heat transferred from the formation to the annulus,

$$q_F = \frac{2\pi}{W}\left[\frac{r_c U_a k_e}{k_e + T_D r_c U_a}\right](T_{ei} - T_a) \, dz \tag{4.57}$$

Or,

$$q_F = \frac{c_P}{A}(T_{ei} - T_a) \, dz \tag{4.58}$$

where,

$$A = \frac{c_{pm} W}{2 \pi} \left[\frac{k_e + (r_c U_a T_D)}{r_c U_a k_e} \right] \qquad (4.59)$$

Heat transferred from the annulus mud to the mud in the drill tube is given by

$$q_{ta} = \frac{2 \pi r_t U_t}{W} (T_a - T_t) \, dz \qquad (4.60)$$

Or,

$$q_{ta} = \frac{c_P}{B} (T_a - T_t) \, dz \qquad (4.61)$$

Where,

$$B = \frac{W c_P}{2 \pi r_t U_t} \qquad (4.62)$$

Hence Equation 4.54 is rewritten as,

$$c_P \left[T_a(z) - T_a(z + dz) \right] = \frac{c_P}{A} (T_a - T_{ei}) \, dz + \frac{c_P}{B} (T_a - T_t) \, dz \qquad (4.63)$$

Or,

$$A \frac{dT_a}{dz} = (T_{ei} - T_a) - (T_a - T_t) \frac{A}{B} \qquad (4.64)$$

Equation 4.64 has two unknowns, the annulus mud temperature, T_a and the tubing mud temperature, T_t. An energy balance for the drill tube mud for the same differential element provides a second expression. Thus.

$$q_t(z+dz) - q_a(z) = -q_{ta} \qquad (4.65)$$

Or,

$$c_p \left(T_t(z+dz) - T_t(z) \right) = c_p \frac{T_t - T_a}{B} dz \qquad (4.66)$$

Or,

$$\frac{dT_t}{dz} = \frac{T_t - T_a}{B} \qquad (4.67)$$

Or,

$$T_a = T_t - B \frac{dT_t}{dz} \qquad (4.68)$$

Using Equation 4.68 to eliminate T_a from Equation 4.64, we obtain,

$$A \frac{dT_t}{dz} - A B \frac{dT_t^2}{d^2z} = T_{ei} + B \frac{dT_t}{dz} - T_t + A \frac{dT_t}{dz} \qquad (4.69)$$

Formation temperature, T_{ei}, is usually assumed to linearly increase with depth. Hence,

$$T_{ei} = T_{ew} + g_T z \qquad (4.70)$$

And,

$$A B \frac{d^2T_t}{dz^2} + B \frac{dT_t}{dz} - T_t + T_{ew} + g_T z = 0 \qquad (4.71)$$

Equation 4.71 is a second order linear differential equation with the following boundary conditions: $T_a = T_{ai}$ at the wellhead (i. e. when $z = 0$) and heat exchange

between the tubing and wellbore mud is zero, i.e. $dT_t/dz = 0$, at the bottomhole (or $T_t = T_s$ when $z = L$). Equation 4.71, which is a inhomogeneous second order linear differential equation, is rewritten in the following form,

$$AB \frac{d^2 T_t}{dz^2} + B \frac{dT_t}{dz} - T_t = -T_{ew} - g_T z \tag{4.72}$$

$$= f(z)$$

where, $$f(z) = -T_{ew} - g_T z \tag{4.73}$$

The particular solution of Equation 4.72 is easily obtained as

$$T_{tp} = \mu z + \chi \tag{4.74}$$

Noting that the second derivative of T_{tp} is zero, substitution of T_{tp} as a solution to Equation 4.72 gives,

$$B \mu - \mu z - \chi = -T_{ew} - g_t z \tag{4.75}$$

Equating coefficients of z and of the constants, we obtain,

$$\mu = g_T, \qquad \chi = T_{ew} + B g_T \tag{4.76}$$

Thus the particular solution to Equation 4.72 is,

$$T_{tp} = g_T z + T_{ew} + B g_1 \tag{4.77}$$

The complementary solution of Equation 4.72 is deduced from its homogeneous form (obtained by setting f (z) = 0),

$$AB \frac{d^2 T_t}{dz^2} + B \frac{dT_t}{dz} - T_t = 0 \tag{4.78}$$

The characteristic polynomial equation for Equation 4.78 is

$$p(\lambda) = AB\lambda^2 - B\lambda - 1 = 0 \tag{4.79}$$

The solution to the quadratic equation gives the following two roots,

$$\lambda_1 = -\frac{1}{2A} + \frac{1}{2A} \sqrt{1 + \frac{4A}{B}} \tag{4.80}$$

$$= -\frac{1}{2A} + \frac{1}{2A} \sqrt{1 + 4 \left(r_c U_a T_D + k_e \right) \frac{r_t U_t}{r_c U_a k_e}} \tag{4.81}$$

Similarly,

$$\lambda_2 = -\frac{1}{2A} - \frac{1}{2A} \sqrt{1 + 4 \left(r_c U_a T_D + k_e \right) \frac{r_t U_t}{r_c U_a k_e}} \tag{4.82}$$

The complementary solution to Equation 4.72 is then,

$$T_{tc} = \alpha e^{\lambda_1 z} + \beta e^{\lambda_2 z} \tag{4.83}$$

and the complete solution, obtained by adding the particular and the complementary solutions, is

$$T_t = \alpha e^{\lambda_1 z} + \beta e^{\lambda_2 z} + g_T z + B g_T + T_{ew} \tag{4.84}$$

The expression for the annulus mud temperature can now be obtained using Equation 4.68 and Equation 4.84. Thus,

$$\frac{dT_t}{dz} = \alpha \lambda_1 e^{\lambda_1 z} + \beta \lambda_2 e^{\lambda_2 z} + g_T \tag{4.85}$$

And,

$$T_a = T_t - B \frac{dT_t}{dz} \tag{4.86}$$

$$= \left(1 - \lambda_1 B\right) \alpha e^{\lambda z} + \left(1 - \lambda_2 B\right) \beta e^{\lambda_2 z} + g_T z + T_{ew}$$

The constants, α and β are obtained by applying the boundary conditions. Thus, at the wellhead, $z = 0$, $T_a = T_{ai}$, hence

$$T_a = T_{ai} = \left(1 - \lambda_1 B\right) \alpha + \left(1 - \lambda_2 B\right) \beta + T_{ew} \tag{4.87}$$

At the bottomhole ($z = L$), dT_t/dz is zero, i.e.,

$$\frac{dT_t}{dz}\bigg|_L = 0 = \alpha \lambda_1 e^{\lambda_1 L} + \beta \lambda_2 e^{\lambda_2 L} + g_T \tag{4.88}$$

Hence,

$$\alpha = -\frac{\beta \lambda_2 e^{\lambda_2 L} + g_T}{\lambda_1 e^{\lambda_1 L}} \qquad (4.89)$$

Substituting this expression for α into Equation 4.87 and simplifying,

$$\beta = \frac{\left(T_{ai} - T_{ew}\right)\lambda_1 e^{\lambda_1 L} + g_T\left(1 - \lambda_1 B\right)}{\lambda_1 e^{\lambda_1 L}\left(1 - \lambda_2 B\right) - \lambda_2 e^{\lambda_2 L}\left(1 - \lambda_1 B\right)} \qquad (4.90)$$

From Equation 4.89, then

$$\alpha = -\frac{\left(T_{ai} - T_{ew}\right)\lambda_2 e^{\lambda_2 L} + g_T\left(1 - \lambda_2 B\right)}{\lambda_1 e^{\lambda_1 L}\left(1 - \lambda_2 B\right) - \lambda_2 e^{\lambda_2 L}\left(1 - \lambda_1 B\right)} \qquad (4.91)$$

4.3.2 Mud Flow Down the Tubing and Up the Annuli

When mud flows down the tubing and back up the annulus, the flow direction is reversed compared to the last case. Although the general approach for setting up the energy balance for the differential element remains the same, slight changes are needed in some of the expressions. We may still represent the heat flow from the formation to the annulus by Equation 4.58, and the heat flow from the tubing to the annulus by Equation 4.61, because in these cases the temperature difference driving force would appropriately account for the direction of heat flow. However, energy entering the mud in the differential element by convection is $q_a(z+dz)$ while that leaving is $q_a(z)$. Thus, Equations 4.53 and 4.54 are changed as follows,

$$q_a(z+dz) - q_a(z) = q_{ta} - q_F \tag{4.92}$$

Or,

$$c_P \left[T_a(z+dz) - T_a(z) \right] = q_{ta} - q_F \tag{4.93}$$

Using Equations 4.58 and 4.61 Equation 4.93 is rewritten (similar to Equation 4.71) as,

$$A \frac{dT_a}{dz} = \left(T_a - T_t \right) \frac{A}{B} - \left(T_{ei} - T_a \right) \tag{4.94}$$

Energy balance for the mud in the drill tube leads to the following equation, which has the opposite sign to that of Equation 4.65,

$$q_t(z) - q_a(z+dz) = -q_{ta} \tag{4.95}$$

Or,

$$T_a = T_t + B \frac{dT_t}{dz} \tag{4.96}$$

Combining Equations 4.94 and 4.96 to eliminate T_a, we obtain,

$$A B \frac{d^2 T_t}{dz^2} - B \frac{dT_t}{dz} - T_t + T_{ew} + g_T z = 0 \tag{4.97}$$

Equation 4.97 can be solved in a manner similar to Equation 4.91 with the following boundary conditions: $T_t = T_{ti}$ at the wellhead (i. e. when $z = 0$) and $dT_t/dz = 0$ at the bottomhole (i.e. when $z = L$). The solution is,

$$T_t = \gamma e^{\xi_1 z} + \delta e^{\xi_2 z} + g_T z - B g_T + T_{ew} \tag{4.98}$$

And,

$$T_a = \left(1 + \xi_1 B\right)\gamma e^{\xi_1 z} + \left(1 + \xi_2 B\right)\delta e^{\xi_2 z} + g_T z + T_{ew} \tag{4.99}$$

Where,

$$\gamma = -\frac{\left(T_{ti} + B g_T - T_{ew}\right)\xi_2 e^{\xi_2 L} + g_T}{\xi_1 e^{\xi_1 L} - \xi_2 e^{\xi_2 L}} \tag{4.100}$$

$$\delta = \frac{\left(T_{ti} + B g_T - T_{ew}\right)\xi_1 e^{\xi_1 L} + g_T}{\xi_1 e^{\xi_1 L} - \xi_2 e^{\xi_2 L}} \tag{4.101}$$

$$\xi_1 = \frac{1}{2A} + \frac{1}{2A}\sqrt{1 + 4\left(r_c U_a T_D + k_e\right)\frac{r_t U_t}{r_c U_a k_e}} \tag{4.102}$$

$$\xi_2 = \frac{1}{2A} - \frac{1}{2A}\sqrt{1 + 4\left(r_c U_a T_D + k_e\right)\frac{r_t U_t}{r_c U_a k_e}} \tag{4.103}$$

4.3.3 Effect of Varying Heat Flux During Mud Circulation

We pointed out earlier that the heat flux from the formation to the annular fluid changes with the operation time. The concept of varying heat flux can be applied to the mud circulation system using the same principle that was earlier used in the single pipe system. Heat flux at any time is a function of previous heat flux and can be expressed as,

$$\phi_n = \frac{c_p}{A_n}(T_{ei} - t_{a,n}) + T_D(t_{D,n} - t_{D,n-1})\frac{\phi_{n-1}}{B_n} - \frac{1}{B_n}\sum_{i=1}^{n-1}(\phi_i - \phi_{i-1})T_D(t_{D,n} - t_{D,i-1}) \quad . \quad (4.104)$$

where,

$$A_n = \frac{W c_p}{2\pi}\left[\frac{k_e + r_c U_a T_D(t_{D,n} - t_{D,n-1})}{k_e r_c U_a}\right] \quad (4.105)$$

and

$$B_n = \frac{k_e + r_c U_a T_D(t_{D,n} - t_{D,n-1})}{r_c U_a} \quad (4.106)$$

Heat transferred from the annulus mud to the mud in the tube is given by,

$$\phi_{ta} = \frac{2\pi r_t U_t}{W}(T_a - T_t)$$

$$= \frac{c_p}{E}(T_a - T_t) \qquad where, \quad E = \frac{W c_p}{2\pi r_t U_t} \quad (4.107)$$

The final form of the energy balance over the differential length, dz of the annulus fluid includes two new terms to account for the varying heat flux.

$$c_p \left[T_a(z) - T_a(z + dz) \right] = (\phi_{to} - \phi) \, dz \qquad (4.108)$$

Or,

$$A_n \frac{dT_a}{dz} = (T_{ei} - T_{a,n}) - \frac{A_n}{E}(T_a - T_t) + \frac{A_n \phi_{n-1}}{B_n c_p} T_D (t_{D,n} - t_{D,n-1})$$

$$- \frac{A_n}{B_n c_p} \sum_{i=1}^{n-1} (\phi_i - \phi_{i-1}) \, T_D (t_{D,n} - t_{D,i-1}) \qquad (4.109)$$

The above equation has two unknowns, the annulus mud temperature, T_a and the tubing

mud temperature, T_t. Earlier it was shown that energy balance over the differential length

on the tube side provides the following expression.

$$T_a = T_t - E \frac{dT_t}{dz} \qquad (4.110)$$

Using the above equation to eliminate T_a from Equation 4.109, we obtain,

$$A_n E \frac{d^2 T_t}{dz^2} + T_{ew} + g_t z - T_t + E \frac{dT_t}{dz} + \frac{A_n \phi_{n-1}}{B_n c_p} T_D (t_{D,n} - t_{D,n-1})$$

$$- \frac{A_n}{c_p B_n} \sum_{i=1}^{n-1} (\phi_i - \phi_{i-1}) \, T_D (t_{D,n} - t_{D,i-1}) = 0 \qquad (4.111)$$

This equation is a second order linear differential equation with boundary conditions : at

the wellhead, $Ta = T_{ai}$ and at the bottomhole, heat exchange between the tubing and

annulus is zero , i.e $dT_t/dz = 0$. Equation 4.111, which is a inhomogeneous second order

linear differential equation, can be rewritten in the following form,

$$A_n E \frac{d^2 T_t}{dz^2} + E \frac{dT_t}{dz} - T_t = -T_{ew} - g_t z - \Omega_1 + \Omega_2 \qquad (4.112)$$

where,

$$\Omega_1 = \frac{A_n \phi_{n-1}}{B_n c_p} T_D (t_{D,n} - t_{D,n-1})$$

$$\Omega_2 = \frac{A_n}{c_p B_n} \sum_{i=1}^{n-1} (\phi_i - \phi_{i-1}) T_D (t_{D,n} - t_{D,i-1})$$
(4.113)

The particular solution of Equation 4.112 can easily be obtained as,

$$T_{tp} = g_t z + E g_t + T_{ew} + \Omega_1 - \Omega_2$$
(4.114)

and the complementary solution of the Equation can be deduced from its homogeneous form,

$$A_n E \frac{d^2 T_t}{dz^2} + E \frac{dT_t}{dz} - T_t = 0$$
(4.115)

and has been found to be,

$$T_{tc} = \alpha e^{\lambda_1 z} + \beta e^{\lambda_2 z}$$
(4.116)

where α, β, λ_1 and λ_2 are constants. The solution of the quadratic equation (Equation 4.115) gives the value of λ_1 and λ_2, whereas values of α and β can be obtained by applying the boundary conditions. The complete solution obtained by adding the particular and complementary solution is as follows,

$$T_t = \alpha e^{\lambda_1 z} + \beta e^{\lambda_2 z} + g_t z + E g_t + T_{ew} + \Omega_1 - \Omega_2$$
(4.117)

and the mud temperature in the annulus,

$$T_a = (1-\lambda_1 E)\alpha\, e^{\lambda_1 z} + (1-\lambda_2 E)\beta\, e^{\lambda_2 z} + g_t z + T_{ew} + \Omega_1 - \Omega_2 \qquad (4.118)$$

By applying the boundary conditions the following values of α and β were obtained,

$$\alpha = -\frac{(T_{ai}-T_{ew}-\Omega_1+\Omega_2)\lambda_2 e^{\lambda_2 L} + g_t(1-\lambda_2 E)}{\lambda_1 e^{\lambda_1 L}(1-\lambda_2 E) - \lambda_2 e^{\lambda_2 L}(1-\lambda_1 E)} \qquad (4.119)$$

$$\beta = \frac{(T_{ai}-T_{ew}-\Omega_1+\Omega_2)\lambda_1 e^{\lambda_1 L} + g_t(1-\lambda_1 E)}{\lambda_1 e^{\lambda_1 L}(1-\lambda_2 E) - \lambda_2 e^{\lambda_2 L}(1-\lambda_1 E)} \qquad (4.120)$$

Down the Tube Up the Annulus :

When mud flows down through the tubing and backs up through the annulus, the flow direction is reversed compared to the last case. Although general approach for setting up the energy balance for the differential element remains the same, slight variation is observed in the expression,

$$c_p\left[T_a(z+dz)-T_a(z)\right] = (\phi_{ta} - \phi)\,dz \qquad (4.121)$$

Substituting the values of ϕ_{ta} and ϕ, we obtain

$$A_n\frac{dT_a}{dz} = -(T_{ei}-T_{a,n}) + \frac{A_n}{E}(T_a-T_i) - \frac{A_n\phi_{n-1}}{B_n C_p}T_D(t_{D,n}-t_{D,n-1})$$

$$+ \frac{A_n}{B_n C_p}\sum_{i=1}^{n-1}(\phi_i-\phi_{i-1})\,T_D(t_{D,n}-t_{D,i-1}) \qquad (4.122)$$

Energy balance in the tube leads the following equation.

$$T_a = T_t + E \frac{dT_t}{dz} \qquad (4.123)$$

Using the above equation to eliminate T_a from Equation 4.122, we get,

$$A_n E \frac{d^2 T_t}{dz^2} + T_{ew} + g_t z - T_t - E \frac{dT_t}{dz} + \frac{A_n \phi_{n-1}}{B_n C_p} T_D(t_{D,n} - t_{D,n-1})$$

$$- \frac{A_n}{C_p B_n} \sum_{i=1}^{n-1} (\phi_i - \phi_{i-1}) T_D(t_{D,n} - t_{D,i-1}) = 0 \qquad (4.124)$$

This equation is a second order linear differential equation with boundary conditions : at

the wellhead, $T_t = T_{ti}$ and at the bottomhole, heat exchange between the tubing and

annulus is zero , i.e $dT_t/dz = 0$. Equation 4.124, which is an inhomogeneous second

order linear differential equation, can be rewritten in the following form,

$$A_n E \frac{d^2 T_t}{dz^2} - E \frac{dT_t}{dz} - T_t = -T_{ew} - g_t z - \Omega_1 + \Omega_2 \qquad (4.125)$$

where Ω_1 and Ω_2 are the same constants described earlier. The particular solution of

Equation 4.125 can easily be obtained as.

$$T_{tp} = g_t z + E g_t + T_{ew} + \Omega_1 - \Omega_2 \qquad (4.126)$$

and the complementary solution of the Equation can be deduced from its homogeneous

form

$$A_n E \frac{d^2 T_t}{dz^2} - E \frac{dT_t}{dz} - T_t = 0 \qquad (4.127)$$

and has been found to be,

$$T_{tc} = \gamma e^{\xi_1 z} + \delta e^{\xi_2 z} \qquad (4.128)$$

where γ, δ, ξ_1 and ξ_2 are constants. The solution of the quadratic equation (Equation 4.127) gives the value of ξ_1 and ξ_2, whereas values of γ and δ can be obtained by applying the boundary conditions.

The complete solution obtained by adding the particular and complementary solution is as follows

$$T_t = \gamma e^{\xi_1 z} + \delta e^{\xi_2 z} + g_t z - E g_t + T_{ew} + \Omega_1 - \Omega_2 \qquad (4.129)$$

and the mud temperature in the annulus,

$$T_a = (1 + \xi_1 E) \gamma e^{\xi_1 z} + (1 + \xi_2 E) \delta e^{\xi_2 z} + g_t z + T_{ew} + \Omega_1 - \Omega_2 \qquad (4.130)$$

By applying the boundary conditions the following values of α and β were obtained,

$$\gamma = - \frac{(T_{ti} + E g_t - T_{ew} - \Omega_1 + \Omega_2) \xi_2 e^{\xi_2 L} + g_t}{\xi_1 e^{\xi_1 L} - \xi_2 e^{\xi_2 L}} \qquad (4.131)$$

$$\delta = \frac{(T_{ti} + E g_t - T_{ew} - \Omega_1 + \Omega_2) \xi_1 e^{\xi_1 L} + g_t}{\xi_1 e^{\xi_1 L} - \xi_2 e^{\xi_2 L}} \qquad (4.132)$$

CHAPTER 5

RESULTS AND DISCUSSION

One of the objective of this work is to develop a unified model for void fraction and pressure gradient in two-phase flow. This model is then used to develop a simulator that is uniquely useful to the petroleum industry. The other objective is to study the complex heat transfer problems encountered in wellbores. This includes prediction of temperature profile during production, injection, and mud circulation. In the first section of this chapter we discuss some of the two-phase simulation results. In the second section some of the important aspects of heat transfer is presented.

5.1 Pressure and Void Fraction Profile

Two approaches may be taken to calculate the pressure profile in an wellbore. In both the approaches, the calculations start out with the wellhead or the bottom condition whichever is known to the user. In one method, the pressure gradient is determined at the known condition and the gradient is multiplied by a certain length (usually a small percentage of the total length, i.e., 1%), which gives pressure at the end of this length. The physical properties of the system, including the superficial velocities are calculated at the new point and a new gradient is calculated. The procedure is repeated until the entire well is traversed in this manner. The drawback of this procedure is that the

74

pressure gradient calculated at the beginning of each section is different from the average gradient for the section. The gradient at any point is dependent on fluid properties which are function of system pressure. So, we use Runge Kutta method to better this prediction. The calculation procedure of our program, which uses the second approach, is somewhat different than most of the available programs. We considered pressure as the independent variable, and the dependent variable length is calculated using the pressure gradient. The advantage of taking pressure as the independent variable is that any error in pressure gradient estimation does not directly influence the fluid property and the gradient calculation. Better prediction is expected from this procedure. It is possible to devise other, numerically more efficient procedure, for pressure prediction in an oilwell. However, property correlations are not very accurate and gradient change is not steep enough, for any further sophistication of the numerical procedure.

The pressure and void fraction profile of two different systems as calculated by the models described in the earlier chapters are shown in Figures 5 and 6. The description of the systems are given in Tables 1 and 2 respectively. Figure 5 shows the pressure and void fraction profile for 4355 ft vertical well producing 855 bbl/day of crude. The bottomhole condition is known in this case and simulation progresses from bottom to top. Besides bubbly and slug, single phase flow is observed in this case. Single phase flow persists from the bottomhole to a depth of around 3200 ft. The pressure within this region is high enough for the gas phase to be dissolved in the liquid phase. As the crude passes this depth, the lower pressure causes gas to come out of the liquid phase forming a distinct phase and bubbly flow starts. Bubbly flow continues up to a

Pressure and Void Fraction Profile
Vertical Upward Flow in Pipe
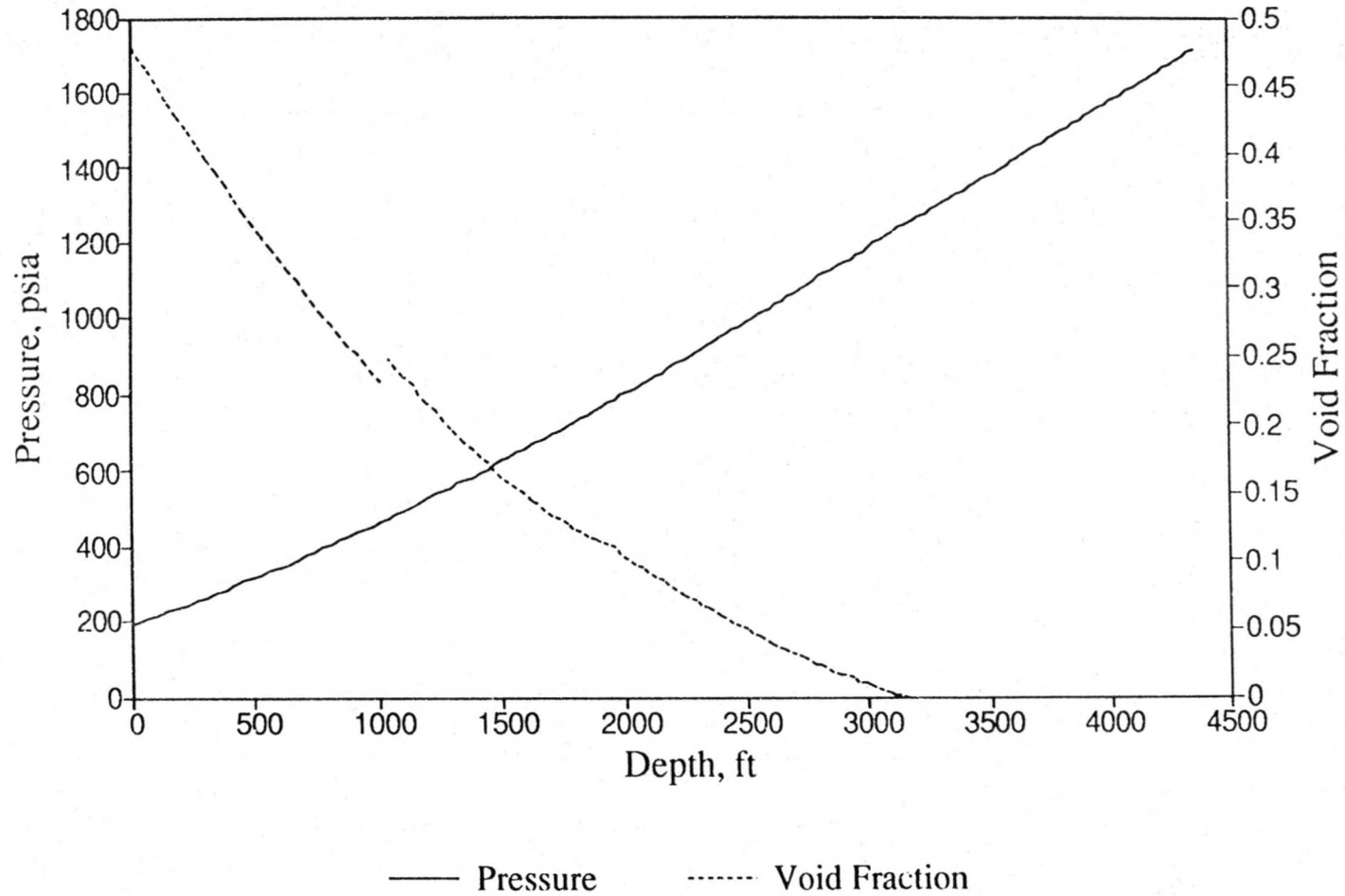
Figure 5. Pressure (and Void Fraction) vs. Depth in Vertical Upward Flow in a Pipe

depth of 1030 ft and transition to slug flow occurs at this depth. An abrupt lowering of void fraction is observed when the pattern changes from bubbly to slug flow. This abrupt change is due to the higher velocity of Taylor bubbles compared to the rise velocity of smaller bubbles that cause the gas phase to move faster and void fraction to decrease.

Figure 6 corresponds to flow in 4450 ft annulus inclined 80° to the horizontal. The flow is in downward direction and the surface condition is known in this case. Simulation progresses from top to bottom. Bubbly flow persists from the wellhead up to a length of about 2150 ft. The conditions are such that slug flow is not observed in this case. At the depth of 2150 ft, the pressure becomes high enough for the gas phase to get dissolved in the liquid phase. Single phase flow starts at that point and it continues up to the bottomhole.

TABLE 1
Wellbore and Fluid Data
(Upward Flow in Vertical Pipe)

Well Depth, ft	4355
Production Rate, STB/day..............................	855
Tube Diameter, in...	0.249
Bottomhole Pressure, psia..............................	1715
Bottomhole Temperature, F............................	153
Gas to Oil Ratio	185
Specific Gravity of Gas	0.75
Specific Gravity of Liquid	0.98
Angle of inclination with Horizontal, deg.......	90
Surface Tension, lb/sec^2..............................	0.058

Figure 6.   Pressure (and Void Fraction) vs. Depth in Inclined Downward Flow in   Annulus

TABLE 2	
Wellbore and Fluid Data	
(Downward Flow in Inclined Annuius)	
Well Depth, ft	4475
Production Rate, STB/day.................................	855
Tube Diameter, in.......................	0.249
Annuli Diameter, in...	0.416
Surface Pressure, psia.......................................	1715
Surface Temperature, F......................................	153
Gas to Oil Ratio	185
Specific Gravity of Gas	0.75
Specific Gravity of Liquid	0.98
Angle of inclination with Horizontal, deg........	80
Surface Tension, lb/sec^2....................................	0.058

5.2 Effect of Varying Heat Flux during Production

In the second section of Chapter 3, we observed that the present approach of estimating fluid temperature during production and injection assumes heat flux to remain constant throughout the production time. However, it is intuitively obvious that heat flux decreases with the production time. We developed two expressions in chapter 4 for estimating fluid temperature in wellbores which account for the variation of heat flux with time. The first expression assumes that the parameter, ψ does not vary significantly with well depth. In reality, however, ψ is a complex function of heat flux, time, and pressure gradient . In deed, the heat flux is zero at the bottomhole (because fluid temperature and

formation temperature are same) and maximum at the wellhead and varies throughout the well depth. In the second approach, we make the more realistic assumption of linear variation of heat flux with depth.

A number of simulations has been run for an oilwell parameters for which are given in Table 3. Besides using the two approaches explained above, numerical solution of the governing differential equation was also sought. Five different solutions with 1, 5, 10, 50, and 100 time steps (= n) were examined for each approach. The number of time step n = 100 signifies that the total production time of 158 hours were divided in 100 equal intervals, and for each 1.58 hour period, the heat flux was assumed to remain at a constant value. Here, n = 1 signifies that heat flux remains constant throughout the entire production time of 158 hours and as such coincides with the solution presently available in the literature. It has been found that although there is significant variation between the results of single step and 100 steps, the results of 50 and 100 time step simulations are close. The simulation with more discritization (such as n = 150) resulted in almost the same profile. So, we concluded that 100 time steps are sufficient for this case. The temperature and heat flux profiles obtained by the simulations are discussed in the following paragraphs. All the profiles will represent the end of production time profile unless otherwise noted.

A number of scenarios have been examined and the results are presented in two different sets of figures. The first set accounts convection in tubing/casing annulus in determining the overall heat transfer coefficient, while the second set does not. The temperature and heat flux profiles with constant ψ assumption are shown in Figures 7

TABLE 3	
Wellbore and Fluid Data During Production in Wellbore	
Well Depth , ft	5400
Production Rate, lb/hr	8856
Tube Diameter, in	2.875
Casing Diameter, in..	7.0
Wellbore Diameter, in..	9.0
Specific Gravity of Crude, API................................	34.3
Formation Thermal Conductivity, Btu/hr ft F...........	0.83
Cement Thermal Conductivity, Btu/hr ft F...............	4.021
Annular Thermal Conductivity, Btu/hr ft F..............	0.383
Specific Heat of fluid, Btu/lb F...............................	0.947
Surface Earth Temperature, F..................................	76
Geothermal Gradient,...	0.005926
Production Time, hr...	158
Thermal Diffusivity, ft/hr^2.......................................	0.04

and 8. The results show significant differences in temperature and heat flux profile as we incorporate the concept of varying heat flux with time. With this approach (ψ=constant), heat flux at any given depth at the end of production time has been found to increase as we discritize the production time. But the physical system suggests that heat flux should decrease if the production time is discritized. This discrepancy suggests that the assumption of constant ψ was probably not a very good one.

The temperature and heat flux profiles with the assumption of linear variation of heat flux with depth are shown in Figures 9 and 10. These simulations also accounted for convection. The solutions have been carried out under the same conditions as the earlier case and five different scenarios at the same number of time steps are presented.

Temperature Profile in the Wellbore
Constant Psi, With Convection
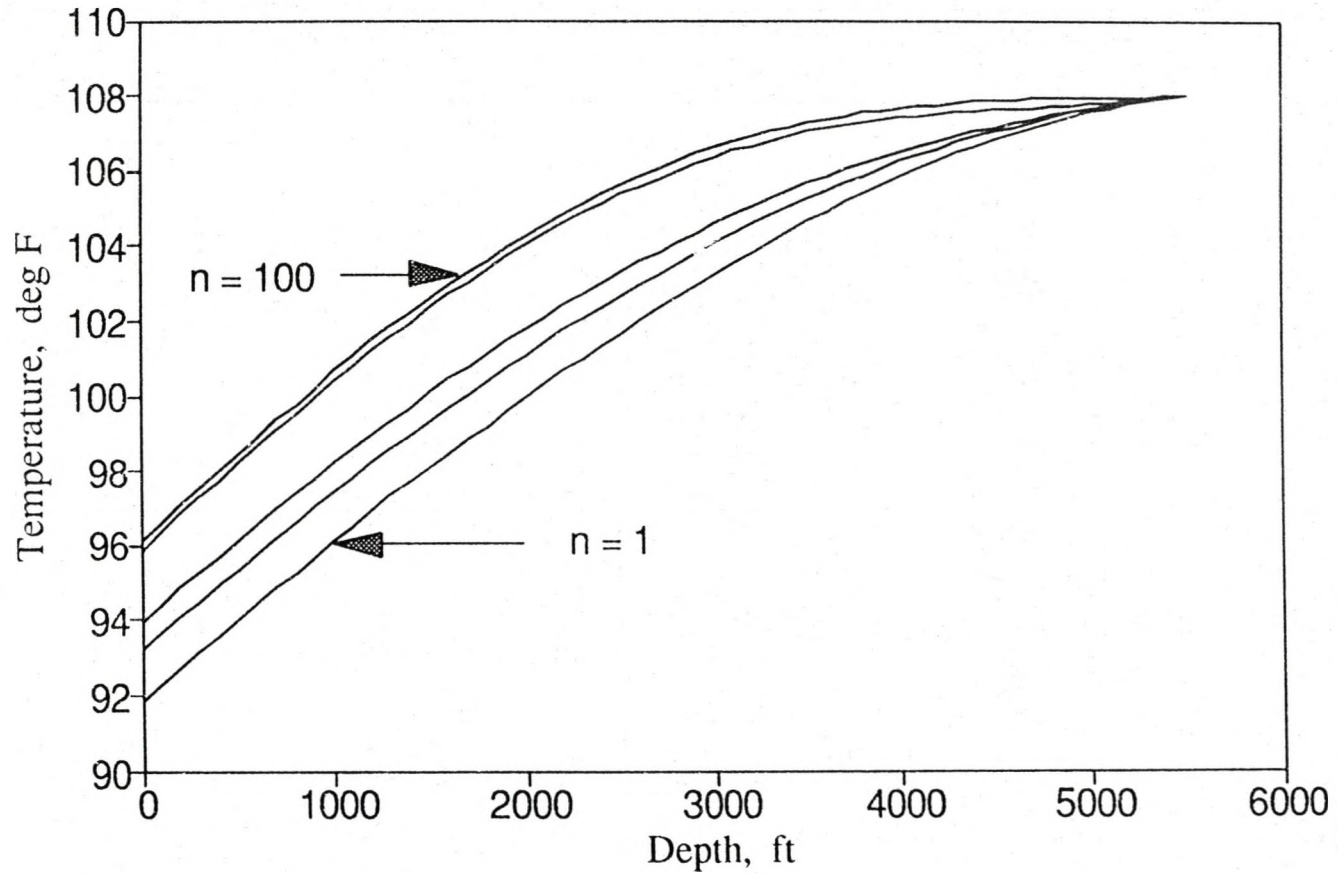
Figure 7.   Temperature vs. Depth in a 5400 ft Wellbore (Constant ψ and With Convection)

Heat Flux Profile in the Wellbore
Constant Psi, With Convection
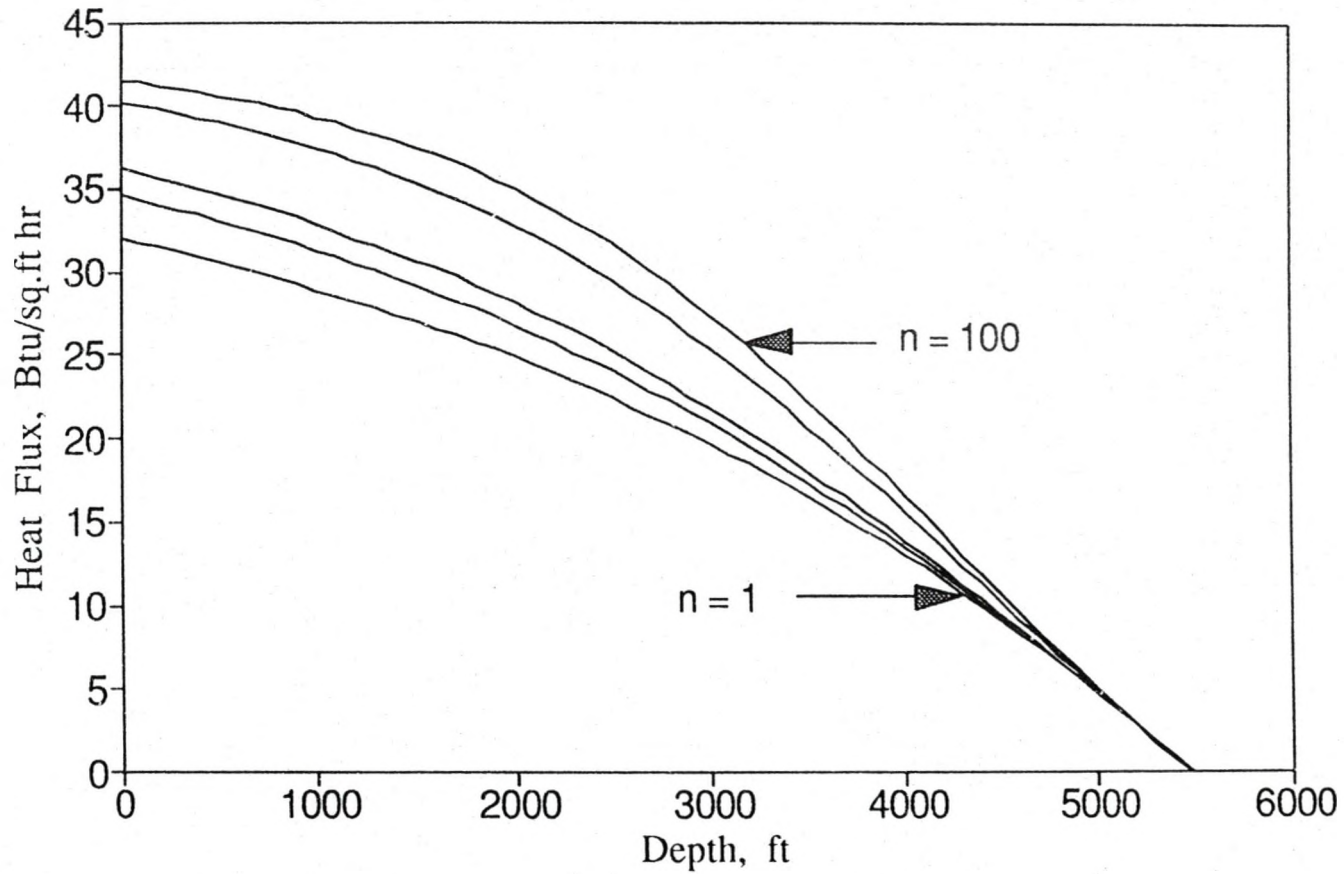
Figure 8.   Heat Flux vs. Depth in a 5400 ft Wellbore (Constant ψ and With Convection)

Temperature Profile in the Wellbore
Linear Phi, With Convection
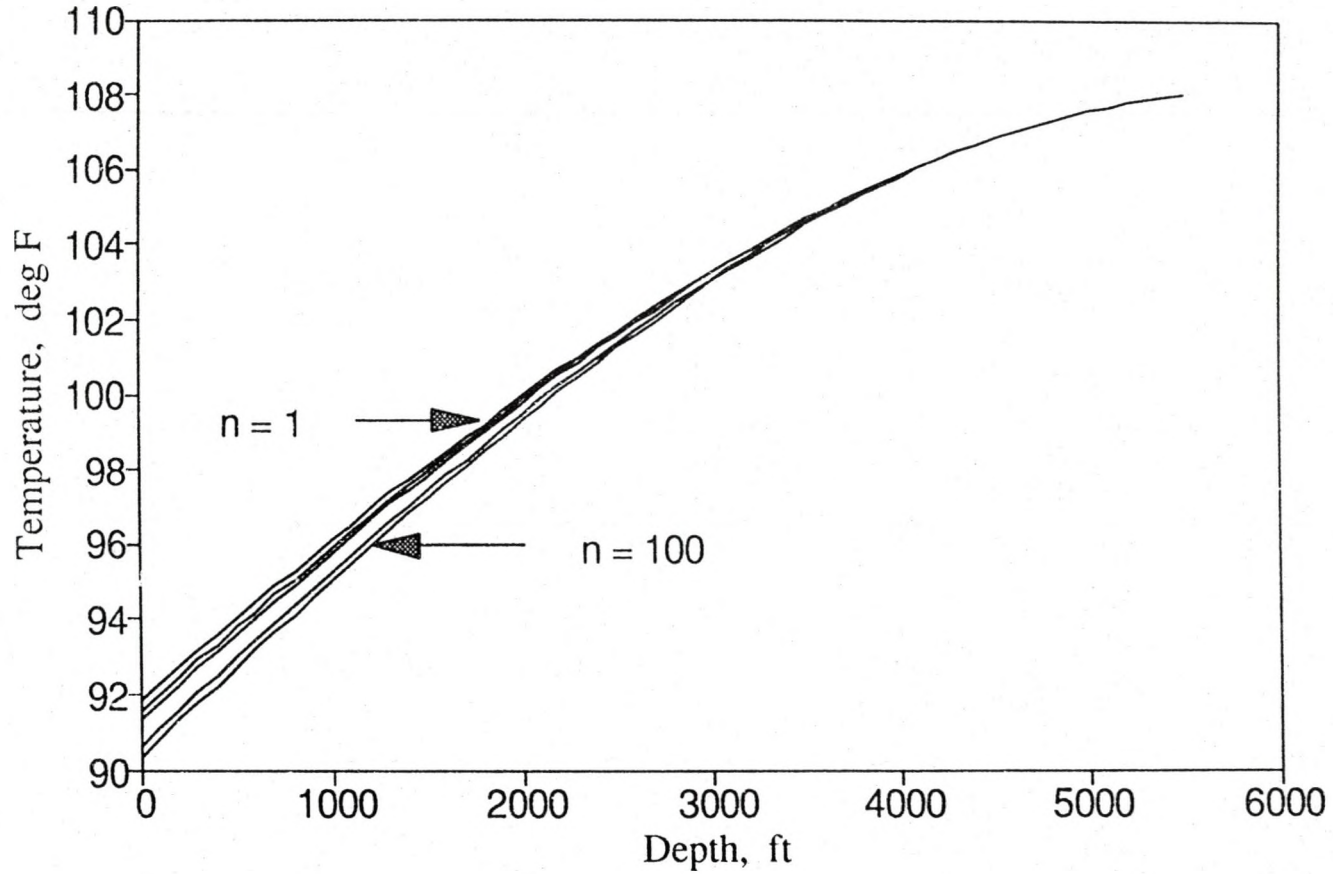
Figure 9.   Temperature vs. Depth in a 5400 ft Wellbore (Linear Heat Flux and With Convection)

Heat Flux Profile in the Wellbore
Linear Phi, With Convection
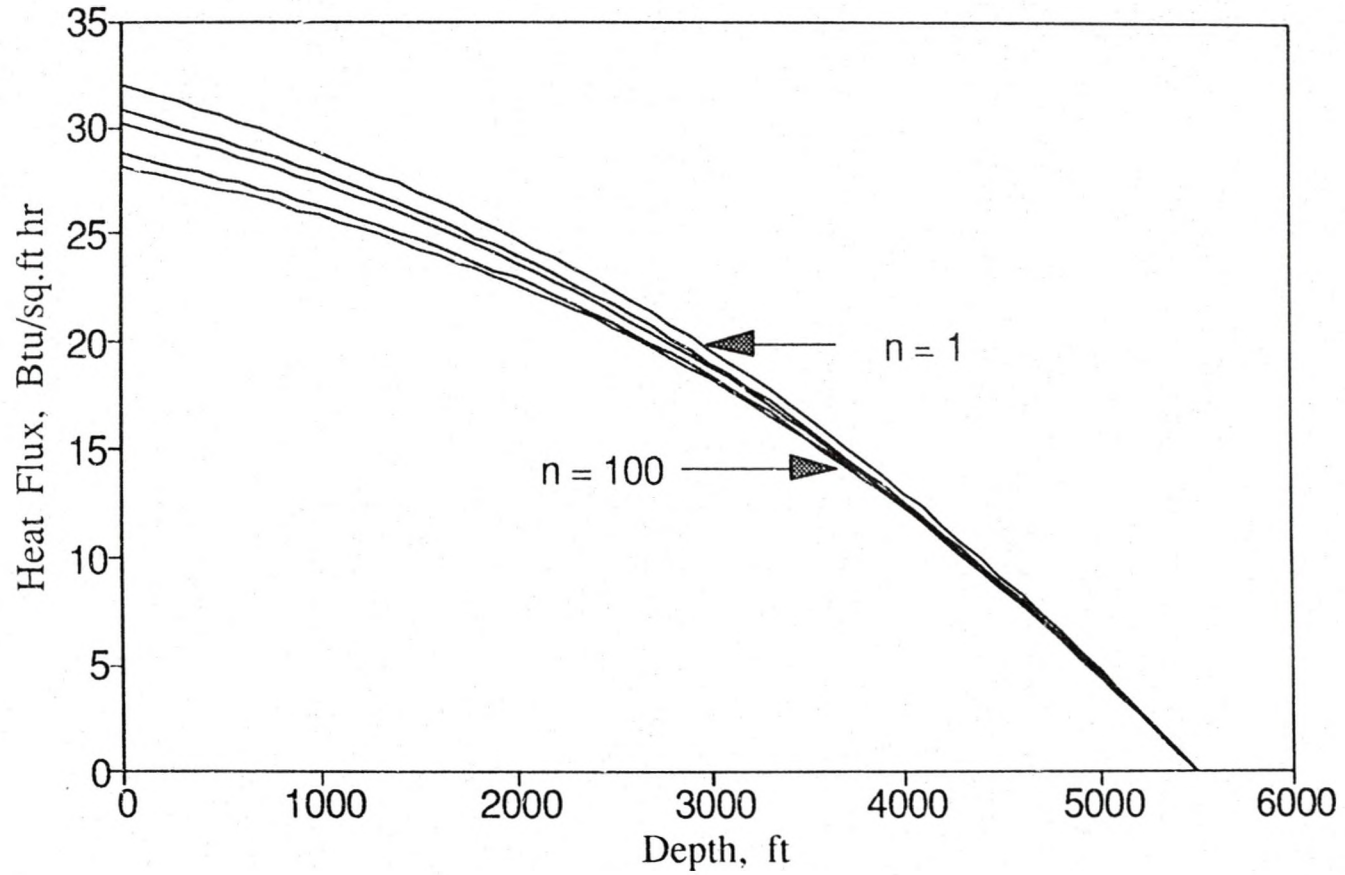
Figure 10.   Heat Flux vs. Depth in a 5400 ft Wellbore (Linear Heat Flux and With Convection)

Temperature Profile in the Wellbore
Numerical Solution
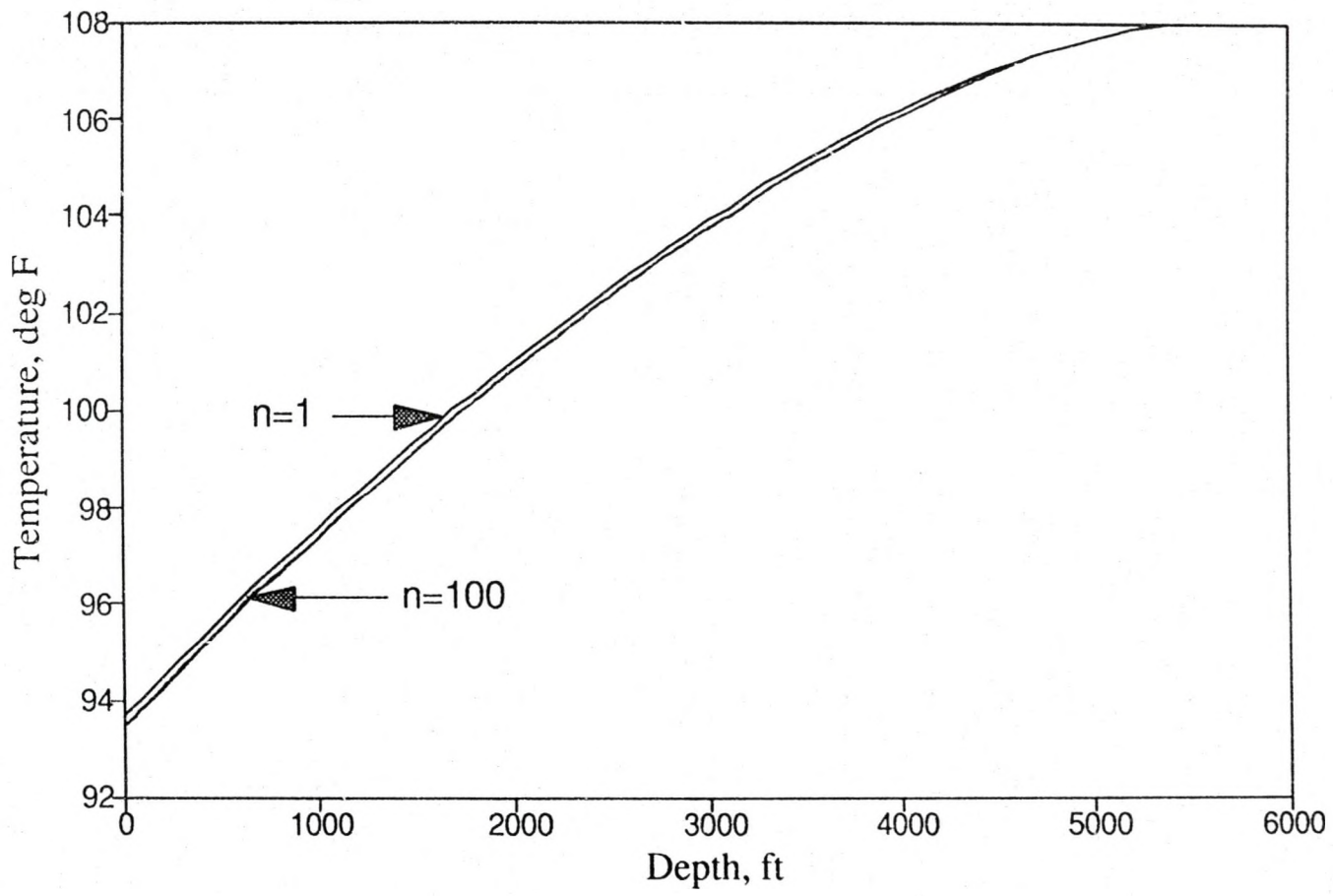
Figure 11.   Temperature vs. Depth in a 5400 ft Wellbore (Numerical Solution)

Heat Flux Profile in the Wellbore
Numerical Solution
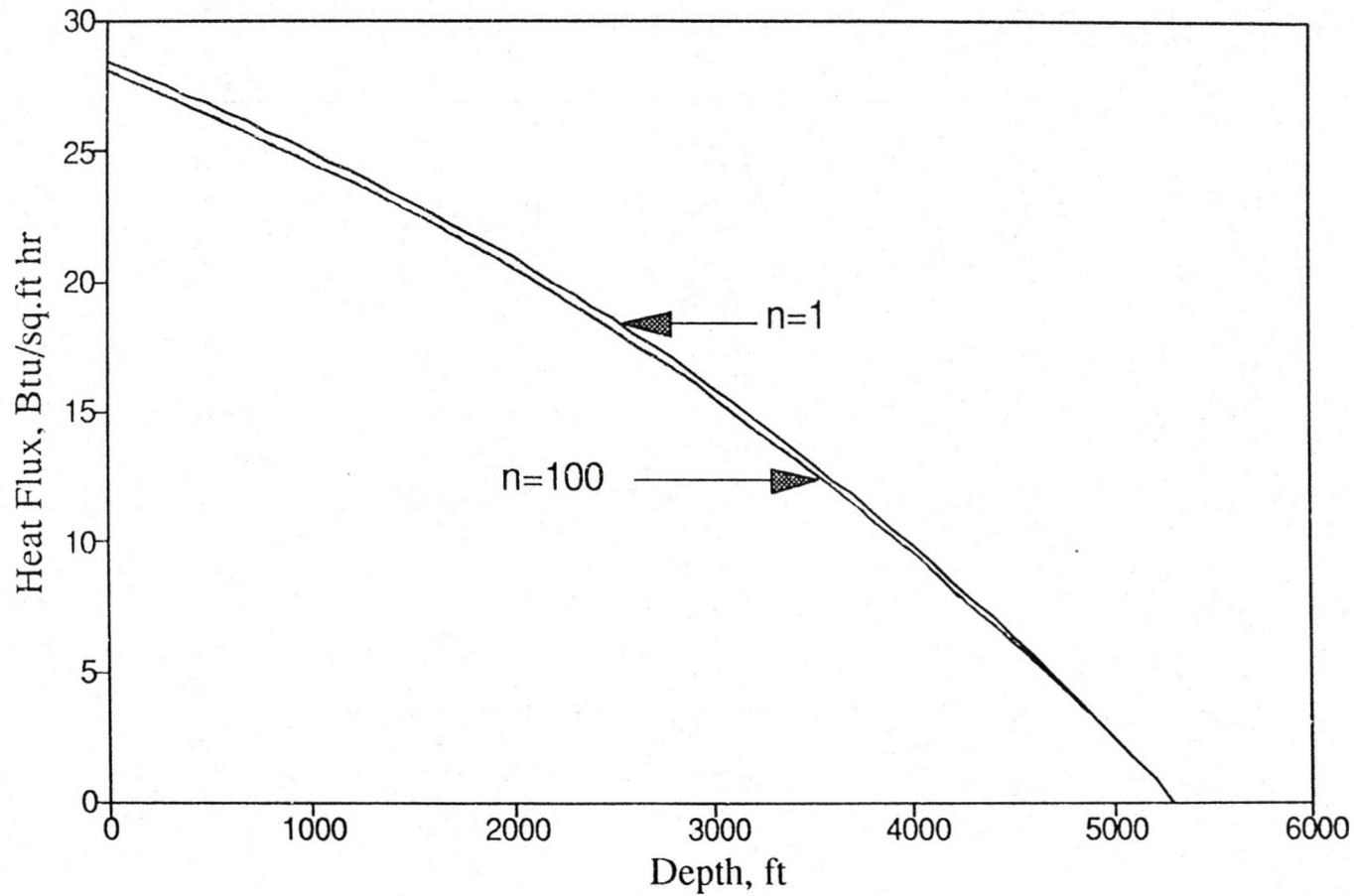
Figure 12.   Heat Flux vs. Depth in a 5400 ft Wellbore (Numerical Solution)

The results show a difference in profile with discritization of production time. But the extent of variation is less compared to the earlier case of constant ψ. The heat flux profiles show that as the total production time is discritized, the heat flux decreases, which is consistent with the physical system. The numerical solutions of the governing differential equation are presented in Figures 11 and 12. The nature of this problem does not easily allow convection to be taken into account in the numerical procedure. The conductivity of formation was changed from 0.83 to 1.40 in order to compensate for convection in the overall heat transfer coefficient term. The numerical solution matches with the solutions obtained from linear variation of heat flux approach. The consistency with the physical system and close match with the numerical results suggest that the linear variation of heat flux with depth assumption is a reasonable one.

The second set of results are shown in Figures 13 to 18. These results do not account for convection in determining the overall heat transfer coefficient. Figure 13 and 14 show the temperature and pressure profile obtained by using the constant ψ assumption. Similarly Figures 15 and 16 show the solution that resulted from the assumption of linear variation of heat flux and Figures 17 and 18 are from numerical solutions. Same conclusion regarding the validity of the linear heat flux assumption can be drawn from this set of results as well. A number of other simulations have been run for a 8000 ft oilwell. The results of these simulations, along with the description of the system, are presented in Appendix C. These results also support the conclusion that linear variation of heat flux assumption is a reasonable one.
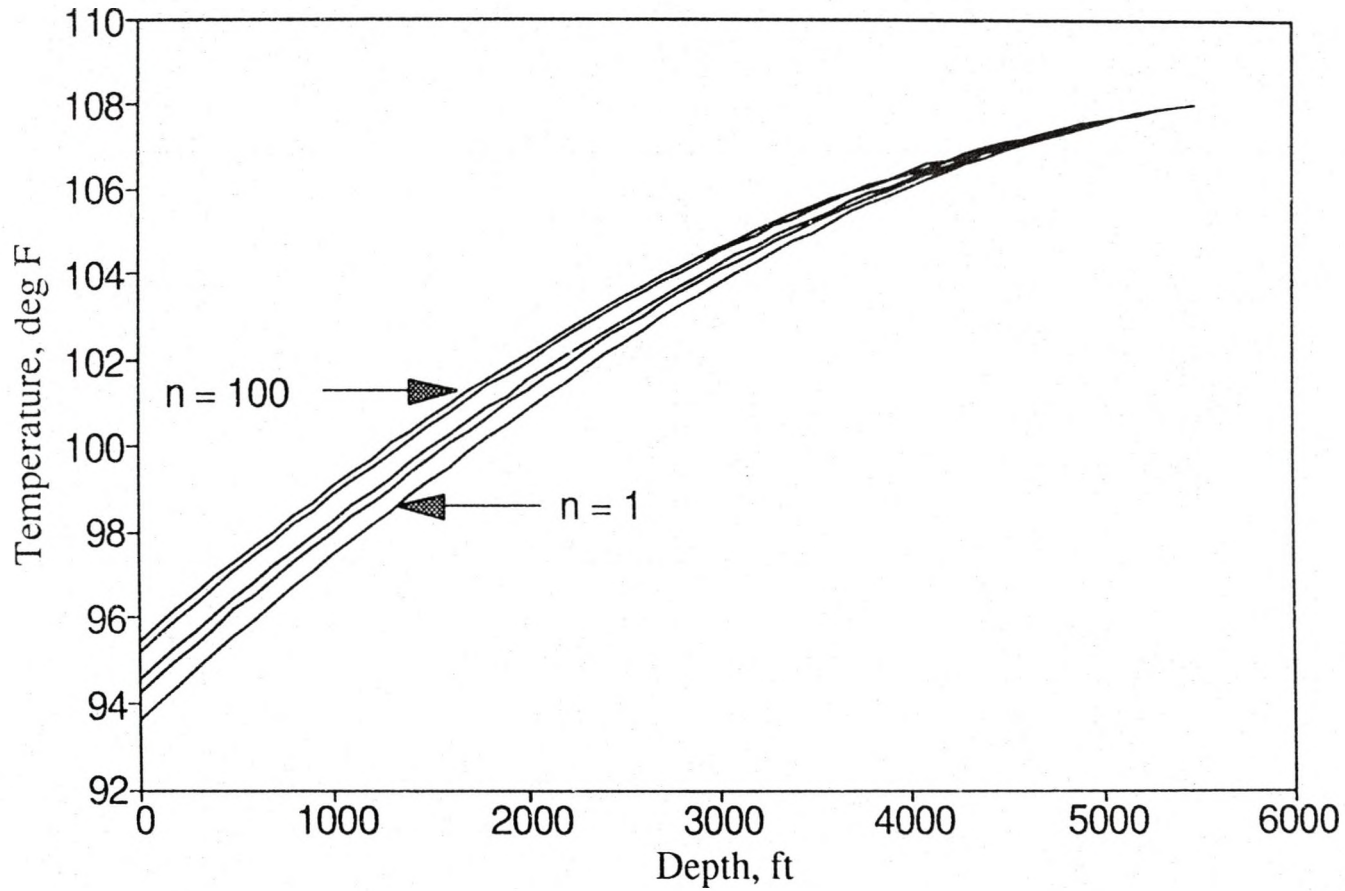
Figure 13. Temperature vs. Depth in a 5400 ft Wellbore (Constant ψ and Without Convection)

Heat Flux Profile in the Wellbore
Constant Psi, Without Convection
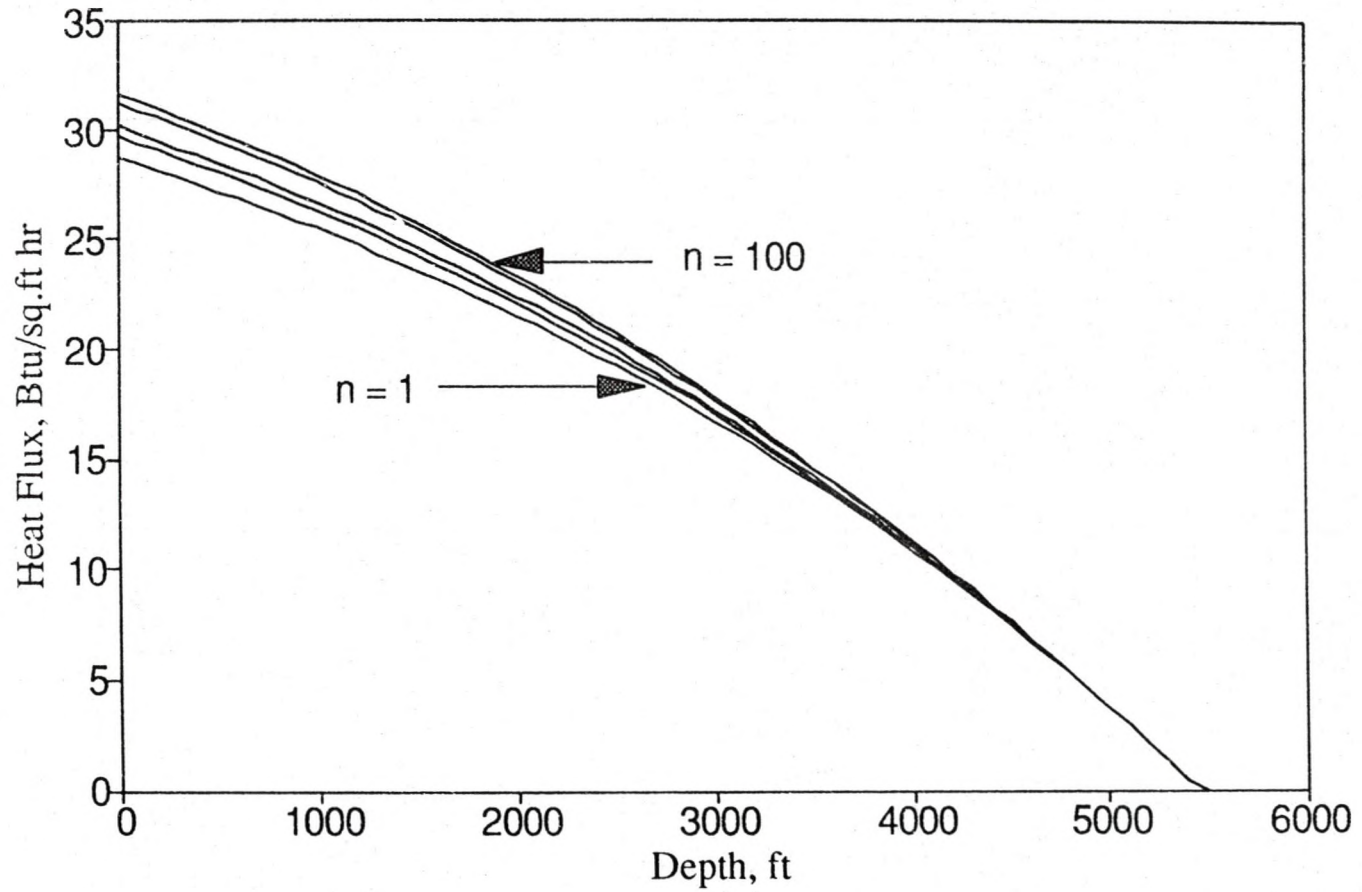
Figure 14.   Heat Flux vs. Depth in a 5400 ft Wellbore (Constant ψ and Without Convection)

Temperature Profile in the Wellbore
Linear Phi, Without Convection
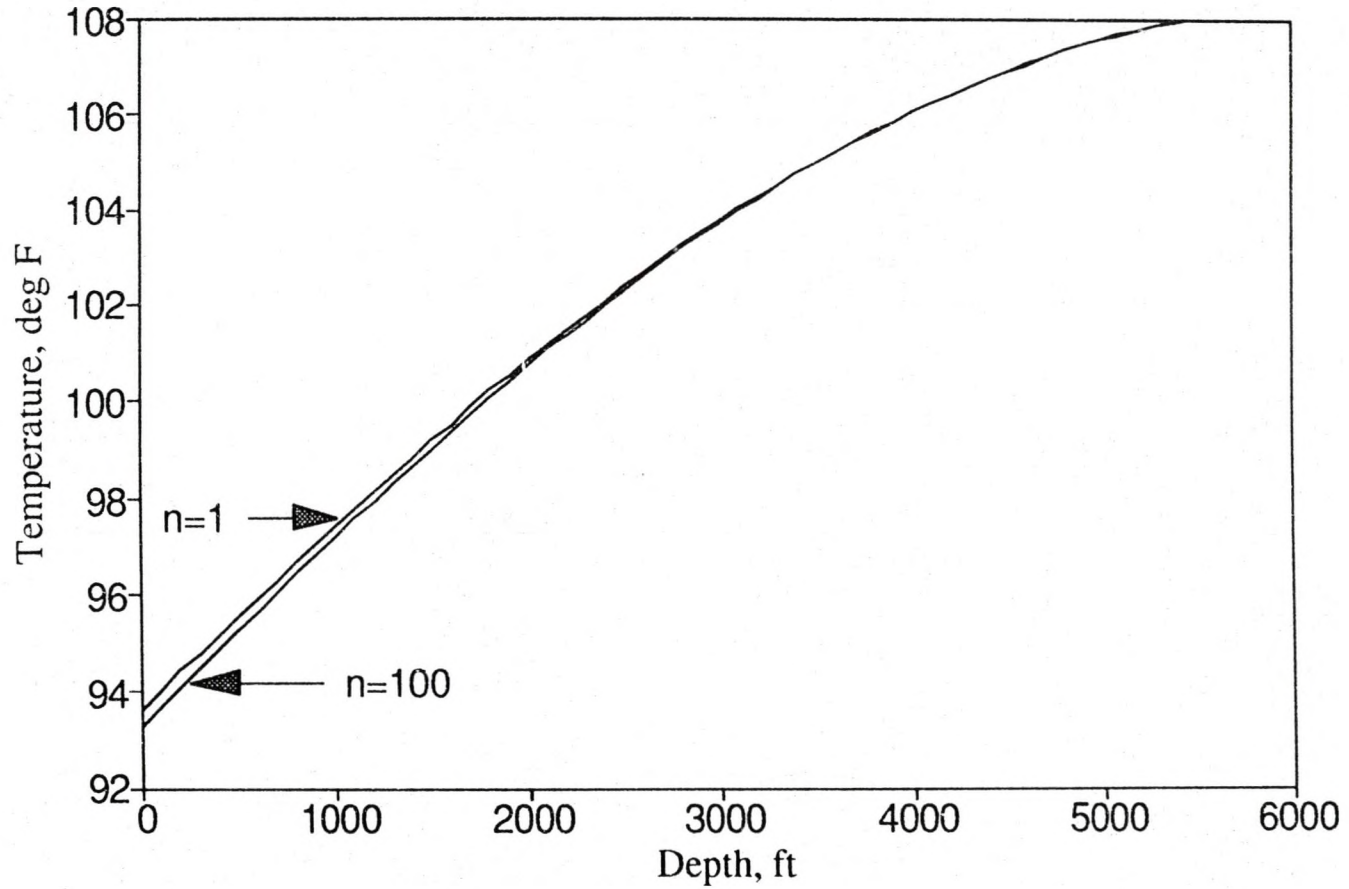
Figure 15.   Temperature vs. Depth in a 5400 ft Wellbore (Linear Heat Flux and Without Convection)

Heat Flux Profile in the Wellbore
Linear Phi, Without Convection
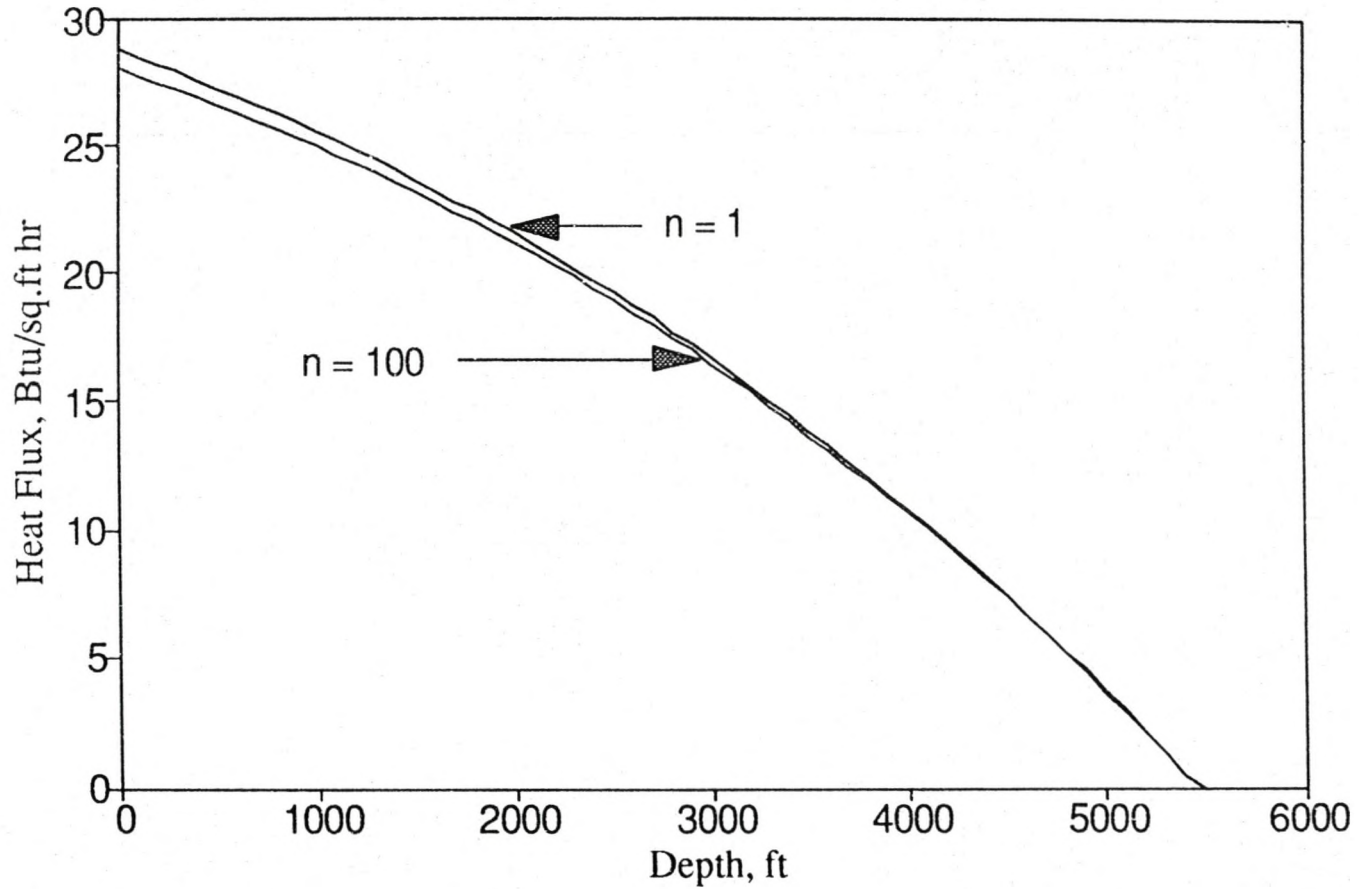
Figure 16. Heat Flux vs. Depth in a 5400 ft Wellbore (Linear Heat Flux and Without Convection)

Temperature Profile in Wellbore
Numerical Solution
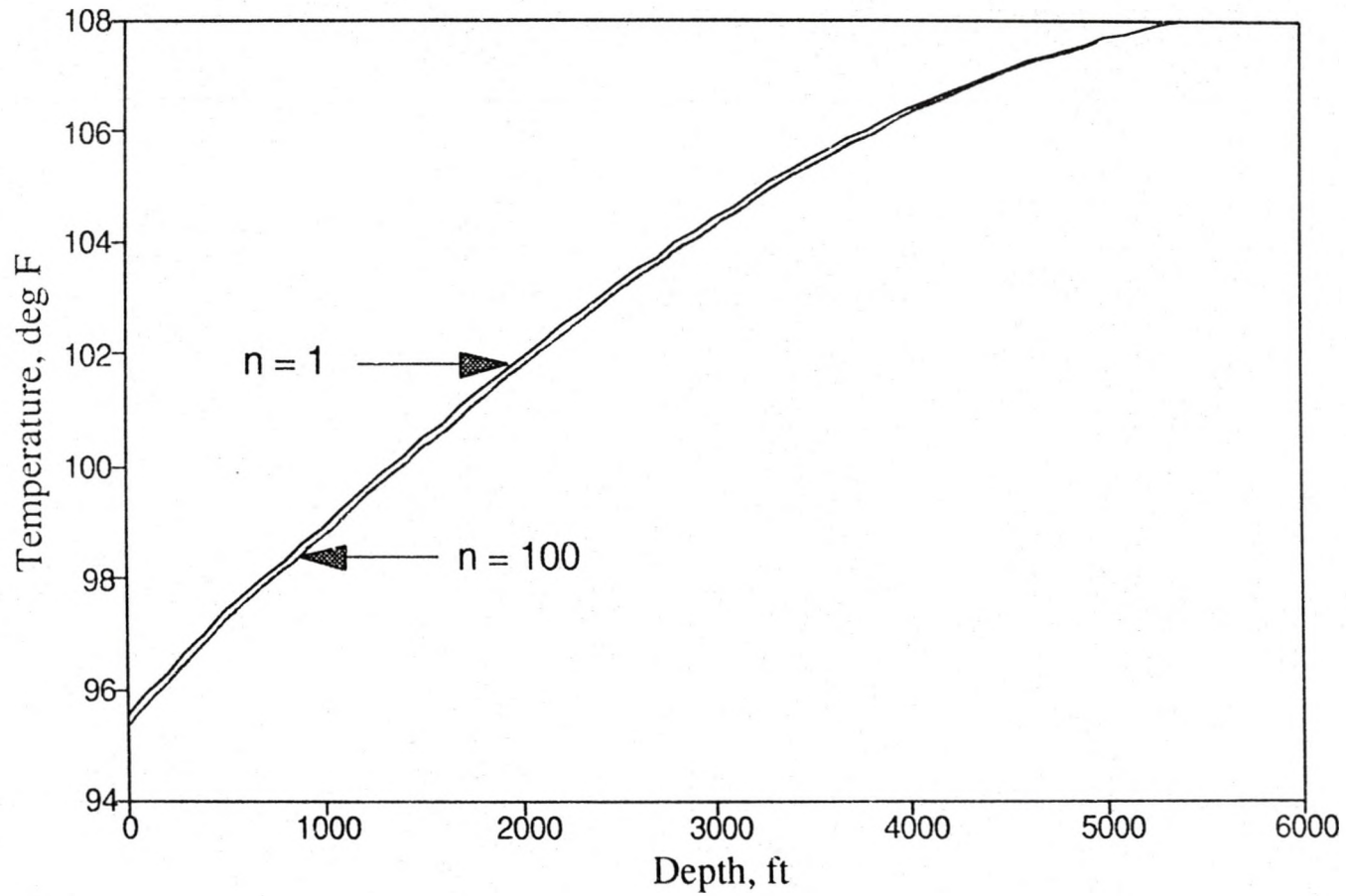
Figure 17.   Temperature vs. Depth in a 5400 ft Wellbore (Numerical Solution)

Heat Flux Profile in the Wellbore
Numerical Solution
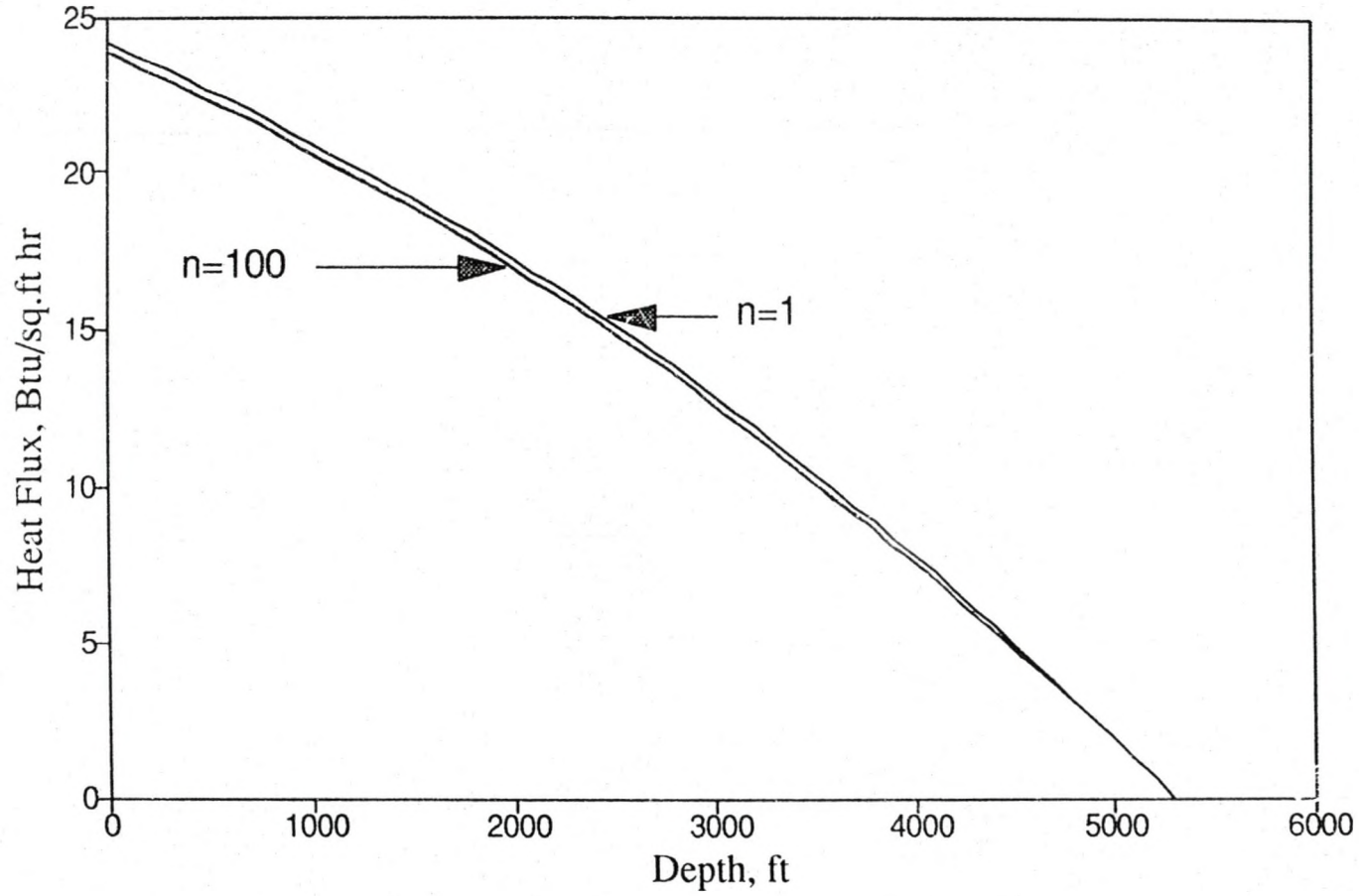
Figure 18. Heat Flux vs. Depth in a 5400 ft Wellbore (Numerical Solution)

5.3 Heat Transfer during Mud Circulation

The knowledge of accurate temperature with time during mud circulation is of prime importance in many operations including drilling, cementing, etc. In the third part of chapter 4, we developed two sets of expressions to estimate circulating fluid temperature in tube and annuli. The first set assumes that heat flux between the annulus fluid and the formation remains constant throughout the whole production time, while the second set accounts for the variation of heat flux with time.

TABLE 4	
Wellbore and Fluid Data during Mud Circulation	
Well Depth, ft	15000.0
Drillstem OD, ft	0.552
Drillbit Size, ft	0.698
Circulation Rate, bbl/hr	300.0
Mud Density, lb/gal	10.0
Formation Density, lb/cu.ft	165.0
Geothermal Gradient	0.0127
Mud Specific Heat, Btu/lb F	0.4
Formation Specific Heat, Btu/lb F	0.2
Mud Viscosity, lb/ft.hr	110.0
Formation Thermal Conductivity, Btu/lb-F	1.3
Mud thermal Conductivity, Btu/lb-F	1.0
Inlet Mud Temperature, F	75.0
Surface Earth Temperature, F	59.5

Both the approaches have been used to estimate the tube and annuli fluid temperatures in a well and the well's description is available in Table 4. The simulations

Temperature Profile in Mud Circulation
Down the Annuli and Up the Tube
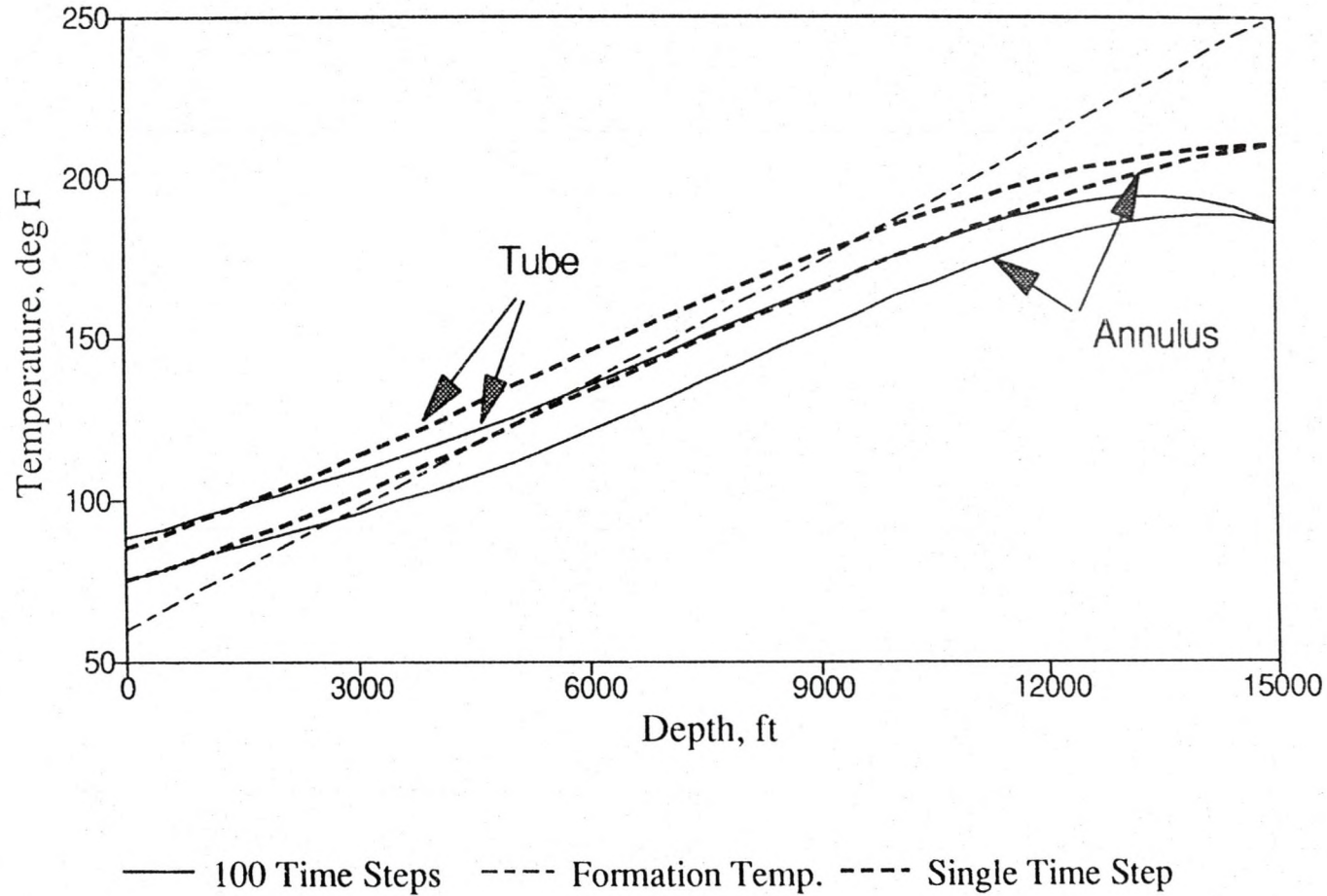
Figure 19. Temperature vs. Depth During Mud Circulation (Down the Annulus, Up the Tube)

Temperature Profile in Mud Circulation
Down the Tube and Up the Annuli
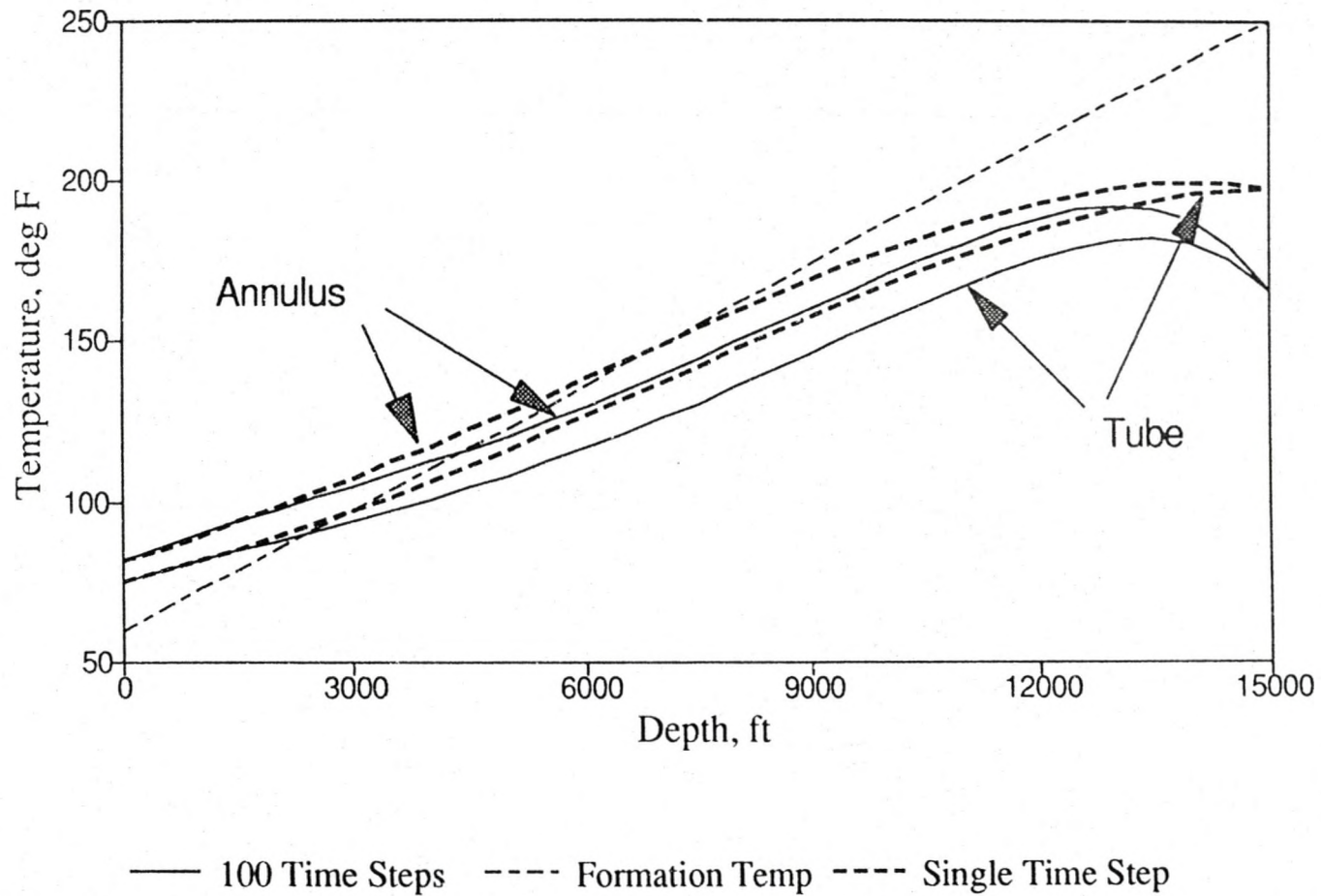
Figure 20. Temperature vs. Depth During Mud Circulation (Down the Tube. Up the Annulus)

were carried out under two different circumstances. In the first case, fluid was assumed to flow down the annulus, and up the tubing, whereas in the second case the flow direction was reversed. While calculating fluid temperature using the varying heat flux concept, the total circulation time was discritized into 100 equal intervals so that convergence could be obtained. The resulting temperature profiles are shown in Figures 19 and 20. A significant difference in temperature profile is observed with the incorporation of varying heat flux concept.

CHAPTER 6

CONCLUSION AND RECOMMENDATION

Conclusions

- A unified model for two-phase flow was developed using the models presently available in the literature. This model was then used to develop a simulator which is useful to the petroleum industry. The simulator first determines the existing flow pattern from flow rates and fluid properties. Then void fraction and pressure gradient were estimated for that pattern. Pressure was taken as the independent variable, and length is calculated for a certain change in pressure. Forward marching technique is used to estimate the length for subsequent pressure change until the total well length is traversed.

- An expression for fluid temperature during production and injection as a function of well depth and operation time was developed from an energy balance between the fluid and the formation. Particular emphasis was given to the appropriate boundary condition in order to account for the variation of heat flux between the wellbore and formation. Significant difference is observerd between the results of the proposed solution and the presently available solution.

- Expressions for fluid temperature in tube and annulus during mud circulation as a function of well depth and circulation time have been developed. Both the cases -

flow down the annulus, up the tube; and flow down the tube, up the annulus, were modeled. The use of superposition principle affects the temperature profiles significantly.

Recommendations

• As the flow pattern changes from bubbly to slug, or slug to churn an abrupt lowering of void fraction is observed. This is due to the higher velocity of Taylor bubbles compared to the smaller bubbles. However, in reality a more gradual transition is expected. We recommend some modifications in the model so that a gradual transition can be accounted for.

• The developed model is applicable only at steady state flow. In practice, under many circumstances, the system does not attain steady state. This type of situations are very common in well testing. Not much work has been done and considerable oppourtunity lies in this area.

• We recommend that the concept of varying heat flux be used in the temperature estimation process during the gas lift operation and also in the pressure transient analysis. The transient heat transfer model presented here could be coupled with the momentum balance in the pressure transient analysis. This heat transfer model would also be useful in various situations where temperature plays an important role, such as in the analysis of transient physical response of the wellbore fluid during phase redistribution.

APPENDICES

APPENDIX A

NOMENCLATURE

A	Inverse relaxation distance , ft (m).
A_n	Inverse relaxation distance for nth time step, ft(m)
B	Constant used in Equation 4.61, defined by Equation 4.62,
c_a	Heat capacity of annulus fluid, Btu/lb °F (kJ/kg °C).
c_p	Heat capacity of wellbore fluid, Btu/lb °F (kJ/kg °C).
c_e	Heat capacity of earth, Btu/lb °F (kJ/kg °C).
C_J	Joule-Thompson coefficient, dimensionless.
C_o	Flow parameter in bubbly flow, dimensionless.
C_1	Flow parameter in slug flow, dimensionless
D	Pipe diameter, ft (m).
D_i	Diameter of inside pipe, ft (m)
D_0	Diameter of outside pipe, ft (m)
E	Entrainment factor, dimensionless
E_g	Gas void fraction, dimensionless
E_1	Liquid Volume Fraction, dimensionless
f	Friction factor, dimensionless.
f_f	Film friction factor in annular flow, dimensionless.
f_g	Gas void fraction, or in-situ volume fraction, dimensionless.
f_m	Friction factor for two-phase flow, dimensionless.
g	Acceleration due to gravity, ft/sec^2 (m/s^2).
g_c	Conversion factor, 32.2 lb$_m$ft/lb$_f$s^2, unity in SI units, dimensionless.
g_T	Geothermal temperature gradient, °F/ft (°C/m).

102

Gr.   Grashof number, defined by Equation 52, dimensionless.

h Heat transfer coefficient, Btu/°F sec ft (kJ/°F s m)

h_c Convective heat transfer coefficient for annulus fluid, Btu/°F s ft (kJ/°C s m)

h_r Radiative heat transfer coefficient for the annulus, Btu/°F sec ft (kJ/°F s m)

h_t Forced convection heat transfer coefficient for the tubing fluid, Btu/°F sec ft (kJ/°C s m)

H Fluid enthalpy, Btu/lb (kJ/kg).

I Definite integral given by Equation 3.23, dimensionless.

J Conversion Factor, 778 ft lb_f/Btu.

J_0 Zero-order Bessel function of the first kind, dimensionless.

J_1 First-order Bessel function of the first kind, dimensionless.

k Conductivity, Btu/ft °F (kJ/m °C).

k_a Conductivity of the annulus fluid Btu/ft °F (kJ/m °C).

k_c Conductivity of the casing material, Btu/ft °F (kJ/m °C).

k_{cem} Cement conductivity, Btu/ft °F (kJ/m °C).

k_e Earth (formation) conductivity, Btu/ft °F (kJ/m °C).

k_{ins} Conductivity of the insulating material, Btu/ft °F (kJ/m °C).

k_t Conductivity of the tubing material, Btu/ft °F (kJ/m °C).

L Length of the well, ft(m)

L_c Length of a *cell* in the cellular model of slug flow, ft (m).

L_s Length of the liquid slug in a *cell* in slug flow, ft (m).

L_T Length of the Taylor bubble portion in a *cell* in slug flow, ft (m).

P Wellbore fluid pressure, psi (kPa).

Pr   Prantl number, defined by Equation 53, dimensionless.

q Heat flow rate from, or to, the wellbore, Btu/hr (kJ/hr).

q_F Heat flow between the formation and wellbore, Btu/hr (KJ/hr)

q_{ta} Heat flow between the tube and annulus, Btu/hr (KJ/hr)

r Radial distance from the wellbore, ft (m).

r_{ci} Inside radius of the casing ft (m).

r_{co} Outside radius of the casing ft (m).

r_{ti}	Inside radius of the tubing ft (m).
r_{to}	Outside radius of the tubing ft (m).
r_{wb}	Outside radius of the wellbore (or cement) ft (m).
t	Time, sec (s).
t_D	Dimensionless time = $\alpha t/r_{wb}$, dimensionless.
T	Temperature, °F (°C).
T_{ci}	Casing inside surface temperature, °F (°C).
T_{co}	Casing outside surface temperature, °F (°C).
T_D	Dimensionless temperature = $(2\pi k_e)(T_{wb} - T_{ei})/(W\phi)$, dimensionless.
T_e	Earth temperature at any given depth and radial distance from well, °F (°C).
T_{ei}	Earth temperature at any given depth and far away from the well, °F (°C).
T_{eibh}	Earth temperature at the bottomhole and far away from the well, °F (°C).
T_{ewh}	Earth temperature at the wellhead and far away from the well, °F (°C).
T_f	Wellbore (tubing) fluid temperature, °F (°C).
T_{ins}	Insulation (outside) surface temperature, °F (°C).
T_{wb}	Wellbore/earth interface temperature, °F (°C).
u	Dummy variable for integration in Eqs. , dimensionless.
V	Fluid velocity, ft/sec (m/s).
V_g	In-situ gas velocity, ft/sec (m/s).
V_{sg}	Superficial gas velocity, ft/sec (m/s).
V_{sl}	Superficial liquid velocity, ft/sec (m/s).
V_m	Two-phase mixture velocity, ft/sec (m/s).
V_t	Terminal rise velocity of small bubbles, ft/sec (m/s).
V_{tT}	Terminal rise velocity of Taylor bubbles, ft/sec (m/s).
W	Total mass flow rate, lb_m/sec (kg/s).
x	Quality, mass fraction of the gas phase, dimensionless.
z	Variable well depth from surface, ft (m).
z_{bh}	Total well depth from surface, ft (m).

105

Greek Letters

α Constant used in the solution of differential equation during mud circulation

α_e Heat transmissivity of earth, $k_e / c_e \rho_e$, ft^2/hr (m^2/hr).

β Constant used in the solution of differential equation during mud circulation

γ Constant used in the solution of differential equation during mud circulation

δ Constant used in the solution of differential equation during mud circulation

θ Pipe inclination angle with horizontal, degree.

μ Fluid viscosity, cp.

ρ Density, lb_m/ft^3 (kg/m^3)

ρ_e Earth density, lb_m/ft^3 (kg/m^3)

ρ_g Gas density, lb_m/ft^3 (kg/m^3)

ρ_l Liquid density, lb_m/ft^3 (kg/m^3)

ρ_m Two-phase mixture density, lb_m/ft^3 (kg/m^3)

σ Surface tension, lb_m/sec^2 (N/m).

λ Constant used in the solution of differential equation during mud circulation

ϕ Heat flux between formation and wellbore, $Btu/ft^2 hr$ $(KJ/m^2 hr)$

χ Constant used in Equation 4.74

ψ Constant used in Equation 4.32, and defined in Equation 4.33.

Ω constant used in Equation 4.112, and defined in Equation 4.113

ξ Constant used in the solution of differential equation during mud circulation

APPENDIX B

OVER-ALL HEAT TRANSFER COEFFICIENT FOR WELLS.

During the production of crudes, the fluid loses heat to the surrounding. Heat being transferred from the wellbore fluid to the earth has to overcome the resistances offered by the tubing wall, the tubing insulation (if any), the tubing-casing annulus, the casing wall, and the cement. This configuration is shown in Figure 21. The resistances are in series, and except for the annulus, the mechanism involved is conductive heat transfer. However, because of the presence of gas or liquid, convective heat transfer dominates in the annulus. In a wellbore/formation system, heat transfer does not really attain steady state. However, heat transfer rate variation is very slow and we assume steady state for a given time period and calculate the overall heat transfer coefficient based on that. In the next time period a new steady state is assumed and a new overall heat transfer coefficient is calculated.

At any steady state, the rate of heat flow through a wellbore per unit length of the well, ϕ, can be expressed as,

$$\phi = 2 \pi r_{to} U_{to} (T_f - T_{wb}) \tag{A.1}$$

where U_{to} is defined as the over-all heat transfer coefficient based on the tubing outside surface area.

106
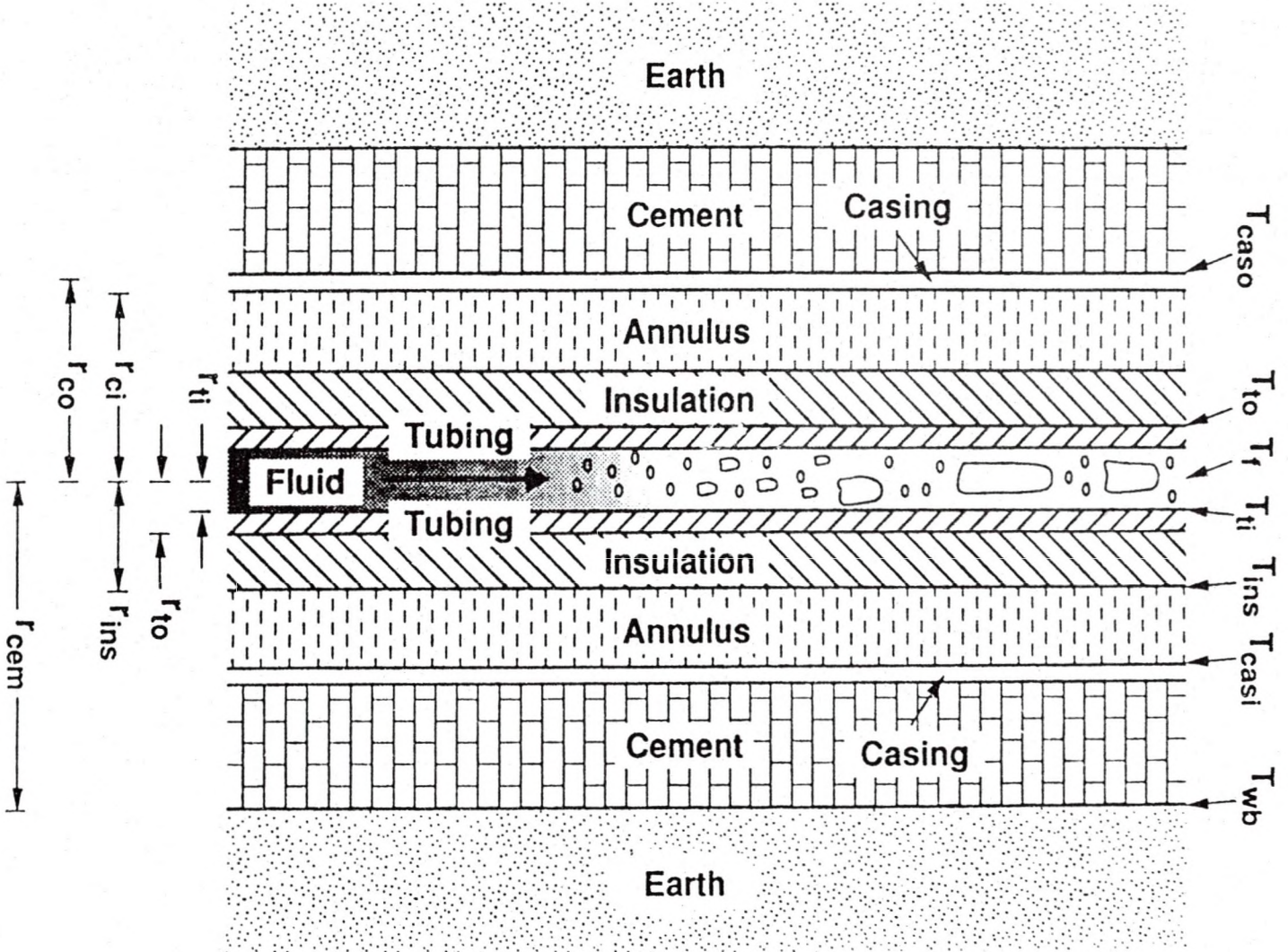
Figure 21. A General Well Configuration involving a variety of elements

107

At steady state, heat flowing through each of the elements mentioned above will be same. This assumption of steady heat transfer allows us to write the rate of heat transfer across each element in terms of the temperature difference across the element and the resistance offered by that element. Thus, the rate of heat transfer between the flowing fluid and inside the tubing wall may be written as,

$$\phi = 2 \pi r_{ti} h_t \left(T_f - T_{ti} \right) \tag{A.2}$$

Equation A.2 may be rewritten for the temperature drop across this element as,

$$T_f - T_{ti} = \frac{\phi}{2 \pi r_{ti} h_t} \tag{A.3}$$

Noting that the sum of the temperature drops across all these elements is equal to the temperature difference between the fluid and the wellbore/earth interface, we can write,

$$T_f - T_{wb} = (T_f - T_{ti}) + (T_{ti} - T_{to})$$
$$+ (T_{to} - T_{ins}) + (T_{ins} - T_{ci})$$
$$+ (T_{ci} - T_{co}) + (T_{co} - T_{wb}) \tag{A.4}$$

Or,

$$T_f - T_{wb} = \frac{\phi}{2 \pi} \left[\frac{1}{r_{ti} h_t} + \frac{\ln \left(r_{to} / r_{ti} \right)}{k_t} + \frac{\ln \left(r_{ins} / r_{to} \right)}{k_{ins}} \right]$$
$$+ \left[\frac{1}{r_{ins} (h_c + h_r)} + \frac{\ln \left(r_{co} / r_{ci} \right)}{k_{cas}} + \frac{\ln \left(r_{wb} / r_{co} \right)}{k_{cem}} \right] \tag{A.5}$$

Or,

$$T_f - T_{wb} = \frac{\phi}{2 \pi r_{to} U_{to}} \tag{A.6}$$

which is another form of Equation A.1, where U_{to} is given by,

$$\frac{1}{U_{to}} = \frac{r_{to}}{r_{ti} h_f} + \frac{r_{to} \ln\left(r_{to}/r_{ti}\right)}{k_t}$$

$$+ \frac{r_{to} \ln\left(r_{ins}/r_{to}\right)}{k_{ins}} + \frac{r_{to}}{r_{ins}\left(h_c + h_r\right)}$$

$$+ \frac{r_{to} \ln\left(r_{co}/r_{ci}\right)}{k_{cas}} + \frac{r_{to} \ln\left(r_{wb}/r_{co}\right)}{k_{cem}} \tag{A.7}$$

Most of the terms in the above Equation can be easily computed except the fourth term. The fourth term, which represents the resistance to heat transfer offered by the annulus, is somewhat difficult to estimate. In most cases of petroleum production, the temperature difference across the annulus, is usually small and one need only to consider convective (natural) heat transfer. Unfortunately, no work on natural convection in vertical annular geometry is reported in the literature. This work adapts, as done by Hasan and Kabir (1991) and Willhite (1967), the correlation proposed by Dropkin and Sommerscales (1965) for heat transfer coefficient for natural convection in fluids between two vertical plates. Their correlation for h_c, expressed for our geometry, is

$$h_c = \frac{0.049 \left(Gr\ Pr\right)^{0.333} Pr^{0.074} k_a}{r_{ins} \ln\left(r_{ci}/r_{ins}\right)} \tag{A.8}$$

The Grashof number Gr, in Equation A.8, is defined as,

$$Gr = \frac{(r_{ci} - r_{ins})^3 \; g \; \rho_a^2 \; \beta \; (T_{ins} - T_{ci})}{\mu_a^2} \qquad (A.9)$$

The Grashof number reflects the extent of motion of the annulus fluid due to the natural convection. The density of the heated fluid next to the insulation layer is less than that next to the casing, creating buoyancy force. The viscous force, working against the buoyancy, generates a circular motion of the fluid in the annulus. Prandtl number, Pr, is a measure of the interaction between the hydrodynamic boundary layer and the thermal boundary layer and is defined as,

$$Pr = \frac{c_{pa} \; \mu_a}{k_a} \qquad (A.10)$$

Not all the components shown in Figure 21 is present in every wells. In addition, some of the elements may offer negligible resistance to heat flow. For example, in most oilwells, tubing insulation is absent. The high values of conductivity of metals, coupled with relatively thin tubing and casing walls, allows us to make the assumption that temperature drop across both the tubing and casing walls may be neglected. In that case, $T_{ti} = T_{to}$ and $T_{ci} = T_{co}$. With this assumption the expression for the overall heat transfer coefficient simplifies to,

$$U_{to} = \left[\frac{1}{h_c} + \frac{r_{to} \; \ln\left(r_{wb}/r_{co}\right)}{k_{cem}} \right]^{-1} \qquad (A.11)$$

We use this equation for estimating the overall heat transfer coefficient, U_{to}. For most oilwells, it adequately represents the overall heat transfer coefficient. In some cases, it is possible to neglect annulus convection in determining the overall heat transfer coefficient. In that case, h_c should be replaced with the conductivity of annular fluid.

PROGRAM LISTING

```
*******************************************************************
*******************************************************************


                    PROGRAM WRITTEN BY
                MOHAMMAD MAHBUBUL AMEEN
            DEPARTMENT OF CHEMICAL ENGINEERING
                UNIVERSITY OF NORTH DAKOTA
                     GRAND FORKS, ND


*******************************************************************
*******************************************************************


$debug

      program flow
      print *,'
      print *,'
      print *,' '
      print *,' '
      print *,' '
      print *,'        *****************************************
     1********'
      print *,'        *****************************************
     1********'
      print *,'        *
     1 *        '
      print *,'        *            Chemical Engr. Deptt.
     1 *  '
      print *,'        *            University of North Dakota.
     1 *  '
```

```
      print *,'                *          Grand Forks, North Dakota 58202.
     1 *     '
      print *,'                *
     1 *     '
      print *,'                *
     1 *     '
      print *,'                *          Welcome to Two-Phase Flow.
     1 *     '
      print *,'                *
     1 *     '
      print *,'                *
     1 *     '
      print *,'                *    This program is written by M. Mahbub Am
     leen      *'
      print *,'                *          and supervised by  Prof. A.R. Hasan
     1 *     '
      print *,'                *
     1 *     '
      print *,'                ******************************************
     1********'
      print *,'                ******************************************
     1********'
      print *,'   '
      print *,'   '
      print *,'Enter 1 if you want to continue'
      read (*,*) iii
      if (iii .eq. 1) go to 601
      print *,'   '
      print *,'   '
      print *,'   '
      print *,'   '
      print *,'   '
      print *,'   '
      print *,'   '
      print *,'   '
      print *,'   '
      print *,'                You have decided not to continue. Bye bye.'
      go to 602
 601  continue
      print *,'   '
      print *,'   '
      print *,'   '
      print *,'   '
      print *,'   '
```

114

```fortran
print *,' '
print *,' '
print *,'
print *,' '
print *,' '
print *,' '
print *,' '
print *,'             You  have  decided to  continue with this '
print *,'          program. So now you have two options. You can '
print *,'          ru.. either  your  own  problem  or a  sample '
print *,'          problem. The  choice  's yours. If  you  want '
print *,'          to run  your  own  problem ,then  enter  2.  '
print *,'          otherwise  for  sample  problem  enter  3.'
print *,' '
print *,' '
print *,' '
print *,' '
print *,' '
print *,' '
print *,' '
print *,' '
print *,' '
print *,' '
read (*,*) jjj
if (jjj .eq. 2) go to 605
if (jjj .eq. 3) go to 606
print *,'             You have selected a wrong option.'
print *,'                Please enter 2 or 3 now.'
print *,' '
print *,' '
print *,' '
print *,' '
print *,' '
print *,' '
print *,' '
print *,' '
print *,' '
print *,' '
print *,' '
print *,' '
read (*,*) jjj
if (jjj .eq. 2) go to 605
if (jjj .eq. 3) go to 606
print *,'                This is not a place for fun. Bye.'
```

```
        go to 602
  605  print *,' '
        print *,'   '
        print *,'            Which condition is known to you ?'
        print *,'            If you know bottom condition, enter 4'
        print *,'            If you know surface condition,enter 5'
        print *,'  '
        print *,'  '
        print *,'  '
        print *,'  '
        print *,'  '
        print *,'  '
        print *,'  '
        print *,'  '
        print *,'  '
        read (*,*) kkk
        if (kkk .eq. 4) go to 607
        if (kkk .eq. 5) go to 608
        print *,'            You have entered a wrong option. '
        print *,'            Please enter 4 or 5 now.        '
        print *,'  '
        print *,'  '
        print *,'  '
        print *,'  '
        print *,'  '
        print *,'  '
        print *,'  '
        print *,'  '
        print *,'  '
        print *,'  '
        print *,'  '
        read (*,*) kkk
        if (kkk .eq. 4) go to 607
        if (kkk .eq. 5) go to 608
        print *,'            This is not a place for fun. Bye.'
        go to 602
  607  a=1.0
        go to 610
  608  a=(-1.0)
  610 continue
        print *,' '
        print *,' '
        print *,' '
```

```
print *,' '
print *,' '
print *,'                    Now you will have to enter some'
print *,'              values. Please remember that this is'
print *,'              not a user friendly program, so if you'
print *,'              make any mistake, then you will have'
print *,'              to restart.'
print *,' '
print *,' '
print *,' '
print *,' '
print *,' '
print *,' '
print *,' '
print *,'Enter the known pressure (in psia)'
read (*,*) p
print *,'Enter the known temperature (in ferenhite)'
read (*,*) tt
print *,'Enter the gor (in scf/stb)'
read (*,*) gor
print *,'   Enter the diameter of the pipe (in ft)'
print *,'[ If annuli, then enter dia of outside pipe ]'
read (*,*) d
print *,' Enter the diameter of inside pipe (in ft)'
print *,'  [ If single pipe,then enter 0 (zero) ]'
read (*,*) din
print *,'Enter the production rate (in stb/day )'
read (*,*) prod
print *,'Enter specefic gravity of gas'
read (*,*) sgg
print *,'Enter the specefic gravity of oil'
read (*,*) sgl
print *,'Enter the value of degree api'
read(*,*) api
print *,'Enter the roughness parameter epsilon'
read (*,*) eps
print *,'Enter the value of delta p   (in +ve psia)'
read (*,*) dp
print *,'Enter depth of the well in feet '
read (*,*) depth
print *,'Enter the value of dt/dz  (in degree f/ foot, +ve) '
read (*,*) dtdz
print *,'Enter the inclination angle with horizontal'
read (*,*) alpha
```

```fortran
      print *,'Enter the value of surface tension (------)'
      read (*,*) surten
      print *,' What is the direction of flow ?'
      print *,'    If upward, enter 1 '
      print *,'   If downward, enter -1'
      read (*,*) cc
      print *,'If the flow is cocurrent, enter 1'
      print *,'But if it is countercurrent, enter -1'
      read (*,*) cc2

      go to 666
      print *,' '
      print *,' '
      print *,' '
      print *,' '
606   print *,'                        You have decided to go for the'
      print *,'               sample problem. Now if would you like to'
      print *,'               see bottom to surface calculation,'
      print *,'               then enter 6, otherwise if you wish to'
      print *,'               see surface to bottom calculation,'
      print *,'               then enter 7.'
      print *,' '
      print *,' '
      print *,' '
      print *,' '
      print *,' '
      print *,' '
      print *,' '
      print *,' '
      print *,' '
      print *,' '
      print *,' '
      read (*,*) lll
      if (lll .eq. 6) go to 611
      if (lll .eq. 7) go to 612
      print *,'            You have entered a wrong option.'
      print *,'                Please enter 6 or 7 now.'


      print *,' '
      print *,' '
      print *,' '
      print *,' '
      print *,' '
```

```
          print *,' '
          print *,' '
          print *,' '
          print *,' '
          print *,' '
          read (*,*) lll
          if (lll .eq. 6) go to 611
          if (lll .eq. 7) go to 612
          print *,'                        This is not a place for fun. Bye.'
          go to 602



611   open (unit=51,file='bot.dat',status='old')
          read (51,*) p,tt,gor,d,din,prod,sgg,sgl,api,eps,dp,depth,dtdz,a,al
          1pha,surten,cc,cc2
          go to 666



612   open (unit=52,file='sur.dat',status='old')
          read (52,*) p,tt,gor,d,din,prod,sgg,sgl,api,eps,dp,depth,dtdz,a,al
          1pha,surten,cc,cc2



666   open (unit=8,file='res3.dat',status='old')
          write (8,*)'                        input data'
          write (8,552)
552   format ('                        ******************'.///)
          write (8,550)
550   format (3x,'    pressure',4x,'temperature ',3x,'gas oil ratio',3x,
          1'    diameter',4x,'production'./)
          write (8,551)p,tt,gor,d,prod
551   format (5f15.6./)
          write (8,553)
553   format (3x,'   s.G.(Gas)',4x,'s.G.(Liquid)',3x,'    alpha    ',3x,
          1'    epsilon',4x,'    delta p'./)
          write (8,554)sgg,sgl,alpha,eps,dp
554   format (5f15.6./)
          write (8,555)
555   format (19x,'   depth ',3x,'    dt/dz    './)
          write (8,556)depth,dtdz
556   format (15x,2f15.6.///)
          write (8,*)'                        output data'
          write (8,557)
557   format ('                        ******************'.///)
```

```
   open (unit=6,file='res1.dat',status='old')
      write (6,500)
500  format (//,5x,'pressure',5x,'   eg   ',5x,'pipe length',5x,'para
     1meter nnn')
      write (6,504)
504  format (5x,'========',5x,'==========-=',5x,'===========',5x,'=======
     1======'./)

      g=32.2
      gc=32.174
      degree=0.0174532*alpha
      dz=0.0
      wp=p
      wtt=tt
      sumh=0.0
      sumf=0.0
      sumv=0.0
      write (6,505) p,tt,dz
505  format (5x,f8.2,5X,f10.4,5X,f10.4./)


 50  continue
      call overall (p,tt,d,gor,prod,sgg,sgl,api,eps,g,gc,dpdzt,nnn,a,dpd
     1zh,dpdzf,dpdzv,degree,eg,din,surten,cc,cc2,alpha,valphat,vmix,vsg)
      dzdp=1.0/dpdzt
      dzdp01=dzdp
      p01=p
      tt01=tt
      tt=tt+dtdz*dzdp01*dp
      p=p-dp*a
      dpdzh1=dpdzh
      dpdzf1=dpdzf
      dpdzv1=dpdzv


      call overall (p,tt,d,gor,prod,sgg,sgl,api,eps,g,gc,dpdzt,nnn,a,dpd
     1zh,dpdzf,dpdzv,degree,eg,din,surten,cc,cc2,alpha,valphat,vmix,vsg)
      dzdp=1.0/dpdzt
      dzdp02=dzdp
      tt=tt01+dtdz*dzdp01*dp*0.5
      P=p01-dp*0.5*a
      dpdzh2=dpdzh
      dpdzf2=dpdzf
      dpdzv2=dpdzv
```

```
      call overall (p,tt,d,gor,prod,sgg,sgl,api,eps,g,gc,dpdzt,nnn,a,dpd
     1zh,dpdzf,dpdzv,degree,eg,din,surten,cc,cc2,alpha,valphat,vmix,vsg)
      dzdp=1.0/dpdzt
      dzdp03=dzdp
      dpdzh3=dpdzh
      dpdzf3=dpdzf
      dpdzv3=dpdzv


      dzdpa=(dzdp01+dzdp02+4.0*dzdp03)/6.0
      dpdzha=(dpdzh1+dpdzh2+dpdzh3*4.0)/6.0
      dpdzfa=(dpdzf1+dpdzf2+dpdzf3*4.0)/6.0
      dpdzva=(dpdzv1+dpdzv2+dpdzv3*4.0)/6.0

      p=p01-dp*a
      tt=tt01+dtdz*dzdpa*dp
      dzv=(-dzdpa)*dp*a
      dz=dz+dzv

      pipel=dz/sin(degree)
      write (6,501) p,eg,pipel,nnn,valphat,vmix,vsg
  501 format (5x,f8.2,5X,f10.4,5X,f10.4,11X,i2,3f10.6)

      sumh=sumh+dpdzha
      sumf=sumf+dpdzfa
      sumv=sumv+dpdzva
      checka=depth-dzv
      if (dz .gt. checka) go to 745
      go to 50

  745 checkb=depth-dz
      coeff=checkb/dzv
      p04=p
      tt04=tt
      p=p-0.5*dp*coeff*a
      tt=tt+dtdz*dzdpa*0.5*dp*coeff
      call overall (p,tt,d,gor,prod,sgg,sgl,api,eps,g,gc,dpdzt,nnn,a,dpd
     1zh,dpdzf,dpdzv,degree,eg,din,surten,cc,cc2,alpha,valphat,vmix,vsg)

      dpp=dpdzt*checkb
      p=p04+dpp
      tt=tt04-dtdz*dpp*a/dpdzt
      dz=dz+checkb
```

```
      sumh=sumh+dpdzh
      sumf=sumf+dpdzf
      sumv=sumv+dpdzv
      suma=(sumh+sumf+sumv)
      frach=sumh/suma
      fracf=sumf/suma
      fracv=sumv/suma
      delp=abs(wp-p)
      delph=delp*frach
      delpf=delp*fracf
      delpv=delp*fracv

      write (6,502)
502   format ('*********************************************')
      pipelen=depth/sin(degree)
      write (6,503)p,eg,pipelen
503   format (5x,f8.2,5X,f10.4,5X,f10.4)



      write (8,560)
560   format (7x,'pressure',3x,' temperature','  parameter nnn',8x,'delp
     1(h)',7x,'delp (f)',/)
      write (8,561)p,tt,wnnn,delph,delpf
561   format (5f15.5,//)


      print *,' '
      print *,' '
      print *,' '
      print *,'               data entered by the user '
      print *,'               **********************'
      print *,' '
      print *,'   pressure    temperature    delta p    diame
     1ter'

c     print *,'   --------    -----------    -------    -----
c     1---'
      print *,wp,wtt,dp,d
      print *,' '
      print *,'     s.g.(gas)    s.g.(liquid)    production    go
     1r'
c     print *,'     ---------    ------------    ----------    ---
c     1--'
      print *,sgg,sgl,prod,gor
      print *,' '
```

```
      print *,'          alpha          depth          epsilon       dt/
     1dz'
c     print *,'          -----          -------        ---------     ----
c    1---'
      print *,alpha,depth,eps,dtdz
      print *,' '
      print *,' '
      print *,'                A very brief look at the results'
      print *,'                  (Conditons at the other end)'
      print *,'       Detailed results are in res1.dat, res2.dat, res3.dat
     1files'
      print *,'    ****************************************************
     1***** '
      print *,' '
      print *,'       presssure      temperature       nnn          dp/
     1dz'
c     print *,'       ---------      -----------       -------       -----
c    1---'
      wnnn= nnn
      print *,p,tt,wnnn,dpdzt
      print *,' '
      print *,'    delta p(t)      delta p(h)      delta p(f)      delt
     1a p(v)'
c     print *,'    ----------      ----------      ----------      ----
c    1------'

      print *,delp,delph,delpf,delpv
      go to 629
602   continue
      print *,' '
      print *,' '
      print *,' '
      print *,' '
      print *,' '
      print *,' '
      print *,' '
      print *,' '
      print *,' '
      print *,' '
      print *,' '
      print *,' '
      print *,' '
629   continue
      end
```

```
$debug
      subroutine overall (p,tt,d,gor,prod,sgg,sgl,api,eps,g,gc,dpdzt,nnn
     1,a,dpdzh,dpdzf,dpdzv,degree,eg,din,surten,cc,alpha,valphat,vmix,vs
     1g)

      call property (p,tt,d,gor,prod,sgg,sgl,api,vsg,vsl,rhog,rhol,fg,rs
     1,din)

c     print *, 'temperature in ferenhite =',tt,'     free gas =',fg
c     print *, 'density  of gas =',rhog,'   density of liquid =',rho
c     print *, 'velocity of gas =',vsg,'velocity of liquid =',vsl

      call viscosit (tt,visg,visl,rs)

      call pattern (vsg,vsl,vmix,rhog,rhol,rhoc,rhom,visg,visl,d,eg,nnn,
     1g,degree,din,surten,cc,alpha,valphat)

c     print *,' eg =',eg,rhol,rhog,rhom

      call gradient (vsg,vmix,rhol,rhom,rhoc,visg,visl,eps,d,eg,p,dpdzt,
     1g,gc,nnn,a,dpdzh,dpdzf,dpdzv,degree,din,cc)

      return
      end




$debug
      subroutine property (p,tt,d,gor,prod,sgg,sgl,api,vsg,vsl,rhog,rhol
     1,fg,rs,din)

      t=tt+460.0
      if (api .Le. 10.0) go to 103
      qmo=650.0-11.0*api+(1.9E-7)*(api**5.0)
      fl=(p*sgg)/t

      if (fl .ge. 1.0) go to 101
      yg=0.43*fl**1.2-0.12*fl**4.0
      go to 102
101   yg=0.56*alog10(fl)+0.315
```

```
102  continue

     rs=((379.3*350.0*sgl)/qmo)*(yg/(1.0-yg))
     go to 111

103  continue

     rs=sgg*((p/18.0)*((10**(0.0125*api))/(10**(0.00091*tt))))**1.20481
     193

111  fg=gor-rs
     if (fg .gt. 0.0) go to 112
     rs=gor
     fg=0.0

112  pc=692.0-30.0*sgg-8.0*sgg**2.0
     pr=p/pc
     tc=162.0+328.0*sgg
     tr=t/tc

     prtr=pr/(tr**2.0)
C    if (tr .lt. 1.1 .or. prtr .gt. 1.0) go to 106

     cm=0.51*tr**(-4.133)
     cn=0.038-0.026*tr**(0.5)
     if (tr .gt. 2.4) go to 104
     zzz=0.0003
     go to 105
104  zzz=0.0007
105  z= 1.0-cm*pr+cn*pr**2.0+zzz*pr**3.0
C 106  continue

c    Calculate by some other method in this space

     area=(3.1416*(d**2.0-din**2.0)/4.0)
     bo=0.972+0.000147*((rs*(sgg/sgl)**0.5)+1.25*tt)**1.175
     r=10.73
     print *,'area =',area,p
     vsg=(fg*prod*t*14.69*z)/(24.0*3600.0*520.0*p*area)
     vsl=(prod*bo*6.49*10.0**(-5.0))/area
     rhog=(29.0*sgg*p)/(z*r*t)

     rhol=(350.4*sgl+rs*sgg*0.0764)/(5.615*bo)
     open (unit=7,file='res2.dat',status='old')
```

```
      write (7,505)p,tt,fl,yg,qino,rs,fg,z,rhog,rhol,vsg,vsl
505   format (2x,12f9.3)
      return
      end




$debug
      subroutine pattern (vsg,vsl,vmix,rhog,rhol,rhoc,rhom,visg,visl,d,e
     1g,nnn,g,degree,din,surten,cc,alpha,valphat)


c     check for bubbly flow


      valpha=1.53*((g*surten*((rhol-rhog)/(rhol**2)))**0.25)
      c0=1.2
      if (cc .eq. -1) c0=1.12
      vmix=vsl+vsg
      eg=vsg/(c0*vmix+cc*valpha)
      rhom=rhol*(1.0-eg)+rhog*eg


c     first check


      check1=(0.429*vsl+cc*0.357*valpha)*sin(degree)
      if (check1 .gt. vsg) go to 150


c     second check


      de=d-din
      check2=4.68*(de**0.48)*((g*((rhol-rhog)/surten))**0.5)*((surten/rh
     1ol)**0.6)*((rhol/visl)**0.08)
      check3=vmix**1.12
      if (check3 .gt. check2 .and. eg .lt. 0.52) go to 150
      go to 151


c     bubbly flow

150   if (vsg .le. 0.000000001) go to 152
      nnn=1
      go to 200
152   nnn=0
      go to 200
```

```
c       no bubbly flow

  151   continue

c       check for slug flow

        if (check3 .lt. check2) go to 170
        go to 171

c       slug flow

  170   nnn=2
        go to 199

c       no slug flow

  171   continue

c       check for churn flow

        check9=3.1*(surten*g*(rhol-rhog)/(rhog**2.0))**0.25
        if (check9 .gt. vsg) go to 173
        go to 181

  173   nnn=3
        c1=1.15
        if (alpha .le. 70) c1=1.2
        if (cc .eq. -1)    c1=1.12
        go to 197

  199   c1=1.2
        if (cc .eq. -1) c1=1.12
  197   continue

c       Calculation of v(alpha-t) follows, then eg and rhom

        anf=(((de**3.0)*g*(rhol-rhog)*rhol)**0.5)/visl
        aneo=(g*(de**2)*(rhol-rhog))/surten
        if (anf .gt. 250.0) go to 155
        if (anf .gt. 18.0) go to 156
        am=25.0
        go to 159
  155   am=10.0
```

```
       go to 159
156  am=69.0*(anf**0.35)
159  continue
     ca2=0.345*(1.0-exp((-0.01)*anf/0.345))*(1.0-exp((3.37-aneo)/am))

     valphat=(0.345+0.1*(din/d))*((sin(degree))**0.5)*((1+cos(degree))*
    1*1.2)*((g*d*(rhol-rhog)/rhol)**0.5)
C    print *,'valphat =',valphat, valpha

     egt=vsg/(c1*vmix+cc*valphat)
     if (vsg .le. 1.312333) go to 166

     qlsl=0.1*((c0*vmix+cc*valpha)/vsg)
     qltl=1.0-qlsl
     eg=qltl*egt+0.1
     go to 167

166  qlsl=0.0762*(c0*vmix+cc*valpha)
     qltl=1.0-qlsl
     eg=qltl*egt+0.0762*vsg

167  rhom=rhog*eg+rhol*(1.0-eg)
     go to 200

c    Annular flow ( no check needed )

181  nnn=4
     xx=(vsg*rhog)/(vsg*rhog+vsl*rhol)
     x=((rhog/rhol)**0.5)*(((1.0-xx)/xx)**0.9)*((visl/visg)**0.1)
     eg=(1.0+x**0.8)**(-0.378)

     vcgs=(vsg*visg*(rhog/rhol)**0.5)/surten
     if (vcgs .ge. 0.0004) go to 185
     e=0.0055*((vcgs*10000.0)**2.86)
     go to 186

185  e=0.857*(log10(vcgs*10000.0))-0.2
186  continue
c    Another way of calculating eg

     rhoc=(vsg*rhog+e*vsl*rhol)/(vsg+e*vsl)
200  continue
     return
     end
```

```
$debug
      subroutine viscosit (tt,visg,visl,rs)

c     calculation of viscosity

c     dead oil

      dla=1.54*10.0**8.0
      dlm=3.12
      Visdl=dla/(tt**dlm)

c     live oil

      ela=0.6*exp((-0.0032)*rs)+0.4*exp((-0.00011)*rs)
      elb=0.3*exp((-0.0035)*rs)+0.7*exp((-0.00022)*rs)
c     visl=(ela*visdl**elb)*0.0006719
      visl=0.000672

C     Program needed to evaluate gas viscosity & liq. surface tension

      visg=0.00000672
      return
      end




$debug
      subroutine gradient (vsg,vmix,rhol,rhom,rhoc,visg,visl,eps,d,eg,p,
     1dpdzt,g,gc,nnn,a,dpdzh,dpdzf,dpdzv,degree,din,cc)

c     gradient for annular flow

      de=d-din
      if (nnn .ne. 4) go to 201
      reg=(0.975*de*vsg*rhoc)/visg

      fc=0.0791*(1.0+75.0*(1.0-eg))/(reg**0.25)
      dpdzx=(+1.0)*((g*rhoc)+(2.0*fc*cc*rhoc*vsg**2.0)/(d*sin(degree)))/
     1(gc*144.0*(1.0-(rhoc*vsg**2.0)/(p*144*gc*sin(degree))))
      dpdzt=dpdzx*(-a)
      open (unit=11, file='res4.dat',status='old')
```

```fortran
      write(11,1001)p,rhoc,reg fc,dpdzt
 1001 format (2x,2f8.3,1X,1f12.3,1X,2f10.3)
      go to 300


c     Common calculation for bubbly, slug and churn

 201  re=(de*vmix*rhol)/visl
      fa=((eps/de)**1.1098)/2.8257+(7.149/re)**0.8981
C     f=(1.0/(4.0*log((eps/d)/3.7065-(5.0452*log(fa))/re)))**2.0
      if (re .gt. 100000) go to 202
      f=0.0791/(re**0.25)
      go to 203
 202  f=0.046/(re**(0.2))
 203  if (nnn .le. 1) go to 211


c     gradient for slug and churn flow

      dpdzf=(((-2.0*cc*a)*f*vmix**2.0*rhol*(1.0-eg))/(gc*d))/sin(degree)
      dpdzh=((a*(-rhom)*g)/gc*sin(0.0174532*90))
      dpdzv=0.0

      dpdzt=(dpdzf+dpdzh+dpdzv)/144.0

      open (unit=12,file='res5.dat',status='old')
      write (12,1002)p,rhom,re,f,dpdzt
 1002 format (2x,f10.3,2X,f8.5,2X,f12.3,1X,2f10.3)
      go to 300


c     gradient for bubblyflow

 211  dpdzf=(((-2.0*cc*a)*f*vmix**2.0*rhom)/(gc*de))/sin(degree)
      dpdzh=(a*(-rhom)*g)/gc*sin(0.0174532*90)
      dpdzv=0.0
      dpdzt=(dpdzf+dpdzh+dpdzv)/144.0
      open (unit=13,file='res6.dat',status='old')
      write (13,1003)p,rhom,re,f,dpdzt
 1003 format (2x,f10.3,2X,f8.5,2X,f12.3,1X,2f10.3)
 300  continue
      return
      end
```

```
$debug
c      subroutine super

       real kann,kcem,kfor
       dimension dqr'z(110,1'0),consp(110,110)
       dimension tin.e(110).(imed(110),timedd(110,110),timerd(110,110)
       dimension tdd(1/0,110)

c      This program calculates the fluid temperature
c      using superposition

       data  cpliq, cpgas / 0.947, 0.200 /
       data  kann, kcem, kfor / 0.383, 4.021, 0.83 /
       data  dia, dcin, dcout, dcem / 0.2376, 0.5375, 0.5833, 0.75 /
       data  alpha, beta, geograd / 0.04, 0.00011, 0.005926 /
       data  p, gor, api, sgg / 113, 68, 34.3, 1.04 /

C      istep= # of time steps.
C      kstep= # length of depth step.
C      nflag= 1 for analytical solution.
C             2 for linear variation of phi.
C      mflag= 4 includes convection
c             5 excludes convection

       print *,' enter the value of istep, kstep, nflag & mflag'
       read (*,*) istep,kstep,nflag,mflag

       zbh=5400
       tforbi=108
       tottim=158

c      viscosity and rhol should come from another subroutine.

       visl=3.8
       rhol=62.3

C      wg and wl comes from main prog.

       wg=0.00
       wl=2.46

       wtot=wg+wl
       qual=wg/wtot
       cpm=cpgas*qual+cpliq*(1-qual)
```

```
        klstep=zbh/kstep
        kk=klstep+2
        do 19 k=2,kk,1
        dqdz(1,k)=0.0
        dqdz(2,k)=0.0
19    continue

        cons=-0.002978+1.006E-6*p+1.906E-4*wtot-1.047E-6*gor+3.229E-5*api+
        14.009E-3*sgg-0.3551*geograd

        timed(1)=0.0
        timed(2)=0.0

        delti=tottim/istep
        ii=istep+2
        do 29 l=3,ii,1
        time(l)=time(l-1)+delti
29    continue

        do 401 l=3,ii,1
        timed(l)=4*alpha*time(l)/(dcem**2)

        do 402 m=1,l-1,1
        timedd(l,m)=timed(l)-timed(m)
        timerd(l,m)=timedd(l,m)**0.5
        tdd(l,m)=(0.4063+0.5*log(timedd(l,m)))*(1+0.6/timedd(l,m))
        if (timedd(l,m) .le. 1.5) Tdd(l,m)=1.12812*timerd(l,m)*(1-0.3*time
        1rd(l,m))

402   continue

401   continue

        do 777 i=3,ii,1

        dz=0.0
        tfluid=tforbi

        do 888 j=2,kk,1

        z=zbh-dz
        dt=5.00

100   Iter=0
```

```
         go to 102

101   dt=dto+(dt-dto)*0.2

102   continue

      kfor=0.83
C     if (z .lt. 1001) kfor= 1.4-0.00057*z

      if (mflag .eq. 5) go to 105

      prnum=(cpliq*visl)/kann
      gras=((((3600**2)*32.2)/8)*((dcin-dia)**3)*(rhol**2)*beta*dt)/visl
     1**2
      convec=0.049*((prnum*gras)**0.333)*(prnum**0.074)*kann
      if (convec .le. kann)  go to 106
      go to 107
105   kfor=kfor*1.687

106   convec=kann

107   resann=((0.5*dia)*log(dcin/dia))/convec
      rescem=((0.5*dia)*log(dcem/dcout))/kcem
      uto=1/(rescem+resann)

      tfor=tforbi+geograd*(-dz)
c     print *, cpm,wtot,kfor,tdd(i,i-1),dia,uto

      afact=((cpm*wtot*3600)*(kfor+tdd(i,i-1)*(dia/2)*uto))/(3.1416*dia*
     1kfor*uto)

      bfact=(kfor+(dia/2)*uto*tdd(i,i-1))/((dia/2)*uto)
c     print *, afact,bfact

      sum=0.0
      do 403 l=3,i,1
      sum=sum+(dqdz(l-1,j)-dqdz(l-2,j))*tdd(i,l-2)

403   continue

      if (nflag .eq. 2) go to 39

      if (z .eq. zbh) go to 37
      dqdz(i,j)=((cpm*(tfor-tfluid))/afact)+(tdd(i,i-1)*dqdz(i-1,j)/bfac
```

```
1t)-(sum/bfact)

      go to 36

37    dqdz(i,j)=0.0

36    dto=dt

      consp(i,j)=cons+((tdd(i,i-1)*dqdz(i-1,j))/(cpm*bfact))-(sum/(bfact
     1*cpm))

      tfact=afact*(-1.0/(778*cpm)+consp(i,j)+geograd)
      expo=exp((-zbh+z)/afact)
      if (expo .eq. 1.0) expo=0.99999
      tfluid=tfor+tfact-expo*(tfact)

      q1=-dqdz(i,j)*wtot*3600

      if (mflag .eq. 5) Go to 45

      dt=(-dqdz(i,j)*wtot*3600)/((3.1416*dia)*convec)

      go to 47

39    if (z .eq. zbh) go to 301
      dqdz(i,j)=((cpm*(tfor-tfluid))/(afact*(zbh-z)))+(tdd(i,i-1)*dqdz(i
     1-1,j)/bfact)-(sum/bfact)
      go to 302
301   dqdz(i,j)=0.0
302   dto=dt

      ft=geograd-(tdd(i,i-1)*afact*dqdz(i-1,j))/(bfact*cpm)+(afact*sum)/
     1(cpm*bfact)

      tfact=afact*(-1.0/(778*cpm)+cons+ft)
      expo=exp((-zbh+z)/afact)
      if (expo .eq. 1.0) expo=0.99999
      tfluid=tforbi-(zbh-z)*ft+tfact-expo*(tfact)
      q1=-dqdz(i,j)*(zbh-z)*wtot*3600

      if (mflag .eq. 5) go to 45
      dt=(-dqdz(i,j)*(zbh-z)*wtot*3600)/((3.1416*dia)*convec)

47    continue
```

```
c       print *,z,dqdz(i,j)
        if (dt .le. 0.0000001)  dt=0.00001
        cky001=abs((dt-dto)/dt)
        iter=iter+1

        if (iter .gt. 199) go to 45
        if (cky001 .ge. 0.001) go to 101

45      continue

        if (i .eq. ii) go to 10

        if (z .eq. 5400) go to 10
        if (z .eq. 5300) go to 10
        if (z .eq. 5200) go to 10
        if (z .eq. 5100) go to 10
        if (z .eq. 5000) go to 10
        if (z .eq. 4500) go to 10
        if (z .eq. 4000) go to 10
        if (z .eq. 3500) go to 10
        if (z .eq. 3000) go to 10
        if (z .eq. 2500) go to 10
        if (z .eq. 2000) go to 10
        if (z .eq. 1500) go to 10
        if (z .eq. 1000) go to 10
        if (z .eq. 500) go to 10
        if (z .eq. 100) go to 10
        if (z .eq. 000 ) go to 10

        go to 12

10      open (unit=7,file='ress.dat',status='old')
        write(7,11)z,tfor,tfluid,dt,q1,afact,bfact,uto
11      format (8f12.5)
12      tfluid=tfluid-geograd*0.5*kstep
888     dz=dz+kstep

        print *,'  I =',i,'  j =',j

777     dtime=dtime+delti

        stop
        end
```

```
$debug
      program dan

c     This program calculates the fluid temperature (in the tube &
c     in the annuli) using superposition. Numerical solution
c     wt & wa same.

      real kfor
      dimension dqdz(220,110)
      dimension time(110),timed(110),timedd(110,110),timerd(110,110)
      dimension tdd(220,110),tft(500),tfa(500)

c     This program calculates the fluid temperature
c     using superposition

c     Down the annuli & up the tube, mmm=+1
c     Down the tube & up the annuli, mmm=-1

      data   cpliq, cpgas / 0.400, 0.200 /
      data   kfor, mmm / 1.30, -1 /
      data   diat, diaa / 0.46875, 0.697916 /
      data   alpha, geograd / 0.039, 0.0127 /
      data   uta, utt / 32.1, 30.0 /

      print *,' enter the value of istep and kstep '
      read (*,*) istep,kstep

      zbh=5000
      tforti=59.5
      tai=75.0
      tti=75.0
      tottim=44.17
      delz=50

c     Viscosity and rhol should come from another subroutine.

      visl=3.8
      rhol=62.3

C     wg and wl comes from main prog.

      wg=0.00
      wl=35.0
```

```
      wtot=wg+wl
      qual=wg/wtot
      cpm=cpgas*qual+cpliq*(1-qual)

      klstep=zbh/kstep
      kk=klstep+2
      kkk=kk-2
      do 19 k=2,kk,1
      dqdz(1,k)=0.0
      dqdz(2,k)=0.0
19    continue

      timed(1)=0.0
      timed(2)=0.0

      delti=tottim/istep
      ii=istep+2
      do 29 l=3,ii,1
      time(l)=time(l-1)+delti
29    continue

      do 401 l=3,ii,1
      timed(l)=4*alpha*time(l)/(diaa**2)

      do 402 m=1,l-1,1
      timedd(l,m)=timed(l)-timed(m)
      timerd(l,m)=timedd(l,m)**0.5
      tdd(l,m)=(0.4063+0.5*log(timedd(l,m)))*(1+0.6/timedd(l,m))
      if (timedd(l,m) .le. 1.5) tdd(l,m)=1.12812*timerd(l,m)*(1-0.3*time
     1rd(l,m))
402   continue
401   continue

      do 777 i=3,ii,1

      zbh=5000
      tforti=59.5
      tai=75.0
      tti=75.0
      tft(2)=tti
      tfa(2)=77

      z=0.0
      dz=0.0
```

```
      do 888 j=2,kkk,1
      z=dz
      z1=z+50
      z2=z1+50

100   continue

      tfor=tforti+geograd*dz
      afact=((cpm*wtot*3600)*(kfor+tdd(i,i-1)*(diaa/2)*uta))/(3.1416*dia
     1a*kfor*uta)
      bfact=(kfor+(diaa/2)*uta*tdd(i,i-1))/((diaa/2)*uta)
      bbfact=(wtot*3600*cpm)/(2*3.1416*(diat/2)*utt)

      sum=0.0
      do 403 l=3,i,1
      sum=sum+(dqdz(l-1,j)-dqdz(l-2,j))*tdd(i,l-2)
403   continue

      dqdz(i,j)=((cpm*(tfor-tfa(j)))/afact)+(tdd(i,i-1)*dqdz(i-1,j)/bfac
     1t)-(sum/bfact)

c     q1=-dqdz(i,j)*wtot*3600
      con1=((afact*dqdz(i-1,j))/(bfact*cpm))*tdd(i,i-1)
      con2=(afact/(cpm*bfact))*sum

      if (mmm .Eq. -1) go to 22

      tlam1=(-1/(2*afact))+(1/(2*afact))*sqrt(1+4*((diaa/2)*uta*tdd(i,i-
     11)+kfor)*(((diat/2)*utt)/((diaa/2)*uta*kfor)))

      tlam2=(-1/(2*afact))-(1/(2*afact))*sqrt(1+4*((diaa/2)*uta*tdd(i,i-
     11)+kfor)*(((diat/2)*utt)/((diaa/2)*uta*kfor)))

      talpha=-((tai-tforti-con1+con2)*tlam2*exp(tlam2*zbh)+geograd*(1-tl
     1am2*bbfact))/(tlam1*(exp(tlam1*zbh))*(1-tlam2*bbfact)-tlam2*(exp(t
     1lam2*zbh))*(1-tlam1*bbfact))

      tbeta= ((tai-tforti-con1+con2)*tlam1*exp(tlam1*zbh)+geograd*(1-tla
     1m1*bbfact))/(tlam1*(exp(tlam1*zbh))*(1-tlam2*bbfact)-tlam2*(exp(tl
     1am2*zbh))*(1-tlam1*bbfact))
c     print *,tlam1,tlam2,talpha,tbeta

      if (j .eq. 2) then
```

```
        tft(j)=tai

        tft(j+1)=(1-tlam1*bbfact)*talpha*exp(tlam1*z1)+(1-tlam2*bbfact
     1)*tbeta*exp(tlam2*z1)+geograd*z+tforti+con1-con2

        tft(j+2)=-((delz**2)/(afact*bbfact))*(bbfact*(tft(j+1)-tft(j))
     1/delz-tft(j)+tforti+geograd*z+con1-con2)+2*tft(j+1)-tft(j)

        der0=(tft(j+1)-tft(j))/delz
        tfa(j)=tft(j)+bbfact*der0
        tfa(j+1)=tft(j+1)+bbfact*der0

        der1=(tft(j+2)-tft(j+1))/delz
        tfa(j+2)=tft(j+2)+bbfact*der1

      else

        tft(j+2)=-((delz**2)/(afact*bbfact))*(bbfact*(tft(j+1)-tft(j))
     1/delz-tft(j)+tforti+geograd*z+con1-con2)+2*tft(j+1)-tft(j)

        der1=(tft(j+2)-tft(j+1))/delz
        tfa(j+2)=tft(j+2)+bbfact*der1
        print *,z,der1
      end if


c     tft=talpha*exp(tlam1*z1)+tbeta*exp(tlam2*z)+geograd*z1+bbfact*geog
c     1rad+tforti+con1-con2

      go to 24

22    tlam1=(1/(2*afact))+(1/(2*afact))*sqrt(1+4*((diaa/2)*uta*tdd(i,i-1
     1)+kfor)*(((diat/2)*utt)/((diaa/2)*uta*kfor)))

      tlam2=(1/(2*afact))-(1/(2*afact))*sqrt(1+4*((diaa/2)*uta*tdd(i,i-1
     1)+kfor)*(((diat/2)*utt)/((diaa/2)*uta*kfor)))

      tgamma=-((tti-tforti+bbfact*geograd-con1+con2)*tlam2*exp(tlam2*zbh
     1)+geograd)/(tlam1*(exp(tlam1*zbh))-tlam2*(exp(tlam2*zbh)))

      tdelta= ((tti-tforti+bbfact*geograd-con1+con2)*tlam1*exp(tlam1*zbh
     1)+geograd)/(tlam1*(exp(tlam1*zbh))-tlam2*(exp(tlam2*zbh)))

c     tft=tgamma*exp(tlam1*z)+tdelta*exp(tlam2*z)+geograd*z-bbfact*geogr
```

```fortran
c       1ad+tforti+con1-con2

c       tfa=(1+tlam1*bbfact)*tgamma*exp(tlam1*z)+(1+tlam2*bbfact)*tdelta*e
c       1xp(tlam2*z)+geograd*z+tforti+con1-con2
        if (j .eq. 2) then

            tft(j)=tti

            tft(j+1)=tgamma*exp(tlam1*z1)+tdelta*exp(tlam2*z1)+geograd*z1-
         1bbfact*geograd+tforti+con1-con2          !-0.0062

            tft(j+2)=((delz**2)/(afact*bbfact))*(bbfact*(tft(j+1)-tft(j))/
         1delz+tft(j)-tforti-geograd*z2-con1+con2)+2*tft(j+1)-tft(j)

c           print *,j,tft(j+1),tft(j+2)

            der00=(tft(j+1)-tft(j))/delz
            der01=(tft(j+2)-tft(j+1))/delz
            der0=der00-(der01-der00)

            print *,der00,der01,der0

            tfa(j)=tft(j)+bbfact*der0
            tfa(j+1)=tft(j+1)+bbfact*der00
            tfa(j+2)=tft(j+2)+bbfact*der01

        else

            tft(j+2)=((delz**2)/(afact*bbfact))*(bbfact*(tft(j+1)-tft(j))/
         1delz+tft(j)-tforti-geograd*z2-con1+con2)+2*tft(j+1)-tft(j)

            der1=(tft(j+2)-tft(j+1))/delz
            tfa(j+2)=tft(j+2)+bbfact*der1

        end if

24      open (unit=7,file='ress.dat',status='old')

        if (j .eq. 2) then

        write (7,13) z,tfa(j),tft(j),con1,con2

13      format (5f12.5)
```

```fortran
      else
      write(7,11)z2,tfa(j+2),tft(j+2),con1,con2
11    format (5f12.5)
      end if
888   dz=dz+kstep

      print *,' I =',i,' j =',j

777   dtime=dtime+delti

      stop
      end


$debug
      program da

c     This program calculates the fluid temperature (in the tube &
c     in the annuli) using superposition.
C     wt & wa same.

      real kfor
      dimension dqdz(100,60)
      dimension time(100),timed(100),timedd(100,100),timerd(100,100)
      dimension tdd(100,100)

c     This program calculates the fluid temperature
c     using superposition

c     Down the annuli & up the tube, mmm=+1
c     Down the tube & up the annuli, mmm=-1

      data  cpliq, cpgas / 0.400, 0.200 /
      data  kfor / 1.30 /
      data  diat, diaa / 0.46875, 0.697916 /
      data  alpha, geograd / 0.039, 0.0127 /
      data  uta, utt / 32.1, 30.0 /

      print *,' enter the value of istep, kstep and mmm'
      read (*,*) istep,kstep,mmm

      zbh=15000
      tforti=59.5
      tai=75.0
```

```
        tti=75.0
        tottim=44.17

C       viscosity and rhol should come from another subroutine.

        visl=3.8
        rhol=62.3

C       wg and wl comes from main prog.

        wg=0.00
        wl=35.0

        wtot=wg+wl
        qual=wg/wtot
        cpm=cpgas*qual+cpliq*(1-qual)

        klstep=zbh/kstep
        kk=klstep+2
        do 19 k=2,kk,1
        dqdz(1,k)=0.0
        dqdz(2,k)=0.0
19      continue

        timed(1)=0.0
        timed(2)=0.0

        delti=tottim/istep
        ii=istep+2

        do 29 l=3,ii,1
        time(l)=time(l-1)+delti
29      continue

        do 401 l=3,ii,1

        timed(l)=4*alpha*time(l)/(diaa**2)

        do 402 m=1,l-1,1

        timedd(l,m)=timed(l)-timed(m)
        timerd(l,m)=timedd(l,m)**0.5

        tdd(l,m)=(0.4063+0.5*log(timedd(l,m)))*(1+0.6/timedd(l,m))
```

```
      if (timedd(l,m) .le. 1.5) tdd(l,m)=1.12812*timerd(l,m)*(1-0.3*time
    1rd(l,m))

402   continue

401   continue

      do 777 i=3,ii,1

      zbh=15000
      tforti=59.5
      tai=75.0
      tfa=tai

      z=0.0
      dz=0.0

      do 888 j=2,kk,1

      z=dz

100   continue

      tfor=tforti+geograd*(dz)

      afact=((cpm*wtot*3600)*(kfor+tdd(i,i-1)*(diaa/2)*uta))/(3.1416*dia
    1a*kfor*uta)
      bfact=(kfor+(diaa/2)*uta*tdd(i,i-1))/((diaa/2)*uta)
      bbfact=(wtot*3600*cpm)/(2*3.1416*(diat/2)*utt)

      sum=0.0
      do 403 l=3,i,1
      sum=sum+(dqdz(l-1,j)-dqdz(l-2,j))*tdd(i,l-2)

403   continue

      dqdz(i,j)=((cpm*(tfor-tfa))/afact)+(tdd(i,i-1)*dqdz(i-1,j)/bfact)-
    1(sum/bfact)

      q1=-dqdz(i,j)*wtot*3600

      con1=(((afact*dqdz(i-1,j))/(bfact*cpm)))*tdd(i,i-1)
      con2=(afact/(cpm*bfact))*sum
```

```
      if (mmm .eq. -1) go to 22

      tlam1=(-1/(2*afact))+(1/(2*afact))*sqrt(1+4*((diaa/2)*uta*tdd(i,i-
     11)+kfor)*(((diat/2)*utt)/((diaa/2)*uta*kfor)))

      tlam2=(-1/(2*afact))-(1/(2*afact))*sqrt(1+4*((diaa/2)*uta*tdd(i,i-
     11)+kfor)*(((diat/2)*utt)/((diaa/2)*uta*kfor)))

      talpha=-((tai-tforti-con1+con2)*tlam2*exp(tlam2*zbh)+geograd*(1-tl
     1am2*bbfact))/(tlam1*(exp(tlam1*zbh))*(1-tlam2*bbfact)-tlam2*(exp(t
     1lam2*zbh))*(1-tlam1*bbfact))

      tbeta= ((tai-tforti-con1+con2)*tlam1*exp(tlam1*zbh)+geograd*(1-tla
     1m1*bbfact))/(tlam1*(exp(tlam1*zbh))*(1-tlam2*bbfact)-tlam2*(exp(tl
     1am2*zbh))*(1-tlam1*bbfact))

      tft=talpha*exp(tlam1*z)+tbeta*exp(tlam2*z)+geograd*z+bbf ct*geogra
     1d+tforti+con1-con2

      tfa=(1-tlam1*bbfact)*talpha*exp(tlam1*z)+(1-tlam2*bbfact)*tbeta*ex
     1p(tlam2*z)+geograd*z+tforti+con1-con2

      go to 24

22    tlam1=(1/(2*afact))+(1/(2*afact))*sqrt(1+4*((diaa/2)*uta*tdd(i,i-1
     11)+kfor)*(((diat/2)*utt)/((diaa/2)*uta*kfor)))

      tlam2=(1/(2*afact))-(1/(2*afact))*sqrt(1+4*((diaa/2)*uta*tdd(i,i-1
     11)+kfor)*(((diat/2)*utt)/((diaa/2)*uta*kfor)))

      tgamma=-((tti-tforti+bbfact*geograd-con1+con2)*tlam2*exp(tlam2*zbh
     1)+geograd)/(tlam1*(exp(tlam1*zbh))-tlam2*(exp(tlam2*zbh)))

      tdelta= ((tti-tforti+bbfact*geograd-con1+con2)*tlam1*exp(tlam1*zbh
     1)+geograd)/(tlam1*(exp(tlam1*zbh))-tlam2*(exp(tlam2*zbh)))

      tft1=tft
      tft=tgamma*exp(tlam1*z)+tdelta*exp(tlam2*z)+geograd*z-bbfact*geogr
     1ad+tforti+con1-con2

      tfa=(1+tlam1*bbfact)*tgamma*exp(tlam1*z)+(1+tlam2*bbfact)*tdelta*e
     1xp(tlam2*z)+geograd*z+tforti+con1-con2
```

```
c  23    print *,afact,tlam1,tlam2,tgamma,tdelta

   24    open (unit=7,file='ress.dat',status='old')
         write(7,11)z,tfor,tft,tfa,dqdz(i,j),con1,con2
   11    format (7f12.5)

  888    dz=dz+kstep

         print *,'  I =',i,'  j =',j

  777    dtime=dtime+delti

         stop

         end
```

APPENDIX D

PROFILES IN A 8000 FT OILWELL

TABLE 5	
Wellbore and Fluid Data During Production	
Well Depth , ft	8000
Production Rate, lb/hr	8856
Tube Diameter, in	2.875
Casing Diameter, in..	7.0
Wellbore Diameter, in...	9.0
Specific Gravity of Crude, API...	34.3
Formation Thermal Conductivity, Btu/hr ft F............	0.83
Cement Thermal Conductivity, Btu/hr ft F................	4.021
Annular Thermal Conductivity, Btu/hr ft F................	0.383
Specific Heat of fluid, Btu/lb F................................	0.947
Surface Earth Temperature, F...................................	76
Geothermal Gradient,...	0.005926

Temperature Profile in the Wellbore
Constant Psi, With Convection
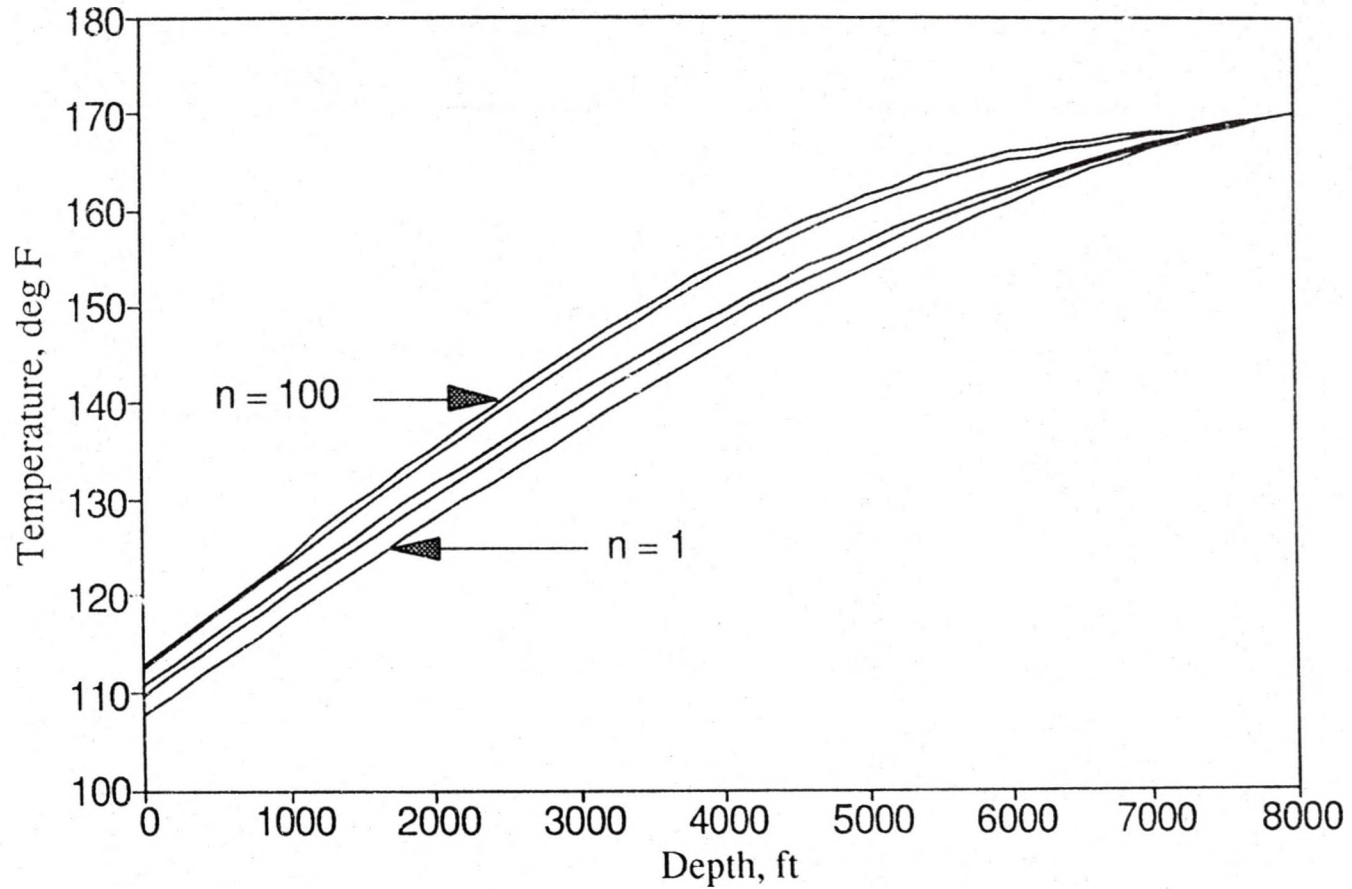
Figure 22. Temperature vs. Depth in a 8000 ft Wellbore (Constant ψ and With Convection)

Heat Flux Profile in the Wellbore
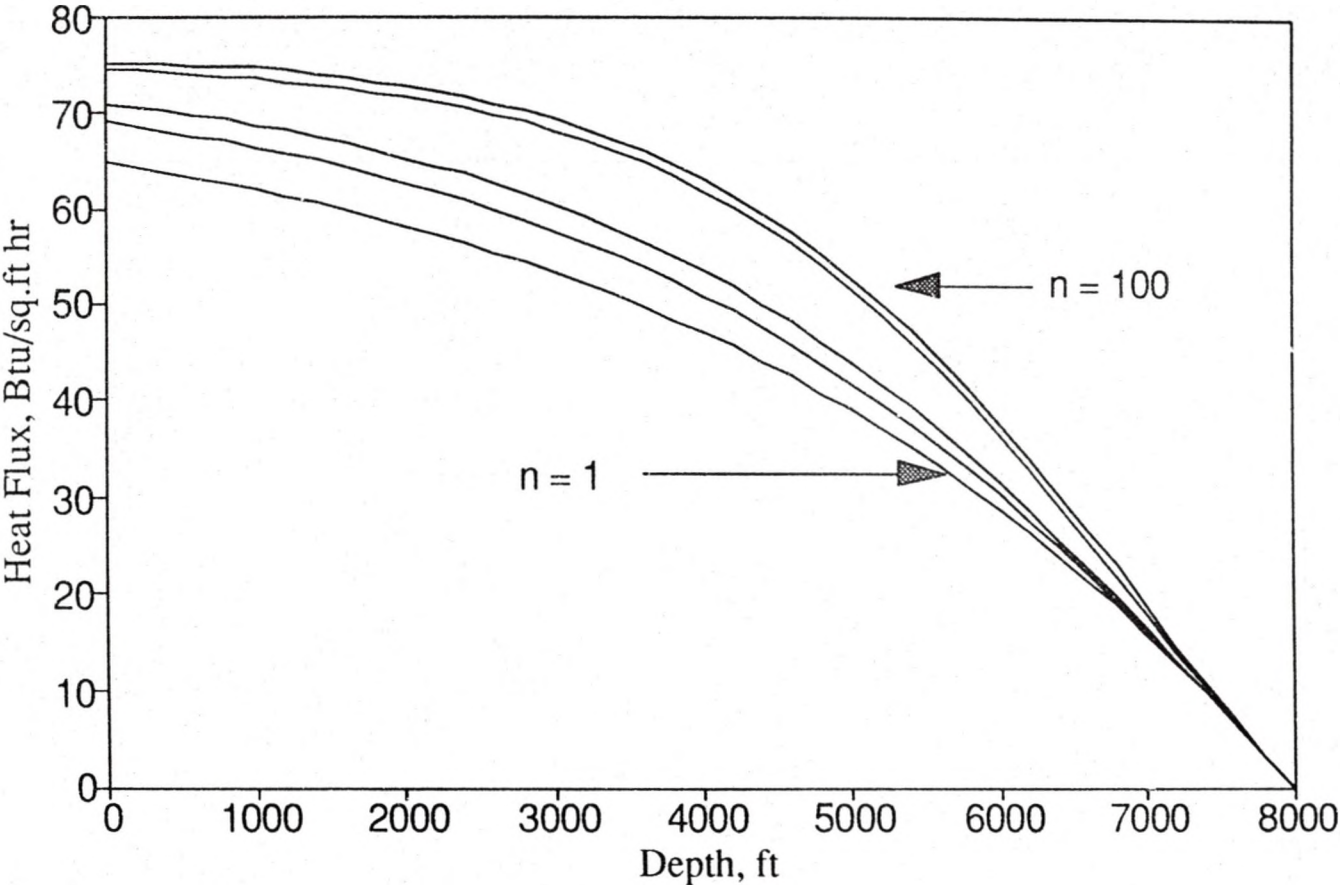### Constant Psi, With Convection

Figure 23.   Heat Flux vs. Depth in a 8000 ft Wellbore (Constant ψ and With Convection)

Temperature Profile in the Wellbore
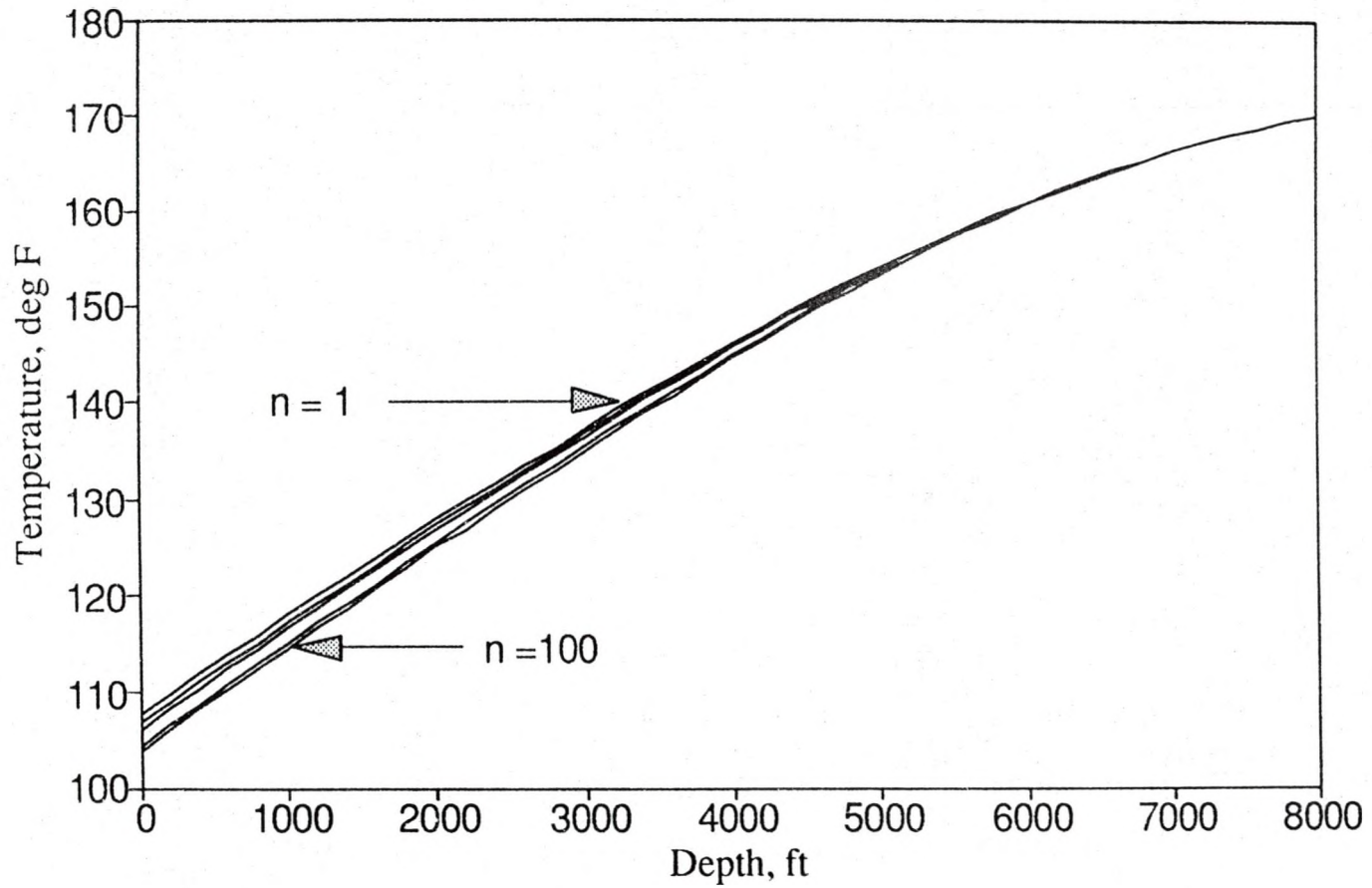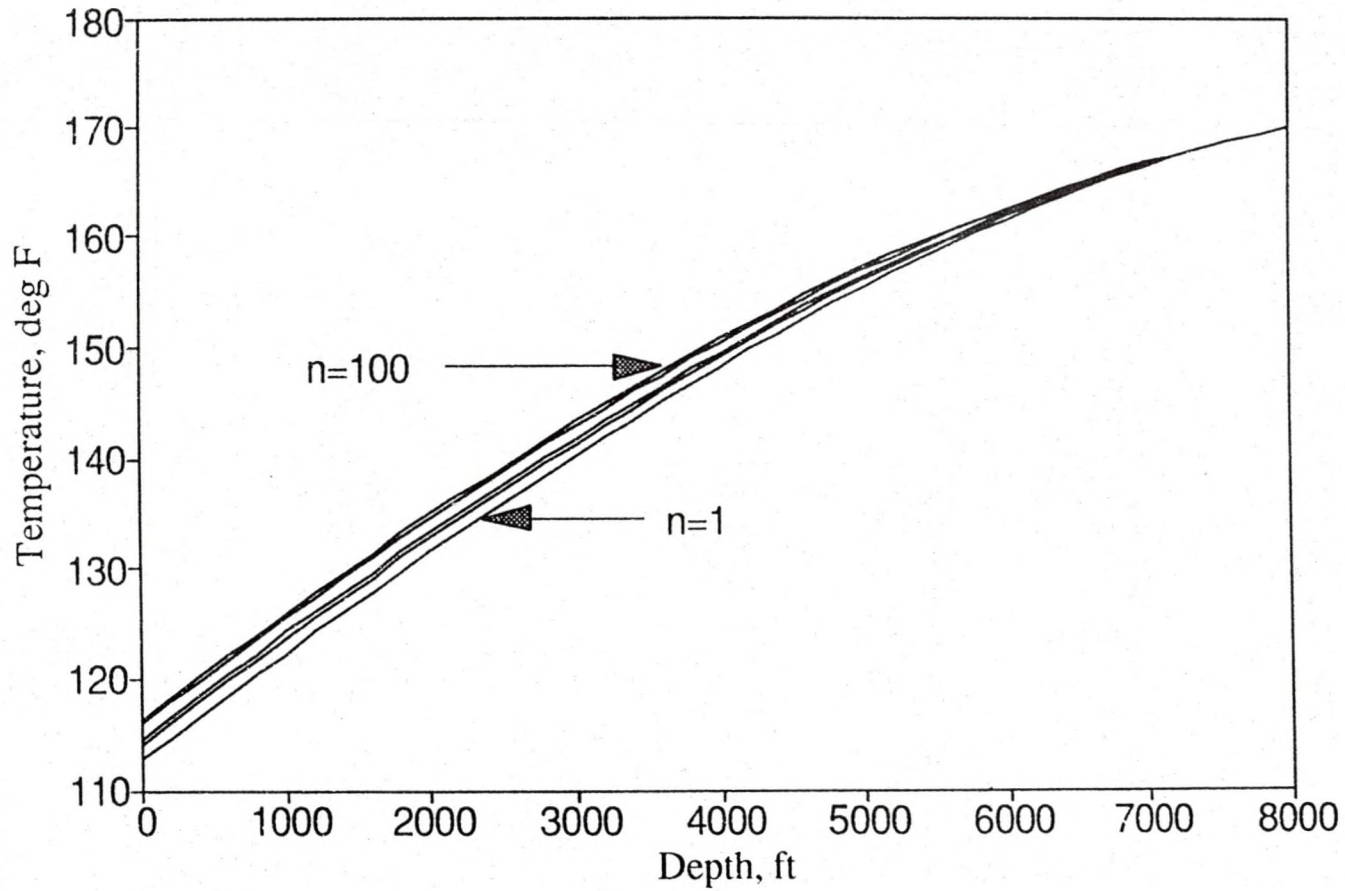## Linear Phi, With Convection

Figure 24. Temperature vs. Depth in a 8000 ft Wellbore (Linear Heat Flux and With Convection)

Heat Flux Profile in the Wellbore
Linear Phi, With Convection
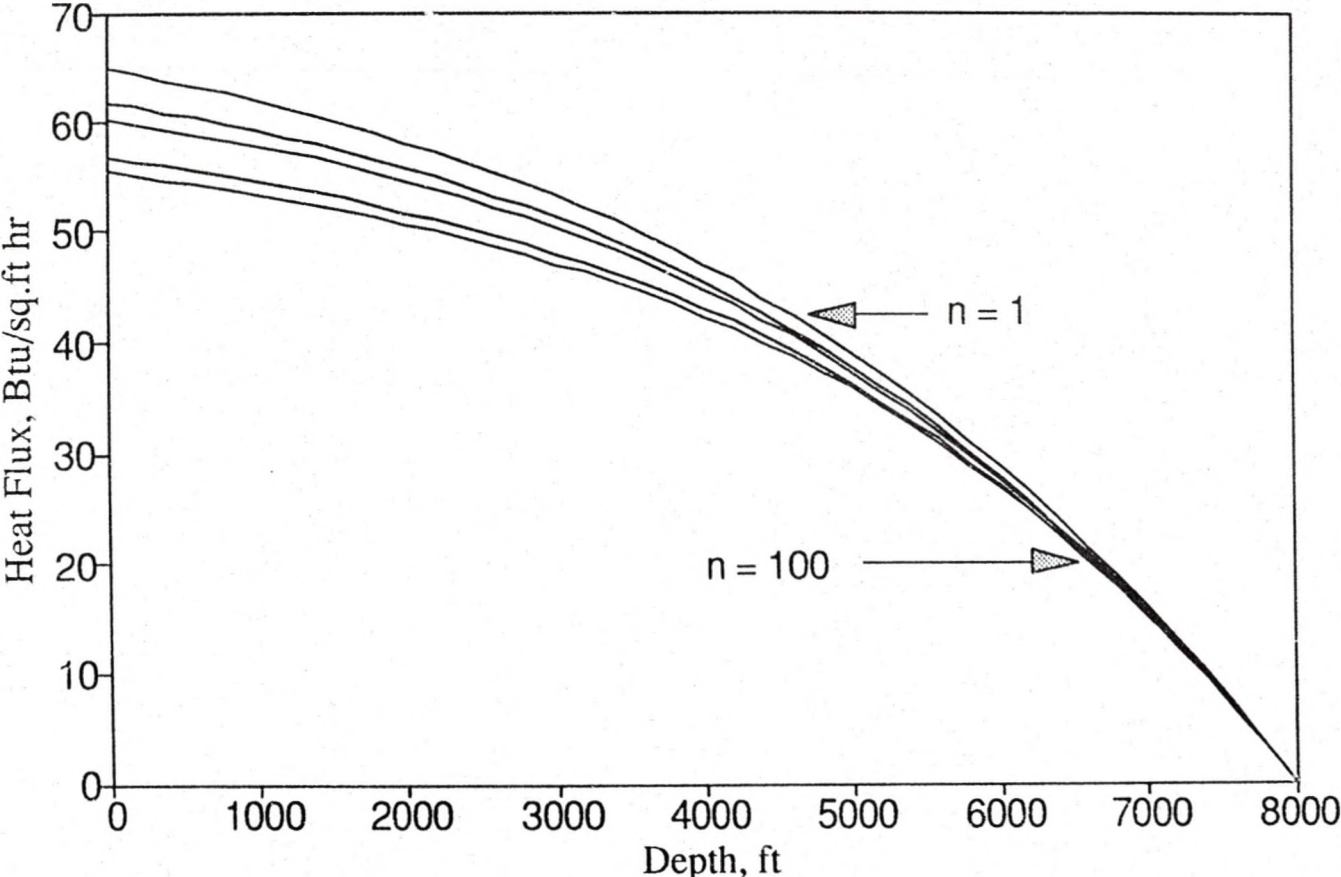
Figure 25.   Heat Flux vs. Depth in a 8000 ft Wellbore (Linear Heat Flux
and With Convection)

Temperature Profile in the Wellbore
Constant Psi, Without Convection

Figure 26. Temperature vs. Depth in a 8000 ft Wellbore (Constant ψ and Without Convection)

Heat Flux Profile in the Wellbore
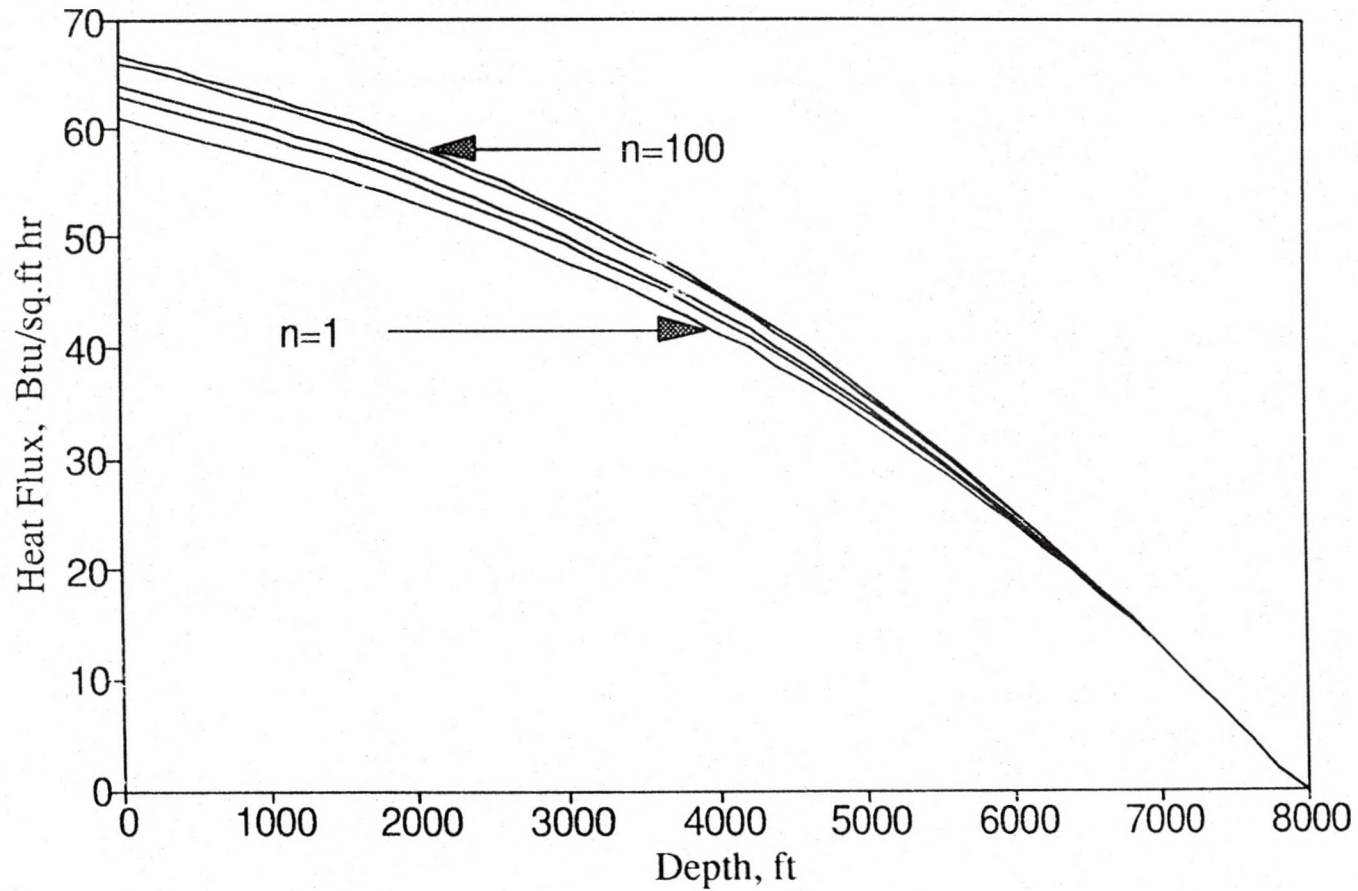## Constant Psi, Without Convection

Figure 27. Heat Flux vs. Depth in a 8000 ft Wellbore (Constant ψ and Without Convection)

Temperature Profile in the Wellbore
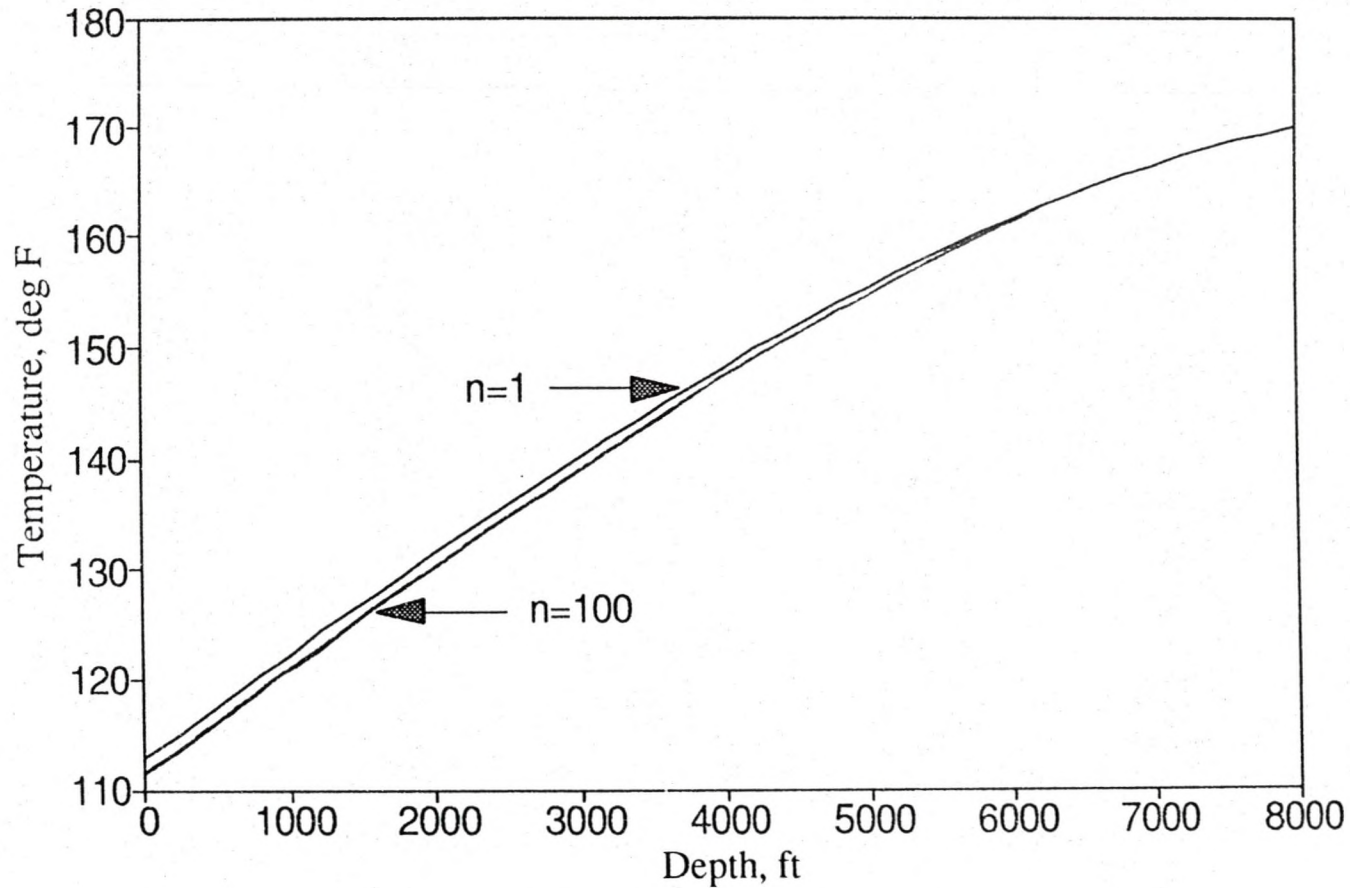## Linear Phi, Without Convection

Figure 28. Temperature vs. Depth in a 8000 ft Wellbore (Linear Heat Flux and Without Convection)

Heat Flux Profile in the Wellbore
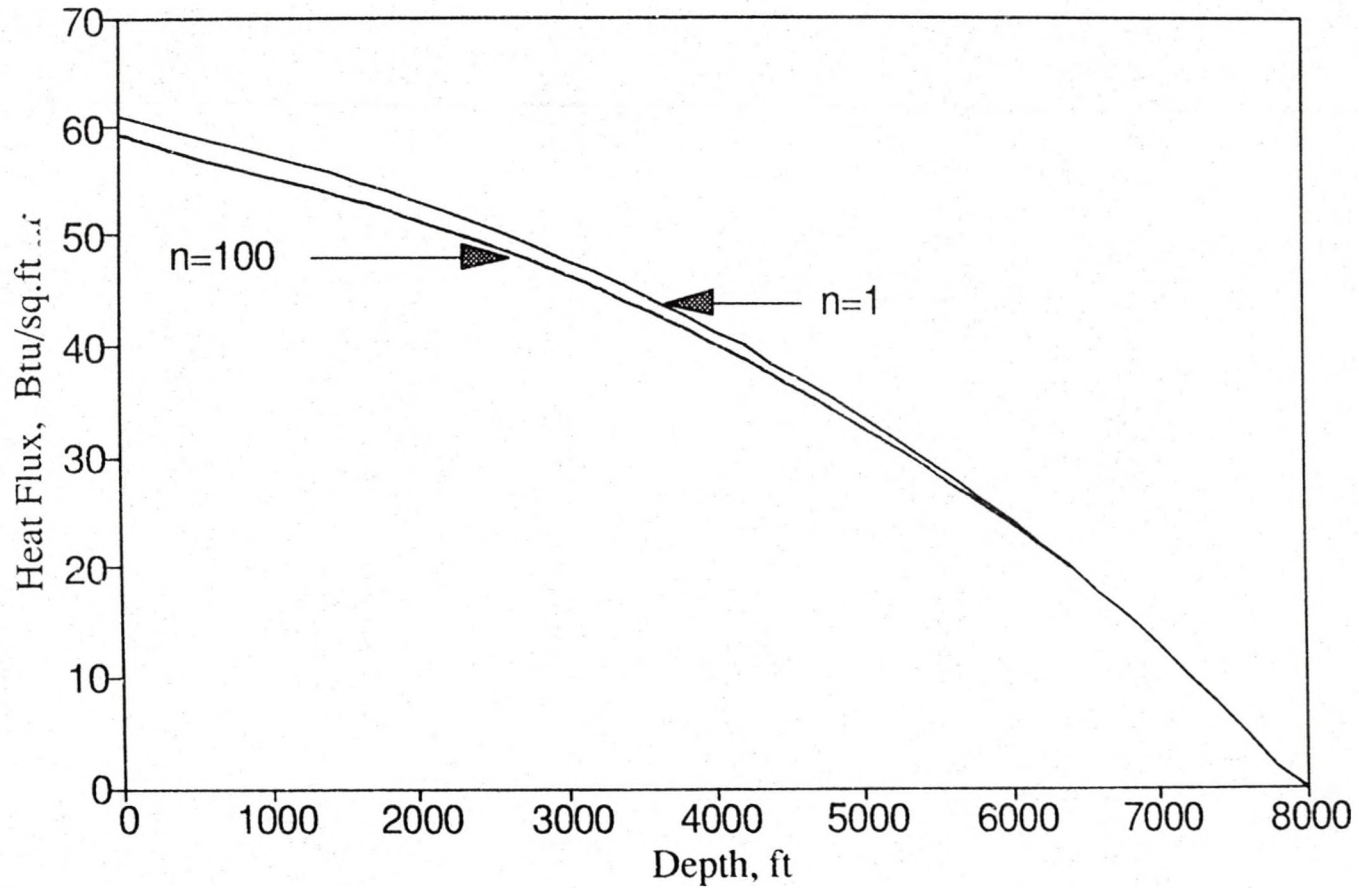## Linear Phi, Without Convection

Figure 29. Heat Flux vs. Depth in a 8000 ft Wellbore (Linear Heat Flux and Without Convection)

REFERENCES

Aziz, K., Govier, G.W. and Fogarasi, M.: "Pressure drop in Wells Producing Oil and Gas," *J. Cdn. Pet. Tech.* (July-Sept.1972) 38-47.

Barnea, D., Shoham, O., Taitel, Y., and Dukler, A. E.: "Gas-Liquid Flow in Inclined Tubes: Flow Pattern Transition for Upward Flow," *Chem. Engr. Sci.* **40**, (1985) 131-36.

Brauner, N. and Barnea, D.: "Slug/Churn Transition in Upward Gas-Liquid Flow. *Chem. Engr. Sci.* **41**, (1986) 159-162.

Beggs, H.D. and Brill, J.P.: " A Study of Two-Phase Flow in Inclined Pipes," *J. Pet. Tech.* (May, 1973) 607-17

Bird, J.M.: "Interpretation of Temperature Logs in Water-and Gas-Injection Wells and Gas-Producing Wells," *Drill and Prod. Prac.* API (1954) 187-95.

Bird, R.B., Stewart, W.E., and Lightfoot, E.N.: *Transport Phenomena*, John Wiley and Sons, Inc., New York (1960) 285-288.

Brauner, N. and Barnea, D.: "Slug/churn Transition in Upward Gas-liquid Flow," *Chem. Engr. Sci.*, **41**, (1986) 159-162.

Carslaw, H.S. and Jaeger, J.C.: *Conduction of Heat in Solids*, Oxford U. Press, Amen House, London (1950).

Dropkin, D., and Sommerscales, E.: "Heat Transfer by Natural Convection in Liquids Confined by Two Parallel Plates Inclined at Various Angles with Respect to the Horizontal," *J. Heat Transfer; Trans., ASME*, Series C (Feb. 1965), **87**, 77-84.

Dumitrescu, D. T.: " Stromung an einer Luftblase in senkrechtem Rohr." *Z. Angew. Math. Mech.* (1943) **23**, No. 3, 139-49.

Edwardson, M.J. et al.: "Calculation of Formation Temperature Disturbances Caused by Mud Circulation," *J. Pet. Tech.* (April 1962) 416-26; Trans., AIME, 225.

Fair, W.B.: "Pressure Buildup Analysis with Wellbore Phase Redistribution," *Soc. Pet. Engr. J.* (April 1981) 257-70.

Fernandes, R. C.., Semiat, R., and Dukler, A. E.: "Hydrodynamic Model for Gas-liquid Slug Flow in Vertical Tubes," *AIChE J.* **29** (1983) 981-989.

Govier, G.W. and Aziz, K.: *The Flow if Complex Mixtures in Pipes*, Van Nostrand Reinhold Publishing Co., New York City (1972)

Griffith, P. and Synder, G.A.: " The Bubbly-Slug Transition in a High Velocity Two-Phase Flow," report no 5003-29 (TID 20947), Massachusetts Inst. of Technology, Cambridge (1962)

Griston, S. and Willhite, G.P.: "Numerical Model for Concentric Steam Injection Wells," paper SPE 16337 presented at SPE California Meeting, Ventura, CA, April 8-10, 1987.

Harmathy, T.Z.: "Velocity of Large Drops and Bubbles in Media of Infinite or Restricted Extent," *AIChE J.* (1960) **6** 281-88.

Hasan, A. R.: "Void Fraction in Bubbly, Slug, and Churn Flow in Vertical Two-Phase Up-flow," *Chem. Engr. Comm.* **6** (April 1988) 101-111.

Hasan, A.R. and Kabir, C.S.: "A Study of Multiphase Flow Behavior in Vertical Wells," *SPE Prod. Engr.* (May 1988) 263-72.

Hasan, A.R. and Kabir, C.S.: "Predicting of Multiphase Flow Behavior in a Deviated Well," *SPE Prod. Engr.* (Nov. 1988) 474-82.

Hasan, A. R. and Kabir, C.S.: "Heat Transfer During Two-Phase Flow in Wellbores : Part I : Formation Temperature." Paper SPE 22866 presented at the 1991 SPE Annual Technical Conference, Dallas, TX. Oct. 6-9.

Hasan, A. R. and Kabir, C.S.: "Heat Transfer During Two-Phase Flow in Wellbores : Part II : Wellbore Fluid Temperature." Paper SPE 22948 presented at the 1991 SPE Annual Technical Conference, Dallas, TX. Oct. 6-9.

Herrera, J.O., Birdwell, B.F., and Hanzlik, E.J.: "Wellbore Heat Losses in Deep Steam Injection Wells, SJ-B Zone, Cat Canyon Field," SPE 7117, presented at the SPE California Regional Meeting, San Francisco, April 12-14, 1978.

Hong, K.C. and Griston, S.: "New Methods for Controlled Injection of Steam into Multiple Sands", SPE 15472 presented at the Annual SPE Technical Conference, New Orleans, LA, Oct. 5-8, 1986.

Ishii, M.: *Thermo-Fluid Dynamics Theory of Two-phase Flow*, Eyrolles, Paris (1975)

Jakob, M.: *Heat Transfer*. Vol. I. John Wiley & Sons. Inc. N.Y. (1950).

Jones, O.C. and Zuber, N.: " Slug-Annular Transition With Particular Reference to Narrow Rectangular Ducts," Intl. Seminar on the Momentum, Heat and Mass Transfer in Two-Phase Energy and Chemical Systems, Dubrovnik, Yugoslavia (Sept. 1978)

Kabir, C.S. and Hasan, A.R.: "Performance of a Tow-Phase Gas/liquid Model in Vertical Wells," *J. Pet. Sci. Engr.* 4 (1990) 273-289.

Karman, A. and Biot, E.: *Mathematical Methods in Engineering* McGraw-Hill Book Co. N.Y. (1940) 403.

Kirkpatrick, C.V.: "Advances in Gas-Lift Technology," *Drilling and Production Practices* (March 1959) 24-60.

Lesem, I.B., Greytok, F., Marotta, F. and McKetta, J.J.: "A method of Calculating the Distribution of Temperature in Flowing Gas Wells", *Trans., AIME* (1957) 210,169.

Lok, K. L.: Two-Phase Flow Simulator for a Geothermal Well," MS thesis, U. of North Dakota, Grand Forks, ND (1991)

McAdams, W.H.: *Heat Transmission,* Second Ed., McGraw-Hill Book Co. N.Y. (1942).

Moss, J.T. and White, P.D.: "How to Calculate Temperature Profiles in a Water-Injection Well," *Oil and Gas Jour.* (March 9, 1959) 57, No. 11, 174.

Mukherjee, H.: " An experimental Study of Inclined Two-Phase Flow," PhD Dissertation, U. of Tulsa, Tulsa, OK (1979)

Nicklin, D.J., Wilkes, J. O. and Davidson, J.F.: "Two-Phase Flow in Vertical Tubes," *Trans. Inst. Chem. Engr.* 40 (1962) 61-68.

Orkiszewski, J.: "Predicting Two-Phase Pressure Drop in Vertical Pipes," *JPT* (June 1969) 829-38: *Trans.*, AIME, 240

Patel, R.: "Multi-Phase Flow in Vertical and Inclined Annuli," MS Thesis, U. of North Dakota, Grand Forks, ND (1988)

Ramey, H.J. Jr.: "Wellbore Heat Transmission", *J. Pet. Tech.* (April 1962) 427-435.

Roux, B., Sanyal, S.K., and Brown, S.L.: "An Improved Approach to Estimating True Reservior Temperature from Transient Temperature Data," paper SPE 8888 presented at the SPE Calif. Regional Meeting, Los Angeles, April 9-11, 1980.

Runge, D.E. and Wallis, G.B.: " The Rise Velocity of Cylindrical Bubbles in inclined Tube," USAEC-Euratom R&D Report No. NYO-314-8 (June 1965)

Sadatomi, M., Sato, Y. and Saruwatri, S.: "Two-Phase Flow in Vertical Non-Circular Channels." *Int. J. Multiphase Flow.* 8, 641-655.

Sagar, R.K, Dotty, D.R., and Schmidt, Z.: "Predicting temperature profiles in a flowing well," SPE Annual Tech. Meeting, San Antonio, TX Oct. 8-11, 1989.

Schlumberger, M., Doll, H.G., and Perebinossoff, A.A.: "Temperature Measurements in Oil Wells," *J. Inst. Pet. Technologists* (Jan. 1937) 23, 159.

Seyer, W., and Langden, I.: "Estimation of Bottomhole Temperature from Surface Condition in Cyclic Steam Injection," paper CIM/SPE 90-110, CIM/SPE Int. Tech. Meeting, Calgary, June 10-13, 1990.

Shiu, K.C. and Beggs, H.D.: "Predicting Temperatures in Flowing Oil Wells," *I Energy Resources Technology* (March, 1980) Trans., ASME.

Srinevasan, S.: "Void Fraction in Countercurrent Two-Phase Flow." MS Thesis, U. of North Dakota, Grand Forks. (1993) in preparation

Steen, D. A. and Wallis, G.B.: "Pressure Drop and Liquid Entrainment in Annular Two-phase Flow," AEC Report No. NYO-3114-2 (1964).

Taitel, Y., Barnea, D. and Dukler, A.E.: "Modelling Flow Pattern Transition For Steady Upward Gas-Liquid Flow in Vertical Tubes," *AIChE J.* (May 1980) 345-54.

Wallis, G.B.: *One Dimensional Two-phase Flow*, McGraw-Hill Book Co. Inc., New York City (1969).

White, E.T. and Beardmore, R.H.: "Velocity of Rise of Single Cylindrical Air Bubbles Through Liquids Contained in Vertical Tubes," *Chem. Engr. Sci.* (1962) **17**, 351-361

Willhite, G.P.: "Over-all Heat Transfer Coefficients in Steam and Hot Water Injection Wells", *J. Pet. Tech.* (May 1967) 607-615.

Witterholt, E.J. and Tixier, M.P.: "Temperature Logging in Injection Wells," paper SPE 4022 presented at the SPE Annual Fall Meeting, San Antonio, Oct. 8-11, 1972.

Zuber, N. and Findlay, J.: "Average Volumetric Concentraition in Two-Phase Flow Systems," *Trans., ASME J. Heat Transfer* (1965) **87**, 453-68

Zukoski, E.E.: " Influence of Viscosity, Surface Tension, and Inclination Angle on Motion of Long Bubbles in Closed Tubes," *J. Fluid Mech.* (1966) **25**, Part 4, 821-37.